Synthesis, Structure and Catalytic Activity of Titanium, Zirconium and Hafnium-Containing Polyoxometalates

by

Ghada Al-Kadamany

A thesis submitted in partial fulfillment of the requirements for the degree of

Doctor of Philosophy in Chemistry

Approved Dissertation Committee

Prof. Dr. Ulrich Kortz (*mentor, Jacobs University*)
Prof. Dr. Gerd-Volker Röschenthaler (*Jacobs University*)
Prof. Dr. Horst Elias (*Technische Universität Darmstadt*)

Defense Date: 28/June/2010
School of Engineering and Science
Jacobs University Bremen

Acknowledgements

To my supervisor, Professor Ulrich Kortz, I owe my deepest gratitude, for he provided the opportunity first and then the guidance and support along the way. Jacobs fellowship was always an honor for me, so special thanks go to Jacobs university and the Dean of School of Engineering and Science in specific, Professor Bernhard Kramer.

My thanks are also due to the committee members Professor Gerd-Volker Röschenthaler and Professor Horst Elias for their precious time and invaluable input.

For the peculiar knowledge and experience I acquired in her laboratory at Boreskov Institute of Catalysis, Novosibirsk, Russia, I express my gratefulness to Professor Oxana Kholdeeva and her coworkers.

I might as well extend my thanks to all the former and current members of the Kortz group for making it such a pleasure to work with, I have to specifically mention here the assistance of Dr. Michael Dickman and Dr. Bassem Bassil in X-Ray Crystallography, and the undergraduate students Prabal Subedi and Borislav Milev.

Last word of appreciation goes deservingly to my mother and my whole family for always encouraging me despite all the strife and work.

Abstract

_____

Polyoxometalates (POMs) represent by now a well-known class of discrete, molecular metal-oxides, which are attractive due to a large structural and compositional variety combined with a multitude of properties. Vacant (lacunary) polytungstate precursors allow for incorporation of a vast number of electrophiles including transition metals. The resulting products often have properties which render them of interest for potential applications in different areas such as catalysis, medicine and materials science.

The exploration of the interaction between lacunary polyoxometalates (POMs) and group 4 (Ti, Zr and Hf) transition metal ions has been mainly driven by the fact that potential products may serve as oxidation catalysts or even as soluble molecular analogues of known Ti and Zr-containing heterogeneous catalysts.

This document is a summary of three-year research conducted in this specific area, that is investigation of titanium containing POMs, the chemistry involved, synthesis, solid state and solution characterization and catalytic performance.

Following an introductory chapter which provides some insight into the structural details of POMs in general and Ti, Zr, Hf-containing POMs in specific, their properties and a thorough review of the literature related, Chapter II presents details on the instrumentation used for characterization and synthetic procedures of precursors. Chapter III can be viewed as the heart of the work for it sums up the description of all polyanions (**2-8**) successfully synthesized and characterized and those with crystallographic disorder (**9-10**). Catalytic studies performed on ruthenium, zirconium and hafnium containing POMs are discussed separately in Chapter IV.

 Polyanions **2**, **3** and **4** are dimeric, trimeric and tetrameric strctures respectively, made up from the interaction of the trilacunary Keggin precursor $Na_{10}[A\text{-}\alpha\text{-}GeW_9O_{34}]$ with two different titanium(IV) sources, $TiOCl_2$ and

$K_8[Ti_4O_4(C_2O_4)_8]$ (**K-1**) (**Ti4**) that crystallizes from any saturated aqueous solution of $K_2TiO(C_2O_4)_2$. The reaction of **Ti4** with $Na_9[A\text{-}\alpha\text{-}PW_9O_{34}]$, on the other hand, lead to a peculiar structure **5**, which exhibits unusual dimerization fashion with the help of oxalate groups attached to the sandwiched titanium atoms.

Attempts were fruitful with the lone pair containing POM precursor $Na_9[B\text{-}\alpha\text{-}AsW_9O_{33}]$, where polyanions **6** and **7** containing two and eight titanium atoms respectively were obtained. The only Wells-Dawson based structure is the dimeric polyanion **8** harboring four titanium atoms incorporated into the tungstate framework and two external ones linking the two half-units.

Two crystallographically disordered molecules **9** and **10** were also briefly reported on.

In Chapter IV, Catalytic studies were discussed for p-xylene oxidation reaction using four organo-ruthenium polyanions (**11-14**) as heterogeneous catalysts. For all four ruthenium-containing polyanions the yields were comparable and significantly higher than those for the blank and the corresponding "all-tungsten" derivatives, that is considered as evidence of the importance of the ruthenium centers for the overall catalytic efficiency of the POMs for this type of reactions. The second part of the chapter dealt with the two novel zirconium and hafnium polyanions (**15** and **16** respectively). They contain an unprecedented octahedral Zr_6/Hf_6 assembly which is stabilized by two (B-α-AsW_9O_{33}) groups and five terminal acetate ligands. The TBA-salts of both **15** and **16** revealed high catalytic activity and selectivity in the liquid-phase oxidation of organic compounds with aqueous H_2O_2. A heterolytic oxidation mechanism is manifested by the high yields of epoxide and diol in the oxidation of cyclohexene.

Table of Contents

Chapter I Introduction

Chapter II Experimental Details

Chapter III Synthetic Results

Chapter IV Catalytic Results

List of Tables

_____

List of Figures

_____

Codes of Compounds

Compound	Code
$K_8[Ti_4O_4(C_2O_4)_8]$	**K-1** (**Ti4**)
$K_9H_5[a,a\text{-}Ge_2W_{18}Ti_6O_{77}].22H_2O$	**K-2**
$Rb_7K_3Na_7[(\alpha\text{-}Ti_3GeW_9O_{37}OH)_3(TiO_3(OH_2)_3)].23H_2O$	**Rb,K,Na-3**
$K_{14}Na_{14}[(Ti_3GeW_9O_{37})_4O_6].60H_2O$	**K,Na-4**
$K_{16}Na_2[P_2W_{18}Ti_8(C_2O_4)_8H_8O_{80}].20H_2O$	**K,Na-5**
$K_{14}[As_2W_{18}Ti_2(C_2O_4)_2O_{66}].18\ H_2O$	**K-6**
$Rb_2K_5Na_{13}[As_2W_{18}Ti_8(C_2O_4)_8(H_2O)_2O_{75}].30H_2O$	**Rb,K,Na-7**
$K_{15}Li_5[P_4W_{32}Ti_6(C_2O_4)_4O_{124}].53H_2O$	**K,Li-8**
$[Ti_{9.3}As_6W_{59.7}O_{244}(H_2O)_4]^{82-}$	**9**
$\{Ti_4P_8W_{48}O_{184}\}$	**10**
$K_5Na_5[Sb_2W_{20}O_{70}(RuC_6H_6)_2].22H_2O$	**K,Na-11**
$Cs_2Na_8[Bi_2W_{20}O_{70}(RuC_6H_6)_2].30H_2O$	**Cs,Na-12**
$Cs_3Na_7[Sb_2W_{20}O_{70}(RuC_{10}H_{14})_2].27H_2O$	**Cs,Na-13**
$Na_{10}[Bi_2W_{20}O_{70}(RuC_{10}H_{14})_2].35H_2O$	**Na-14**
$Cs_9Na_2[Zr_6(\mu_3\text{-}O)_4(OH)_4(H_2O)_2(CH_3COO)_5(AsW_9O_{33})_2].87H_2O$	**Cs,Na-15**
$((n\text{-}C_4H_9)_4N)_7H_4[Zr_6O_4(OH)_4(H_2O)_2(CH_3COO)_5(AsW_9O_{33})_2]$	**TBA$_7$H$_4$-15**
$Cs_{10}Na[Hf_6(\mu_3\text{-}O)_4(OH)_4(H_2O)_2(CH_3COO)_5(AsW_9O_{33})_2].73H_2O$	**Cs,Na-16**
$((n\text{-}C_4H_9)_4N)_6H_5[Hf_6O_4(OH)_4(H_2O)_2(CH_3COO)_5(AsW_9O_{33})_2]$	**TBA$_6$H$_5$-16**

Chapter I
Introduction

1.1 A brief history

The history of the field of Polyoxometalates (POMs) dates back to the first third of the nineteenth century, when Berzelius first reported the formation of Ammonium 12-molybdophosphate $(NH_4)_3[PMo_{12}O_{40}]$ in 1826.[1,2]

There have been attempts in the next hundred years to understand this new class of compounds. Miolati in 1908 and Rosenheim later on, applied the ionic coordination theory, which was criticized by Pauling in 1929. The latter suggested instead, a structure formed by MoO_6 octahedra encapsulating a PO_4^{3-} unit. Pauling made some progress in the right direction, but it was until 1933, that Keggin provided an explicit description of the structure that was named after him. Other types of structures were later reported in literature, the Anderson-Evans in 1948 and the Wells-Dawson in 1953 for instance.[1,2,3]

Nevertheless, it was only in the past few decades that the real burst in the POMs field began, owing to the development of the modern experimental techniques (e.g NMR and single crystal XRD) and the promising potential applications, namely catalysis, that became apparent at the time.

Most of the pioneering systematic studies on the catalytic use of POMs were carried out in Russia (Matveev and coworkers) and Japan (Izumi, Misono, Ono, Otake, Yoneda and co-workers). It was actually in Japan in 1972, that a heteropolyacid $H_4[SiW_{12}O_{40}]$ was industrially employed for the first time, as a homogeneous catalyst for the hydration of propene to 2-propanol.[2,4,5,6]

1.2 General definitions and structural principles

Polyoxometalates (POMs), as their name indicates, are multi-oxygen containing discrete anionic molecules with one or more other elements in their positive oxidation state(s). The 1983 monograph by Pope[1] distinguishes between two classes based on this definition, the isopoly- and the heteropolyoxoanions of the general formulas $[M_mO_y]^{p-}$ and $[X_xM_mO_y]^{q-}$ respectively. M is usually referred to as the "addenda atom" and X, which is typically of lower atomic proportion than M, is called the "heteroatom". M is mostly molybdenum or tungsten in their highest oxidation state (d^0), though a limited number of other transition metals are known so far to exhibit such a chemical phenomenon such as vanadium, niobium and tantalum. The identity of X on the other hand is much less restricted.

Elements that qualify to be addenda atoms have to have the ability to increase their coordination number with oxygen from 4 to 6 as they polymerize in solution upon acidification. This requires a favorable combination of high positive charge and an ionic radius that falls within the range for octahedral packing with oxygens. Another indispensible factor is the accessibility of the addenda atom empty d-orbitals for metal-oxygen π interaction.[3]

This is all better understood through the general principles that mostly govern the formation of polyoxometalates. POMs structures are based on the assemblage of MO_n polyhedra that are most commonly octahedra, connected to each other via one (corner sharing), two (edge sharing) or three oxygens (face sharing).

The addenda metal atom is displaced from the center of the octahedron towards the terminal oxygen(s) due to the M-O π bonding and the greater polarizability of the unshared oxygens towards the addenda atom as compared to other shared oxygens. The surface oxygens as a result are

incapable of further polymerization and thus account for the existence of POMs as discrete species. The strong polarizability and the nonbasicity of the surface oxygen atoms make it unlikely for them to get protonated or even form hydrogen bonds of average strength. The distribution of the negative charge over the large size of heteropoly complexes places the cations at large distances thus minimizing the electrostatic interaction and lowering the lattice energies and solvation energies[3]. In consequence, the hydrodynamic radii and crystallographic radii of POMs are frequently comparable.

Lipscomb rule states that it is very unlikely for a POM to have MO_6 octahedra with more than two unshared oxygen atoms. This can be reasoned based on the strong trans influence of the M=O bonds that facilitates the dissociation of MO_3 from the polyanion.[1,2,7] The 1983 monograph by Pope[1] again classifies polyanions as type I "mono-oxo" and type II "cis-dioxo". The number of terminal oxygen atoms M=O per addenda atom is one for type I and two in cis positions for type II.

In the next two sections, two of the most common POM structures will be introduced and discussed in the form of tungstates only. These are the Keggin and the Wells-Dawson ions.

1.3 The Keggin ion

First discovered by Berzelius in 1826 upon reacting ammonium molybdate with phosphoric acid and later structurally elucidated by J.F. Keggin in 1933 in the form of 12-tungstophosphoric acid,[8] the Keggin structure and its derivatives are by far the most widely investigated.

The Keggin ion is a highly symmetric heteropolyanions generally represented by the formula $[XM_{12}O_{40}]^{x-}$, it is composed of a central XO_4 tetrahedron surrounded by a neutral shell of 12 WO_6 octahedra grouped as four M_3O_{13} units, called triads (Fig. 1.1). Each triad is formed by three edge shared WO_6

octahedra with a central μ_4 oxygen bridge that links it to the central tetrahedron. These triads are connected to each other via corner sharing oxygen atoms. The Keggin is a type I ion with one W=O bond per WO_6 octahedron and a significantly longer trans bond. IR spectroscopy shows separate bands for such types of bonding with the W=O vibration band lying at the high wave number side.
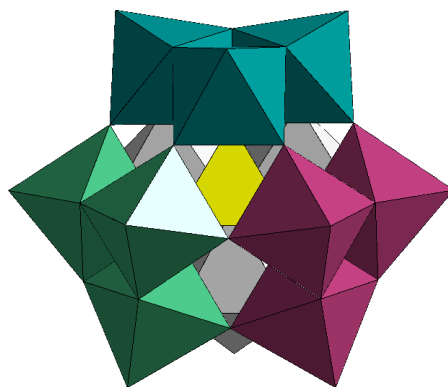
Fig. 1.1 Polyhedral representation of the Keggin ion showing the four triads in four different colors surrounding the central tetrahedron in yellow

Different structural isomers of the α-Keggin depicted in Fig. 1.1 are obtained by 60° rotation of one, two, three or all four triads, thus forming the β, γ, δ and ε isomers respectively. As for the β isomer, it has lowered symmetry (C_{3v}) in comparison to the α (T_d), and involves shorter W...W distances and more acute W-O-W angles between the rotated triad and the rest of the anion. The resulting increased coulombic repulsions and the less favorable pπ-dπ interactions make the β isomer less stable than the α. For the same reasons, γ, δ and ε isomers are less stable than α and β.[1] Stability of each isomer is also dependent on the heteroatom; the β → α isomerization for X= Si(IV) or Ge(IV) is known to be slower than that for X= P(V) or As(V). α and β isomers can be

distinguished by means of UV-spectroscopy or polarography (the reduction potential is higher for the ß isomer).

The plenary α and ß-Keggin ions are stabilized under acidic conditions but they might lose one or more addenda atoms to form lacunary species in solution. For example, α-$[PW_{12}O_{40}]^{3-}$ remains intact up to pH 1.5-2, then it degrades to give the mono-lacunary α-$[PW_{11}O_{39}]^{7-}$. The latter is stable between pH 2 and 8, then further degrades to give the tri-lacunary α-$[PW_9O_{34}]^{9-}$. There exists only one monolacunary α-$[XW_{11}O_{39}]^{y-}$ isomer, where all 12 addenda atoms of the parent Keggin ion are equivalent by T_d symmetry; while there are β_1, β_2 and β_3-$[XW_{11}O_{39}]^{y-}$ isomers (Fig. 1.2) where the lost addenda atom octahedron is unconnected, connected with or part of the rotated triad respectively.

ß-$[XW_{12}O_{40}]^{n-}$

β_1 -$[XW_{11}O_{39}]^{x-}$

β_2 -$[XW_{11}O_{39}]^{x-}$

β_3 -$[XW_{11}O_{39}]^{x-}$
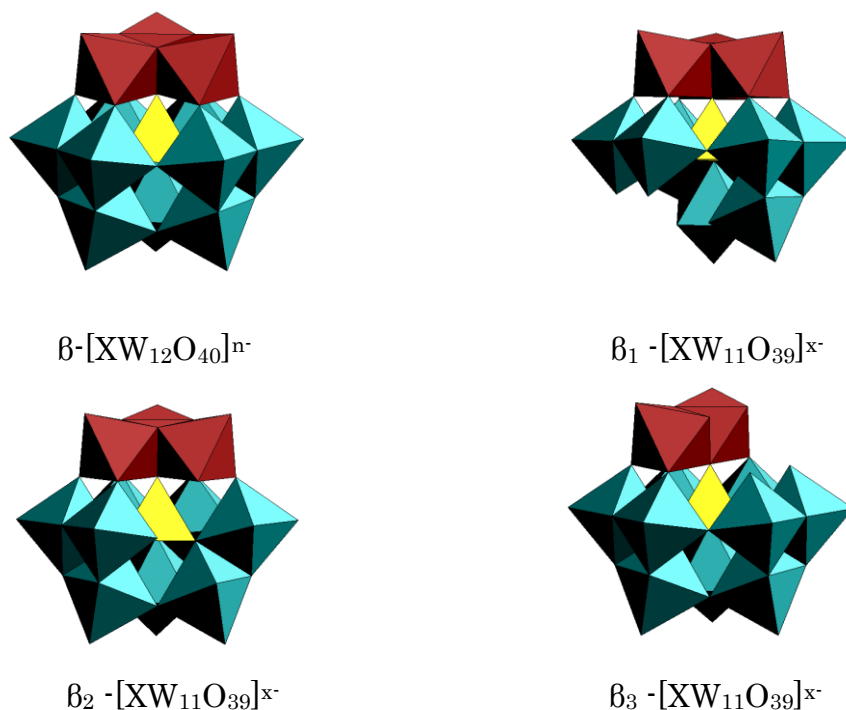
Fig. 1.2 Polyhedral representation of the three monolacunary species derived from the ß-Keggin ion showing the rotated triad in red.

As for the trilacunary $[XW_9O_{34}]^{z-}$ species, whether they originate from an α or ß parent plenary Keggin ion can fall into one of two categories, the A and the B-type. The discrepancy depends on whether the removed M_3 group involves corner shared (A type) or edge shared (B type) octahedra (Fig. 1.3). Unlike the A type, one of the oxygens of the central tetrahedron of the B type is free and pointing out of the lacuna.[1,2,7]
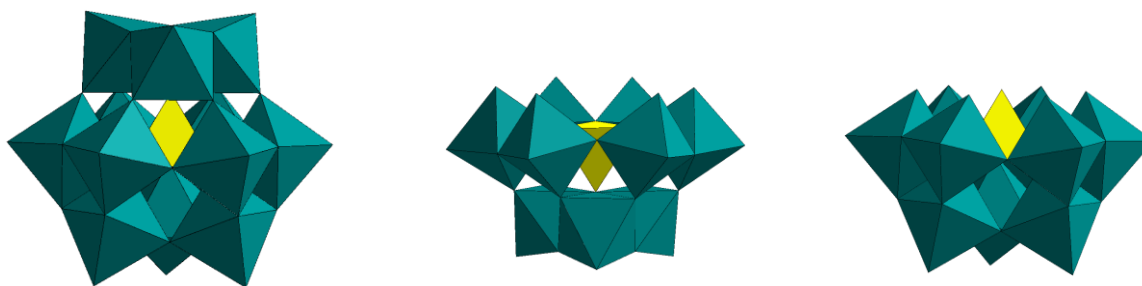
Fig. 1.3 α-$[XM_{12}O_{40}]^{x-}$ A-α-$[XM_9O_{34}]^{y-}$ B-α-$[XM_9O_{34}]^{y-}$

However salts of trilacunary anions have been isolated with a central pyramidal group with a lone pair, such as $[As^{III}W_9O_{33}]^{9-}$ and $[Sb^{III}W_9O_{33}]^{9-}$. These exist exclusively in the B type, and are unable to undergo further condensation to the $As^{III}W_{11}$ or the $Sb^{III}W_{11}$ due to the repulsion exerted by the lone pair of electrons. This renders the chemistry related to these species dissimilar to what is usually associated with $[GeW_9O_{34}]^{10-}$ or $[PW_9O_{34}]^{9-}$ for example.[1,7]

1.4 The Wells-Dawson ion

The Wells-Dawson structure is only known for the heteroatoms P(V) and As(V). It is a dimeric heteropolyanion of the formula $[X_2M_{18}O_{62}]^{x-}$ where M= W(VI) or Mo(VI). The anion is viewed as a fusion between two A-α-XW_9 units through all six oxygens of the lacuna resulting in a virtual D_{3h} symmetry cluster of the α isomer type (Fig. 1.4). Two sets of tungsten form this polyanion, six "polar" and twelve "equatorial" constituting the two caps and the two belts of the anion respectively. The β isomer forms when one of the caps is rotated by 60°. Similar to the β Keggin, the β Wells-Dawson is more easily reduced.
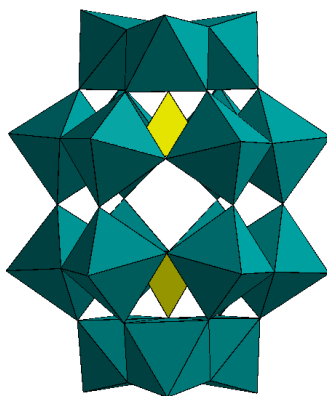
Fig. 1.4 Polyhedral representation of the Wells-Dawson structure, WO_6 octahedra (teal) and XO_4 tetrahedra (yellow)

Stable lacunary species are also derived from α-$[P_2M_{18}O_{62}]^{x-}$ plenary anion upon alkalination. Two isomers of the monolacunary species exist, these are the $α_1$ and the $α_2$-$[P_2W_{17}O_{61}]^{10-}$, where the one addenda is lost from the belt in the first and it is lost from the cap in the second upon reaction with base, typically potassium bicarbonate.[9]

The trilacunary $[P_2W_{15}O_{56}]^{12-}$ and even hexalacunary $[H_2P_2W_{12}O_{48}]^{12-}$ species (Fig. 1.5) can be generated using bases of different strengths, sodium carbonate and tris(hydroxymethyl)amino methane respectively.[1,2,9]
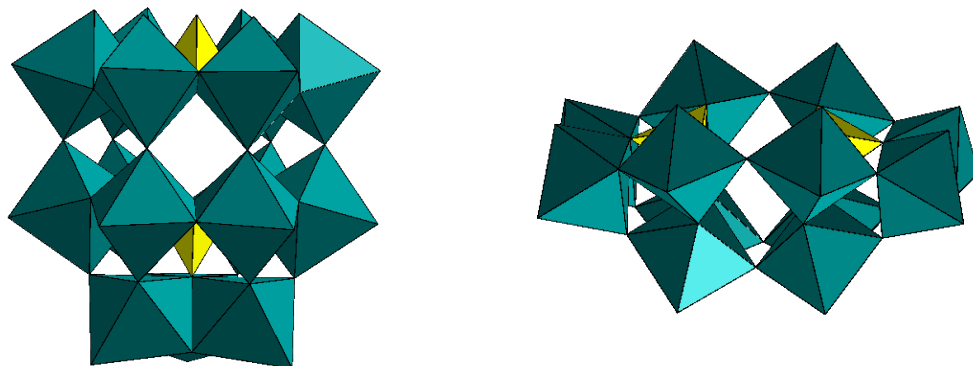
Fig. 1.5 Polyhedral representation of the trilacunary $[P_2W_{15}O_{56}]^{12-}$ (left) and hexalacunary $[H_2P_2W_{12}O_{48}]^{12-}$ (right) species of the Wells-Dawson structure

1.5 Properties

Despite the wide versatility of POMs in terms of size and structure, there are however properties that might be generalized. Polyoxoanions are air and water stable structures of high molecular weight. They usually have low lattice and solvation energies as previously discussed[1], their solubility is therefore mainly determined by the counter cation; where Na salts and heteropolyacids (HPAs, heteropolyanions having H^+ as the only counter cation) are very water soluble and salts of cations of organic nature such as tetrabutylammonium (TBA) are soluble in nonaqueous media for example.[2,3] The pH range in which a polyoxoanion is able to maintain its structure in solution varies widely from one case to the other (pH ~ 1-14). We can nevertheless state that POMs are much more stable towards more acidic

conditions.[1] The tungstate/phosphate system mentioned earlier is an example, where the ^{31}P-NMR study showed that the $[PW_{12}O_{40}]^{3-}$ anion exists predominantly at pH<1.5, while the monolacunary $[PW_{11}O_{39}]^{7-}$ can be stable in the pH range 2.5-7 and further degradation to the phosphate free ion occurs at higher pH values.[2,4]

In one of the early studies of the stability of Heteropolyacids, it was shown that the meta tungstic acid $H_8[W_{12}O_{40}].xH_2O$ decomposes at 50°C while the presence of a heteroatom P or Si in the middle increased the decomposition temperature by 400 or 500 degrees, since it helps reducing the effect of the thermal vibrations. Thermal analytical methods are used for such studies including Thermal Gravimetric Analysis (TGA) and Differential Thermal Analysis (DTA). Heteropoly compounds of the Keggin structure, being the ones mostly investigated and reported on, are generally known for their high thermal stability, this is of high importance if the catalyst is to be employed in heterogeneous catalysis. Thermal decomposition of POMs leads eventually to a mixture of metal oxides, catalytic activity can however be lost long before reaching this stage.[1,4,5,6]

Heteropolyacids of the Keggin and the Wells-Dawson structures are known to be very strong Brønsted acids, though the properties of the Keggin acids are the ones that are well documented. Dissociation constants and Hammett acidity functions in different solvents show that HPAs are stronger than the usual mineral acids like H_2SO_4 or HNO_3. Acidity depends on the identity of the addenda as well as the heteroatom, tungstates are stronger than molybdates and $H_3[PW_{12}O_{40}]$ is the strongest in the Keggin series. Solid Keggin HPAs on the other hand also exhibit Brønsted acidity that is higher than the conventional solid acids like SiO_2-Al_2O_3 and HX and HY zeolites. The order of acidity parallels that in solution and so does the order of catalytic activity in most of the cases in homogeneous and heterogeneous systems.[2,5,6,10] Analytical techniques used to determine the degree of acidity

of solid HPAs are detailed in a book by J.B. Moffat on heterogeneous catalysis and surface properties of POMs.[4]

A mechanistic classification of heterogeneous processes by solid HPAs was developed by Misono *et al.* [6,11,12] Three categories were identified, (i) surface type, that is the conventional case where the activity takes place at the surface of the catalyst, (ii) bulk I type, in which the solid exists in a pseudoliquid phase where active sites in the bulk and on the surface take part in the reaction. This is common for the polar substrates that are capable of penetrating into the flexible bulk of the solid catalyst. (iii) bulk II type, where reaction (mostly oxidation) occurs at the surface along with the diffusion of H^+ and e^- from the bulk.

When redox properties of POMs are discussed, distinction between type I and type II anions should be made. The lowest unoccupied molecular orbital (LUMO) of type I MO_6 octahedra is a nonbonding metal-centered orbital, while the LUMO of type II is antibonding in character. This causes reduction in case of type II anions to be much more difficult and irreversible and makes type I anions, especially those belonging to the Keggin family, the most favorable for oxidation catalysis.

POMs are known as "electron reservoirs" because of their high capacity of accepting electrons without a major change in their structure. The additional negative charge is necessarily accompanied by protonation from the solvent in order to keep electro neutrality; reductions therefore are mostly pH-dependent. Cyclic voltammetry and ESR measurements are conducted in such studies, and they show that deeply colored species are formed upon the one and two-electron reversible reductions of Keggin tungstates for example, these are called the "heteropolyblues". ESR spectroscopy sets forward the evidence that the unpaired electron added to the Keggin undergoes fast hopping amongst all addenda centers at room temperature; while two and four electrons reduced species are ESR silent. The Wells-Dawson ion on the

other hand, when reduced restricts the delocalization of the added electron to the belt tungstens.[1,2,5]

1.6 Applications

The unique properties of POMs including mass, size and electron/proton storage capacities have granted them the application in different areas such as materials science, medicine, and catalysis which was by far the most active area.

Their fairly high thermal stability in the solid state, their solubility in polar solvents and non-polar solvents as well upon choosing the appropriate cation, high H^+ mobility and reversible redox properties gave POMs the advantage to be employed as acid as well as oxidation catalysts.[10]

Heteropolyacids and their salts have even found their way to industrial large scale acid and oxidation catalyzed processes. These include homogeneous systems (liquid phase hydration of butene) and heterogeneous systems (gas phase oxidation of methacrolein to methacrylic acid and of ethylene to acetic acid).[2]

1.6.1 Acid catalysis

The general mechanism of reactions catalyzed by heteropolyacids can be represented by the conventional single proton transfer reaction:

$$S_1 + H^+ \leftrightarrow S_1H^+ + S_2 \rightarrow P + H^+$$
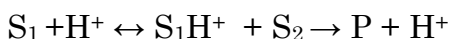
Where S_1 and S_2 are the substrate and P is the product. Consequently, the higher the Brønsted acidity of the heteropolyacid, the more efficient catalyst it becomes. Thus the order of catalytic activity of the Keggin POMs, being the ones that were extensively studied, parallels that of acid strength in

___

homogeneous and heterogeneous systems i.e. $H_3PW_{12}O_{40}$ > $H_4SiW_{12}O_{40}$ > $H_3PMo_{12}O_{40}$ > $H_4SiMo_{12}O_{40}$.[2,7]

HPAs are not only more acidic than the conventional mineral acids, but also more thermally stable and have the advantage of being odorless and non-volatile.

Their high acidity is attributed to the high lability of the crystal lattice nonlocalized protons that exchange rapidly with protons of the crystal water and those of the μ_2 bridging oxygen atoms of the polyanions.[2,7,13]

Highly demanding acid catalyzed reactions such as isomerization of alkanes and Friedel-Crafts as well as mild reactions such as Diels-Alder are examples where HPAs were utilized as catalysts.[5,13]

1.6.2 Oxidation catalysis

Unlike POMs acid catalysis, Oxygenation and oxidative dehydrogenation reactions make use not only of the Keggin-type HPAs but a wide variety of transition metal substituted POMs.

Selective catalytic oxidation of organic compounds is of both academic and industrial interest, especially when it is accomplished with an environmentally benign oxidant of low cost such as O_2 or H_2O_2. Numerous unique properties of POMs such as their thermal and hydrolytic stability and solubility in various media that were mentioned earlier make them suitable candidates for such a task.

Transition metal-substituted POMs, the so called inorganic metalloporphyrins, have the advantage of the inorganic nature of their coordination sphere which made them more thermodynamically stable against oxidative degradation. Their metal active sites and countercations, however, can be synthetically modified. Furthermore, these compounds can function as homogeneous probes of the mechanisms of heterogeneous

catalytic oxidation reactions. Their closely packed arrays of oxide anions can be practically viewed as discrete fragment models of the extended metal oxide lattices known for being efficient heterogeneous catalysts.[2,4,5,6,7,13]

The basic mechanism involved in POM catalyzed oxidation reactions with molecular oxygen is shown in eq. A; where POM_{ox} and POM_{red} are the oxidized and reduced forms of the POM respectively. The substrate is first oxidized by the POM which is then regenerated by the oxidant that is often oxygen to form water. Oxidation of the substrate is often accompanied by proton transfer to the consequently reduced catalyst (eq. A):

$S + [POM]_{ox} + nH^+ \rightarrow H_n[POM]_{red} + P$

$H_n[POM_{red}] + n/4 \ O_2 \rightarrow [POM]_{ox} + n/2 \ H_2O$ (eq. A)
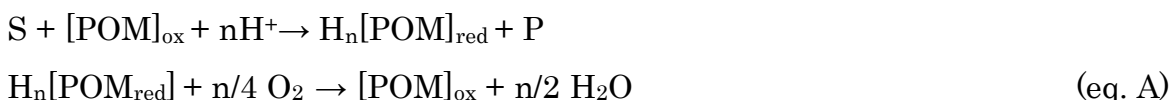
Such a mechanism is thermodynamically favorable under the condition that the reduction potentials of the substrate, POM and molecular oxygen increase in the following order:

$E(S) \leq E(POM) \leq E(O_2)$

This mechanism is usually followed in the formation of carboxylic acids from the corresponding aldehydes (methacrylic acid from methacrolein) and the dehydrogenation of alcohols and aldehydes and carboxylic acids to form C=C and C=O bonds (isobutyric acid transformation to methacrylic acid).[1,2]

Phosphomolybdovanadates were employed first by Kozhevnikov and Matveev as secondary catalysts in the Wacker process for the transformation of ethylene to acetaldehyde; $H_5PV_2Mo_{10}O_{40}$ was found out to be the most efficient in the reoxidation of the primary catalyst $PdCl_2$ according to (eq. B) as a replacement of the halide containing $CuCl_2$.[14]

$Pd^0 + [POM]_{ox} + 2H^+ \rightarrow H_2[POM]_{red} + Pd^{II}$

$H_2[POM]_{red} + 1/2 \ O_2 \rightarrow [POM]_{ox} + H_2O$ (eq. B)
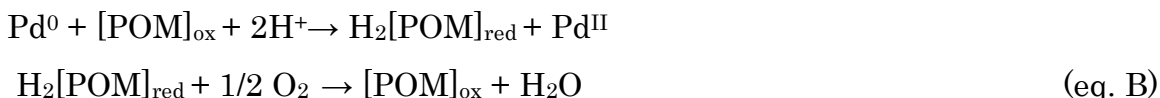
Neumann *et al.* later tried to utilize this catalyst in the direct oxidative dehydrogenation of various organic substrates such as 9,10-dihydroanthracene, dehydrogenation of benzylic alcohol or

dehydrodimerization of activated phenols to diphenoquinones among other numerous reactions.[15,16,17]

POMs are also known to catalyze various organic substrates by H_2O_2, such as epoxidation of olefins, oxidation of alcohols and phenols. Keggin type and related polyanions were widely applied in such systems and detailed examination lead to the discovery that POMs actually serve as precatalysts where they tend to be decomposed by excess H_2O_2 to form oxo-peroxo species, the most renowned of which is the Ishii-Venturello complex $\{PO_4[WO(O_2)_2]_4\}^{3-}$ which was isolated and crystallographically characterized.[18]

Other transition metal substituted POMs are able to interact with the H_2O_2 to form a certain peroxo or hydroperoxo activated complex which further oxidizes the substrate into the desired product(s). The activated complex can however be regenerated in its original form (eq. C).

Oxidant + POM → [POM-Ox]$_{activated}$

[POM-Ox]$_{activated}$ + substrate → POM + product   (eq. C)
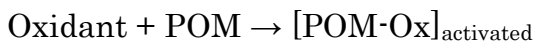
Titanium-containing POMs are shown mostly by Kholdeeva *et al.* to follow this kind of reaction route when applied as oxidation catalysts with H_2O_2.[19]

1.7 Ti-containing polyoxotungstates

Titanium has a high tendency to change its coordination upon reaction and it is able to form peroxo species with H_2O_2 without being extracted from its framework. This is what makes Ti-containing molecular sieves among the best catalysts for selective oxidation with H_2O_2.

The above established facts, in addition to TiO_2 being a well known photocatalyst, were among the most prominent motivations for the synthesis of Ti-containing POMs. They proved to deserve interest, not only because they serve as adequate probes to study the conventional titanium oxide

catalysts or titanium silicates, but also because they, themselves show high potential as oxidation and photo catalysts.[19]

Due to the comparable sizes of the ionic radii of Ti^{IV} (0.75Å) and W^{VI} (0.74Å), Ti is expected to fit perfectly in the polyoxotungstate framework. In addition, this substitution of W^{VI} with Ti^{IV} is particularly interesting because of the expected much higher basicity of the resulting POM.[20,21,22,23,24]

Numerous Ti-polyoxotungstates have already been reported in literature, many of which are shown in Table 1.1. The majority of the compounds are based on the Keggin structure and some are derivatives of the Wells-Dawson in addition to others. Figures are shown where necessary.

The substitution of the tungsten(VI) with the lower valence Ti(IV) leads to an increase in basicity of the POM and thus the high tendency to oligomerize through the Ti-O-Ti bridging bond. This, among other reasons, accounts for the formation of the family of dimers (entries 9 to 12): Alpha or Beta $(Ti_3XW_9O_{38.5})_2$ (Fig. 1.6). These are consisted of two $XW_9Ti_3O_{40}$, trilacunary Keggin ions, each being tri-substituted with Ti (IV) with the three TiO_6 octahedra occupying the vacant sites of the three corner shared WO_6 octahedra.
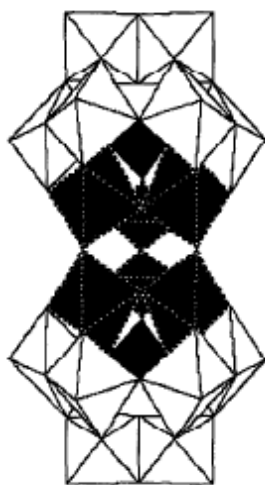
Fig. 1.6 Polyhedral representation of the $[\alpha\text{-}X_2W_{18}Ti_6O_{77}]$ dimer

Table 1.1 Details of a number of Ti-Polyoxotungstates published

	Type	Structure	-substituted	Shorthand-Formula	Year	Ref	Fig.
1	K[a]	monomer	mono	α-PW$_{11}$Ti*	1983	25	7
2	K	monomer	mono	α-PW$_{11}$(TiO$_2$)	1992	26	
3	K	monomer	di	α-PW$_{10}$Ti$_2$*	1983	27	8
4	K	monomer	di	α-PW$_{10}$(TiO$_2$)$_2$	2007	28	
5	K	monomer	mono	α-PW$_{11}$TiCp *	1986	29	
6	K	monomer	tri	XW$_9$(TiCp)$_3$* X=Si,Ge	2000	30	
7	K	dimer	di	(α-PW$_{10}$Ti$_2$)$_2$	2002	21	
8	K	dimer	di	(γ-GeW$_{10}$Ti$_2$)$_2$	2008	31	
9	K	dimer	tri	$\alpha\alpha$-P$_2$W$_{18}$Ti$_6$	2001	32	6
10	K	dimer	tri	$\alpha\alpha$-Si$_2$W$_{18}$Ti$_6$	2001	32	6
11	K	dimer	tri	$\beta\beta$-Si$_2$W$_{18}$Ti$_6$	1993	33	
12	K	dimer	tri	$\alpha\alpha$-Ge$_2$W$_{18}$Ti$_6$	1993	34	6
13	K	tetramer	di	(β-SiW$_{10}$Ti$_2$)$_4$	2004	35	14
14	K[b]	monomer	di	αPW$_{11}$(Ti(ox)(OH))$_2$	2005	23	11
15	K	monomer	tetra	αPW$_{10}$(Ti(ox)(H$_2$O))$_4$	2006	24	
16	WD[c]	monomer	mono	α_2- P$_2$W$_{17}$Ti	1997	36	
17	WD	monomer	mono	αP$_2$W$_{17}$TiCp*#	1986	29	
18	WD	monomer	mono	α_2- P$_2$W$_{17}$(TiO$_2$)	1997	36	
19	WD	monomer	tri	α-P$_2$W$_{15}$Ti$_3$*	1997	36	
20	WD	monomer	tri	P$_2$W$_{15}$(TiO$_2$)$_3$ (OH)$_3$	2004	37	9
21	WD	dimer	mono	(P$_2$W$_{15}$Ti)$_2$	2003,2007	38,39	12
22	WD	dimer	mono	(α_2- P$_2$W$_{17}$Ti)$_2$	2008	40	
23	WD	tetramer	tri	(P$_2$W$_{15}$Ti$_3$)$_4$	2000 to	22,38	13

					2003	41,42,	
24		monomer	di	$As_2W_{19}Ti_2$	2007	43	15
25	L^d	monomer	mono	$(MeO)TiW_5O_{18}$	1996	44	10

a: Keggin ion
b: one host-two guests system meaning two metal cations in one vacant site
c: Wells-Dawson ion
d: Lindqvist ion
*: structures based on IR and NMR (no XRD data)
#: Cp is cyclopentadiene
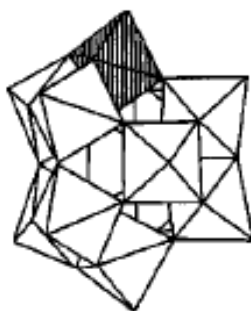
Fig. 1.7 Polyhedral representation of **"$PW_{11}Ti$"**
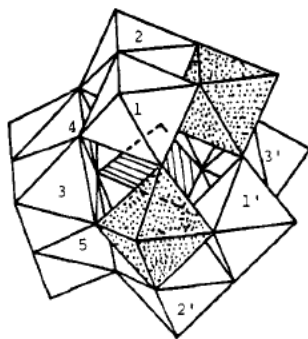
Fig. 1.8 Polyhedral representation of **"$PW_{10}Ti_2$"**
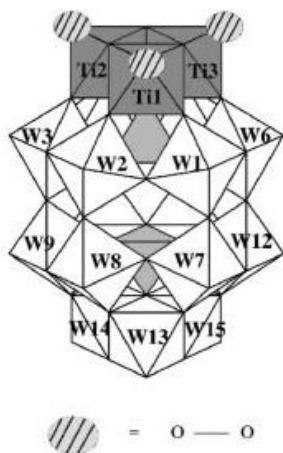
Fig. 1.9 Polyhedral representation of "$P_2W_{15}(TiO_2)_3(OH)_3$"

Despite of what is mentioned above; monomeric Ti-substituted polyoxoanions still exist in literature, such as the monosubstituted monomeric Keggin $[PW_{11}TiO_{40}]^{5-}$ (entry 1) first reported in 1983 by Domaille and Knoth[25] and the monolacunary Lindqvist functionalized by a methoxy titanium group (entry 25) (Fig. 1.10).
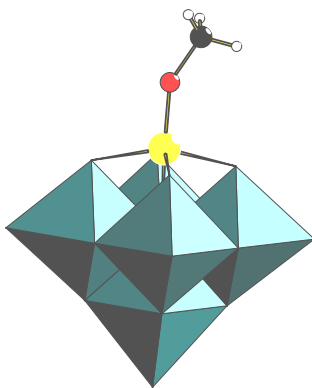
Fig. 1.10 Polyhedral representation of the Linqvist structure $[(MeO)TiW_5O_{18}]^{3-}$

Kholdeeva *et al.* [45], however, reported on the tendency of the monomer to dimerize $[(PW_{11}TiO_{39})_2OH]^{7-}$ in acetonitrile solution upon increase in acidity. According to the scheme proposed, the formation of the dimer occurs after protonation of the monomer $PTiW_{11}O_{40}$ at the terminal Ti=O site, where this oxygen supposedly is the most basic. Then, two protonated molecules $HPTiW_{11}O_{40}$ react to give the dimer.

Another example of a monomer is the monosubstituted Wells-Dawson structure $[\alpha_2\text{-}P_2W_{17}TiO_{62}]^{8-}$ (entry 16) and its peroxo analogue[36] $[\alpha_2\text{-}P_2W_{17}(TiO_2)O_{61}]^{8-}$ which was synthesized same way but with drop wise addition of H_2O_2 at the end. The peroxo metal substituents have higher activity and selectivity in catalytic oxidation reactions than the corresponding POMs.

$[\{Ti(OH)(ox)\}_2(\mu\text{-}O)(\alpha\text{-}PW_{11}O_{39})]^{7-}$ showed in Fig. 1.11 (entry 14) (18) is another example of a monomer. However, this structure involves the combination of one host, the monolacunary Keggin (α-$PW_{11}O_{39}$), and two guests, the titanium metal centers. The compound was found to be stable under acidic conditions of less than pH 1.5. Expectedly, the isolated μ_2-O Ti-O-Ti site showed a significant influence on the catalytic activity for H_2O_2-oxidation reactions in a study dedicated to this purpose.[23]
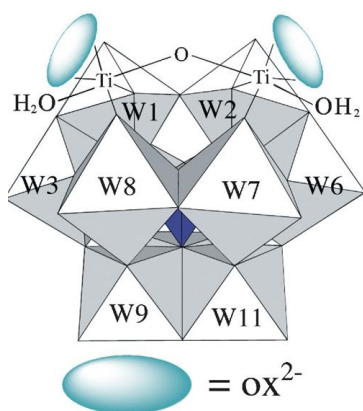
Fig. 1.11 Polyhedral representation of $[\{Ti(OH)(ox)\}_2(\mu\text{-}O)(\alpha\text{-}PW_{11}O_{39})]^{7-}$ where ox^{2-} is the oxalate anion $C_2O_4^{2-}$

The four structures reported by Kortz group (entries 13, 21, 23 and 24) were all oligomers, a dimer $[(TiP_2W_{15}O_{55}OH)_2]^{14-}$ (Fig. 1.12) and a tetramer $[\{Ti_3P_2W_{15}O_{57.5}(OH)_3\}_4]^{24-}$ (Fig. 1.13) with the trilacunary $[P_2W_{15}O_{56}]^{12-}$ were published in 2003.[38] The dimer is linked via two Ti(IV) ions, while in the tetramer, each trilacunary Wells-Dawson is trisubstituted with titanium and the four units are fused together forming a $Ti_{12}O_{46}$ core inside, the highest Ti-content in POMs known to date.
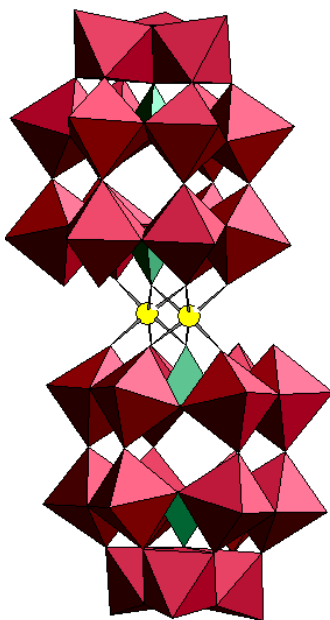
Fig. 1.12 Polyhedral representation of $[(TiP_2W_{15}O_{55}OH)_2]^{14-}$ dimer, color code: WO_6 octahedra (red), PO_4 tetrahedra (green), titanium (yellow), oxygen (red balls)
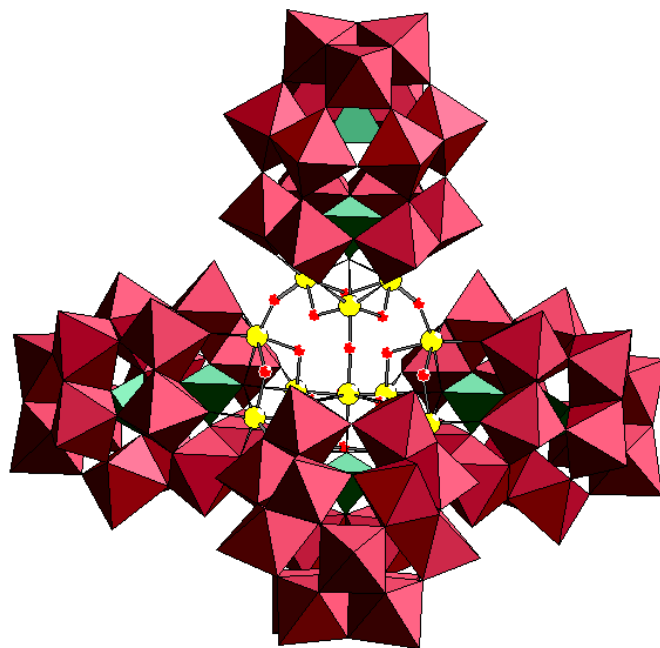
Fig. 1.13 Polyhedral representation of $[\{Ti_3P_2W_{15}O_{57.5}(OH)_3\}_4]^{24-}$ tetramer, color code: WO_6 octahedra (red), PO_4 tetrahedra (green), titanium (yellow), oxygen (red balls)

In 2004, the $[\{\beta\text{-}Ti_2SiW_{10}O_{39}\}_4]^{24-}$ (Fig. 1.14) cyclic tetramer was reported, it is formed by interaction of the solid $TiO(SO_4)$ with the dilacunary Keggin $[\gamma\text{-}SiW_{10}O_{36}]^{8-}$ which undergoes rotation to form the β-isomer.[35]

And lately, the new structure of $[Ti_2(OH)_2As_2W_{19}O_{67}(H_2O)]^{8-}$ (Fig. 1.15) was reported and characterized in the solid state by single-crystal XRD, IR, elemental analysis and TGA. Solution studies involving UV-spectrophotometry and electrochemistry were also performed in addition to a study on the cyclohexene system having the tetra-butyl ammonium TBA salt of the anion as an oxidation catalyst,[43] followed by a more detailed study concerning the influence of the proton content of this catalyst over its performance.[46]
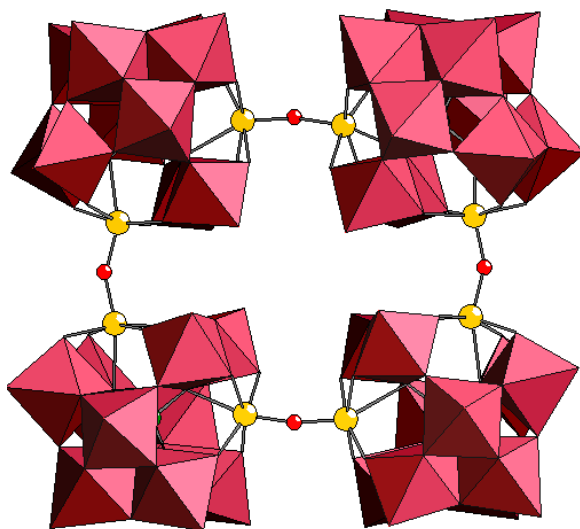
Fig. 1.14 Polyhedral representation of [{ß-Ti$_2$SiW$_{10}$O$_{39}$}$_4$]$^{24-}$, ·, color code: WO$_6$ octahedra (red), titanium (yellow), oxygen (red balls)
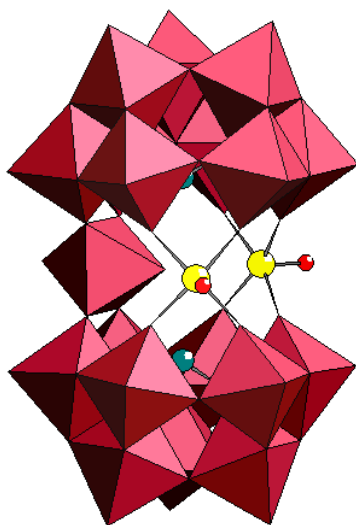
Fig. 1.15 Polyhedral representation of [Ti$_2$(OH)$_2$As$_2$W$_{19}$O$_{67}$ (H$_2$O)]$^{8-}$, color code: WO$_6$ octahedra (red), titanium (yellow), arsenic (green), oxygen (red balls)

This polyanion is consisted of two (B-α-$As^{III}W_9O_{33}$) Keggin moieties with an octahedral {WO_5 (H_2O)} fragment and two square-pyramidal {$TiO_4(OH)$} groups in the belt in a sandwich type structure. The special feature about this compound is that it is arranged in a way that no conventional Ti-O-Ti bonding is involved, but rather two terminal OH groups are pointing out to the same side of the molecule. These can actually be viewed as reactive sites that can enhance the catalytic efficiency; as was illustrated by the high activity in H_2O_2-based cyclohexene oxidation to form the epoxide mainly and the trans-diol, the products typical of a heterolytic oxidation mechanism.

1.8 Zr,Hf-containing polyoxotungstates

The exploration of the interaction between lacunary polyoxotungstates and group 4 (Ti, Zr and Hf) transition metal ions has been mainly driven by the fact that potential products may serve as oxidation catalysts or even as soluble molecular analogues of known Ti and Zr-containing heterogeneous catalysts. Bearing in mind that zirconium(IV) and hafnium(IV) can have coordination numbers larger than titanium(IV), the chemistries of the latter and its heavier congeners are expected to be different, leading to different structural assemblies. This can be illustrated through an example of the two structures resulting from the interaction of the trilacunary {PW_9} with Ti and Zr respectively. Fig. 1.16 shows that Ti (right) manages to replace the missing W perfectly thus forming {$P_2W_{18}Ti_6$} dimer while Zr (left) is too big to fit in the lacuna so the three Zr atoms act as a linker between the two units thus forming {$P_2W_{18}Zr_3$}.
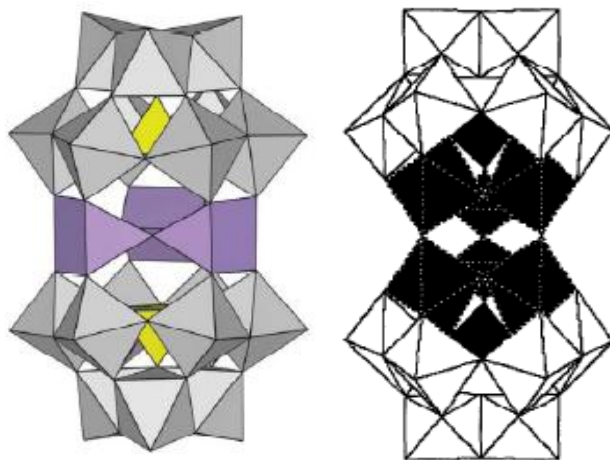
Fig. 1.16 Polyhedral representation of two compounds {$P_2W_{18}Ti_6$}(right) and{$P_2W_{18}Zr_3$}(left) showing the different geometries and assemblies formed by the two elements Ti and Zr.

There are significantly fewer reports in the literature on Zr/Hf-POMs than Ti-POMs, and the former can be classified according to the composing lacunary POM fragments as follows: Keggin type ($[PW_{11}O_{39}]^{7-}$, $[\beta\text{-}SiW_{10}O_{37}]^{10-}$, $[\gamma\text{-}SiW_{10}O_{36}]^{n-}$, $[PW_9O_{34}]^{9-}$ and $[SiW_9O_{34}]^{10-}$), Wells-Dawson type ($[\alpha_2\text{-}P_2W_{17}O_{61}]^{10-}$, $[P_2W_{16}O_{59}]^{12}$ and $[P_2W_{15}O_{56}]^{12-}$),and Lindqvist type ($[W_5O_{18}]^{6-}$). In addition, the unique, asymmetric structure $[Zr_2(\mu\text{-}OH)(H_2O)_2(AsOH)_2(AsW_7O_{28})(AsW_{10}O_{36})]^{9-}$ has resulted from reaction of $[NaAs^{III}_4W_{40}O_{140}]^{27-}$ with Zr^{IV} ions, and does not belong to any of the above mentioned classes.[47] Details of a number of published compounds are listed in Table 1.2.

Table 1.2 Details of a number of Zr,Hf-Polyoxotungstates published

	Type	Structure	-lacunary	Shorthand-Formula	Year	Ref
1	K	monomer	mono	$Hf(\alpha\text{-}PW_{11})$	2007	48
2	K[a]	dimer	mono	$Zr(\alpha\text{-}PW_{11})_2$	2006	49
3	K	dimer	mono	$Hf(\alpha\text{-}PW_{11})_2$	2007	50,51
4	K	dimer	mono	$[(\alpha\text{-}PW_{11}Zr(\mu\text{-}OH)]_2$	2006	52
5	K	dimer	di	$[\gamma\text{-}SiW_{10}Zr(\mu\text{-}OH)]_2$	2007	53
6	K	dimer	di	$(\gamma\text{-}SiW_{10})M_2$, M=Zr, Hf	2007	54
7	K	dimer	di	$(\gamma\text{-}SiW_{10})_2M_4$, M=Zr, Hf	2007	54
8	K	dimer	di	$(\beta\text{-}SiW_{10})_2Zr_4$	2006	55
9	K	trimer	di	$(\beta\text{-}SiW_{10})_3Zr_6$	2006	55
10	K	trimer	di	$(\gamma\text{-}SiW_{10})_3Zr_6(O_2)_6$	2008	56
11	K	dimer	tri	$(A\text{-}\beta\text{-}SiW_9)_2Zr_3$	1989	57
12	K	dimer	tri	$(A\text{-}\alpha\text{-}PW_9)_2M_3$, M=Zr,Hf	2009	58
13	WD[b]	monomer	mono	$Hf(\alpha_1\text{-}P_2W_{17})$	2007	48
14	WD[b]	dimer	mono	$Zr(\alpha_2\text{-}P_2W_{17})_2$	2006	49
15	WD	dimer	mono	$Hf(\alpha_2\text{-}P_2W_{17})_2$	2007	50
16	L[c]	dimer	mono	$[(\mu\text{-}OH)ZrW_5O_{18}]_2$	1984,2004	59,60
17	L[c]	dimer	mono	$[(\mu\text{-}MeO)ZrW_5O_{18}]_2$	2007	61

a: Keggin ion
b: Wells-Dawson ion
c: Lindqvist ion

1.9 Ti, Zr, Hf-POMs in catalysis

It is well established that the high catalytic activity of titanium/zirconium containing micro- and meso-porous materials in the H_2O_2-based oxidation of a wide variety of organic compounds is mainly attributed to the site-isolated titanium/zirconium species. The mechanistic details are yet obscure and the structure-catalytic activity relations remain unraveled. The oxidation resistant Ti-POMs came to serve as convenient models of the heterogeneous catalysts. In this context, most of the early work done by Kholdeeva concentrated on the titanium monosubstituted Keggin ions system[45,62,63,64] in H_2O_2 oxidation reactions; each POM unit with one titanium center adequately resembles a fragment of the extended titanium silicate lattice that can act homogeneously in organic media. Zr-POMs on the other hand can be viewed as potential models for the well known zirconia supported tungsten catalysts. These are environmentally friendly promising candidates for the replacement of the chlorinated $AlCl_3/HCl$ acid catalysts used for skeletal isomerization of light n-alkanes.[59]

The substrates Kholdeeva worked on were mainly thioethers (methyl phenyl sulfide and methyl p-tolyl sulfide), cycloalkenes and trimethyl phenol. The TBA-salt of the Ti-monosubstituted Keggin POM ($PTiW_{11}O_{40}^{5-}$) **1** was studied in the beginning; it was found that the way of preparation of the TBA salt of this anion has a big impact on the catalytic results which led to a close inspection of the structural differences. The TBA salts used were only different in their proton content, a result that had big implications to the indispensible role that protons play in the process. Similar to the titanium silicate catalyzed reactions, adding acid enhanced the catalytic activity while the addition of base had a negative effect. Thus another evidence of the resemblance between TM-POMs and their respective TM-oxides was provided.[65] The non-protonated took a few days to form a peroxo complex **I**

$[PW_{11}(TiO_2)O_{39}]^{5-}$ while the protonated TBA-salt readily converted in a few hours to a colored peroxo complex **II** $[PW_{11}(TiOOH)O_{39}]^{4-}$ upon addition of 30-fold molar excess of 77% H_2O_2; as distinguished from the ^{31}P-NMR signals taken for both. The oxidation of the thioether proceeded more quickly when **II** is formed.

In a later study[45] in 2000, the pH-dependent interconversion in MeCN between **1** and **H2** $[(PTiW_{11}O_{39})_2OH]^{7-}$ the corresponding protonated form of the dimer (Fig. 1.17) was investigated thoroughly. The dimer tends to hydrolyze to give the monomer when the amount of water is sufficient, and thus the relative concentrations of **1**, its conjugate acid **H1** $[P(TiOH)W_{11}O_{39}]^{4-}$,**H2** and its conjugate base **2** $[(PTiW_{11}O_{39})_2O]^{8-}$ depend on both the concentration of H^+ and H_2O. Furthermore, the presence of water is highly crucial in the case of the dimeric species since they need to hydrolyze first before they form the hydro-peroxo active complex. The catalytic activity of these Ti-POM species was found to be in this sequence: **H2>H1>2>1**. It was confirmed again that the rate of thioether oxidation with H_2O_2 correlates with the rate of H_2O_2 decomposition by the catalyst or in other words the rate of formation of the peroxo-titanium complex that has to be protonated in order to show activity.
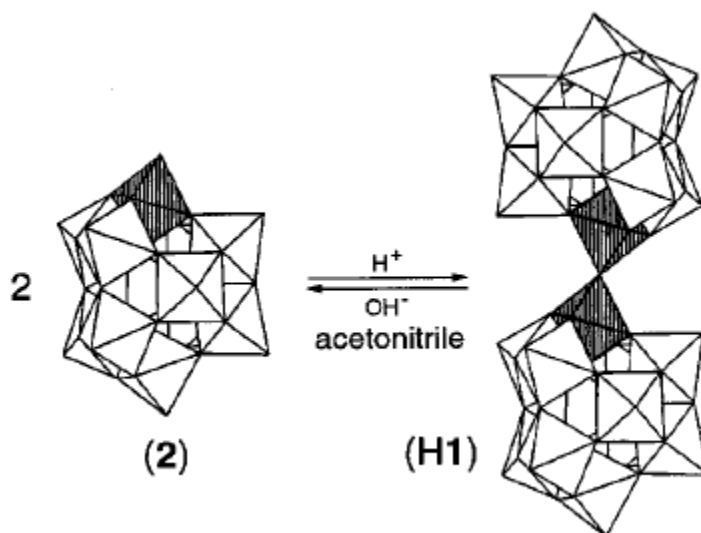
Fig. 1.17 The pH-dependent monomer-dimer interconversion

In an attempt to correlate between these findings and the behavior of titanium oxide heterogeneous catalysts, another study was published in 2001.[64] The outcome was two main points: 1) the formation of the titanyl groups (Ti=O), the so called extra framework titanium in titanium silicates, should be avoided since the Ti=O bond reacts much more slowly with the hydrogen peroxide and 2) the increase in the concentration of titanium in titanium silicates causes a drop in the catalytic performance and that is probably due to the formation of the Ti-O-Ti bond that reacts much more slowly with hydrogen peroxide than the Ti-OH or the Ti-O-Si bonds.

Lately in 2007[62], Kholdeeva *et al.* took a deeper look at the mechanism of oxidation of more than an organic substrate with the presence of Ti/Zr-POMs as catalysts. It was revealed that the active titanium peroxo species **II** mentioned above reacts with organic substrates via homolytic oxidation mechanisms. However when the amount of protons in the Ti-POM increases from 1 to 2 per Ti atom the reaction mechanism changes from homolytic to heterolytic and the nature of the products of the reaction change

consequently. For example, for cyclohexene oxidation, increasing the number of protons from 1 to 2 in the Ti-POM manifests in increasing yield of the diol product at the expense of one-electron oxidation products, the en-ol and the en-one (Fig. 1.18). The study showed that the presence of acid protons is essential also for the activity of Zr catalysts; they however differ from the Ti catalysts in a way that they only operate through homolytic oxidation mechanisms and the Zr-O-Zr bond is resistant to aqueous hydrolysis without the assistance of acid protons, unlike the Ti-O-Ti bond which easily reacts with water to form the reactive Ti-OH species. Same conclusions were drawn in an earlier study by the same group on Zr(IV)-monosubstituted Keggin type dimeric POMs (entry 3 in Table 1.2).[52]
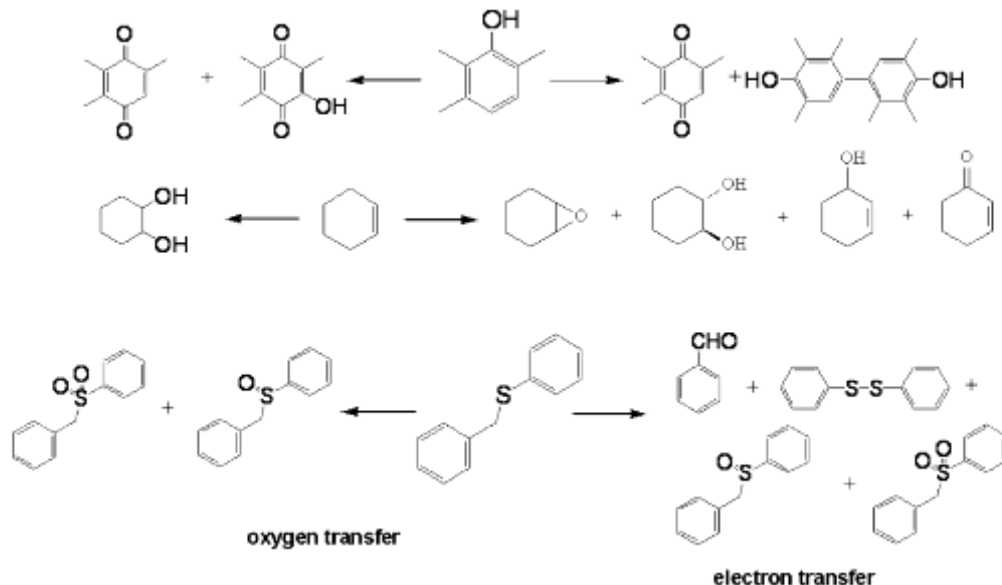
Fig. 1.18 Three substrates with the homolytic oxidation products to the right and the heterolytic oxidation products to the left

Likewise, the TBA salt of $[Ti_2(OH)_2As_2W_{19}O_{67}(H_2O)]^{8-}$ showed a high catalytic activity in H_2O_2-based cyclohexene oxidation in a collaborative study between our group and Kholdeeva's.[43] The main products were the epoxide and *trans*-cyclohexane diol, those typical for a heterolytic oxidation mechanism (Fig. 1.18). The high activity was interpreted based on the unprecedented structure of the molecule where the vicinity of the two Ti-OH groups most likely favors the formation of the diprotonated peroxo-titanium POM species capable of oxygen atom transfer to alkenes. The catalyst was once again looked at in more detail in a study published in 2009 [46], where the selectivity in alkene oxidation revealed marked dependence on the proton content in the cationic part of the catalyst which can be controlled by the pH of precipitation of the TBA salt of the $Ti_2(OH)_2As_2W_{19}O_{67}(H_2O)]^{8-}$ anion.

After the facts about Ti-POMs briefed above were established, another group, Nomiya *et al.* showed interest in similar systematic catalytic studies. In 2007, the interaction between H_2O_2 and the titanium di-substituted Keggin ion $[PW_{10}Ti_2O_{40}]^{7-}$ was assessed. [28] The latter was derived from the corresponding anhydrous dimer $[\alpha\text{-}1,2\text{-}PW_{10}Ti_2O_{39}]_2.18H_2O$ (Fig. 1.19) by hydrolytic cleavage in the very same way the titanium mono-substituted dimer hydrolyzes to give the monomer as mentioned earlier. The interaction ended in an orange solution, this solution, when precipitated with MeOH gave a thermally stable yellow species, while when re-precipitated with EtOH yielded a relatively stable orange compound. Each was collected as a pure powder and then later tested for the ability to oxidize 2-propanol. The orange species was able to transform 2-propanol to acetone detected by ^{1}H NMR while the yellow was not. These results were a clear indication that the orange is the hydroperoxo $K_5[\alpha\text{-}1,2\text{-}PW_{10}(TiOOH)_2O_{38}].5H_2O$ while the yellow is the inactive peroxo complex $K_7[\alpha\text{-}1,2\text{-}PW_{10}(TiO_2)_2O_{38}].8H_2O$.
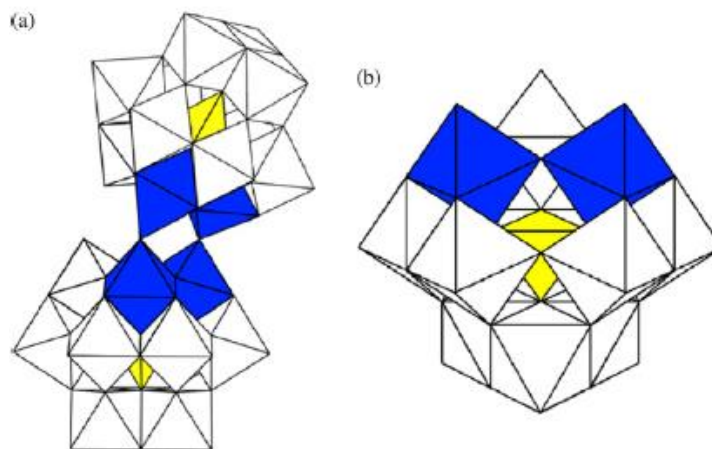
Fig. 1.19 Polyhedral representations of: a) the $[\alpha\text{-}1,2\text{-}PW_{10}Ti_2O_{39}]_2$ dimer and b) the monomer $[PW_{10}Ti_2O_{40}]^{7-}$

Other results were published in 2005 [66] concerning the influence of structures around titanium centers in dimeric mono-, di-, and tri-titanium substituted Keggin polyoxotungstates (Fig. 1.20) on the catalytic efficiency in alkenes epoxidation. Later in 2007 [67], the three structures were compared to the novel 1host-2guest POM mentioned earlier (Fig. 1.11). In summary, there was a non-linear increase in activity with the increase in titanium atoms. The tri-Ti containing $[(\alpha\text{-}1,2,3\text{-}PTi_3W_9O_{37})_2O_3]^{12-}$ exhibited the fastest rate of formation of the active hydroperoxo species facilitated by the intramolecular transfer of protons bound to the surface edge sharing oxygens. And thus it also showed the highest turnover frequency of the epoxidation of alkenes. In comparison, the 1host-2guest was considerably more active than the three dimers showing that it is more about structure rather than titanium content where the μ_2-O Ti-O-Ti site had obviously the significant influence.
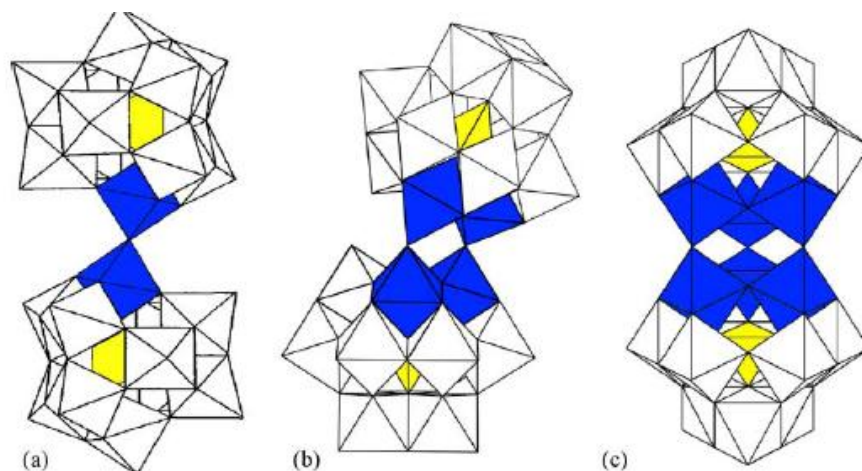
Fig. 1.20 Polyhedral representation of dimeric, Ti–O–Ti bridging forms of (a) $[(PTiW_{11}O_{39})_2O]^{8-}$ b) $[\alpha\text{-}1,2\text{-}PW_{10}Ti_2O_{39}]_2$ c) $[(\alpha\text{-}1,2,3\text{-}PTi_3W_9O_{37})_2O_3]^{12-}$

Zr2, **Hf2**, **Zr4** and **Hf4** are dimeric compounds formed via the reaction of $K_8[\gamma\text{-}SiW_{10}O_{36}]$ with $ZrOCl_2$ and $HfOCl_2$ in the corresponding molar ratios (entries 5 and 6 in Table 1.2). The tetranuclear zirconium and hafnium species **Zr4** and **Hf4** showed high catalytic activity towards the intramolecular cyclization of (+)-citronellal whereas the dinuclear clusters **Zr2** and **Hf2** were almost inactive. **Zr4** and **Hf4** activity was found to be a result of the Lewis acid rather than Brønsted acid sites.[54]

TBA salts of the Hf-containing Keggin and Wells-Dawson monomeric species (entries 1 and 13 in Table 1.2) were also tested in Lewis acid mediated organic reactions such as Mukaiyama aldol and Mannich-type additions. These reactions were made possible due to the enhanced Lewis acidity in the Hf complexes in comparison with the lanthanide-containing analogues.[48]

1.10 References

[1] Pope, M. T. *Heteropoly and isopoly oxometalates;* Springer-Verlag: Berlin ; New York, 1983.

[2] Kozhevnikov, I. *Catalysis by polyoxometalates;* J. Wiley:Chichester, West Sussex, 2002.

[3] Baker, L. C. W.; Glick, D. C. *Chem. Rev.* **1998,** 98, 3.

[4] Moffat, J. B. *Metal-oxygen clusters the surface and catalytic properties of heteropoly oxometalates;* Kluwer Academic/Plenum Publ: New York, NY u.a., 2001.

[5] Kozhevnikov, I. V. *Chem. Rev.* **1998,** 98, 171.

[6] Mizuno, N.; Misono, M. *Chem. Rev.* **1998,** 98, 199.

[7] Pope, M. T.; mueller, A. *Angew. Chem. Int. Ed. Engl.* **1991,** 30, 34.

[8] Keggin, J. F. *Nature* **1933,** 131, 908.

[9] Ginsberg, A. P. *Inorganic syntheses.Volume 27;* Wiley:New York, 1990 *(Chapter III: Early Transition Metal Polyoxoanions).*

[10] Pope, M. T. *Polyoxometalates: from platonic solids to anti-retroviral activity [workshop held at the Center for Interdisciplinary Research at the University of Bielefeld, July 15 - 17, 1992];* Kluwer Academic Publishers: Dordrecht u.a., 1994.

[11] Misono, M. *Catal. Rev. Sci. Eng.* **1987,** 29, 269.

[12] Misono, M. *Catal. Rev. Sci. Eng.* **1988,** 30, 339.

[13] Okuhara, T.;Mizuno, N.;Misono, M. *Adv. Catal.* **1996,** 41, 113.

[14] Kozhevnikov, I. V.; Matveev, K. I. *Russ. Chem. Rev.* **1978,** 47, 1231.

[15] Neumann, R.; Lissel, M. *J. Org. Chem.* **1989,** 54, 4607.

[16] Neumann, R.; Levin, M. *J. Org. Chem.* **1991,** 56, 5707.

[17] Lissel, M.; Jansen in de Wal, H.; Neumann, R. *Tetrahedron Lett.* 33, 1795.

[18] Venturello, C.; Daloisio, R.; Bart, J. C. J.; Ricci, M. *Journal of Molecular Catalysis* **1985,** 32, 107.

[19] Kholdeeva, O. A. *Topics in Catalysis* **2006,** 40, 229.

[20] Nomiya, K.;Arai, Y.;Shimizu, Y.;Takahashi, M.;Takayama, T.;Weiner, H.;Nagata, T.;Widegren, J. A.;Finke, R. G. *Inorg. Chim. Acta* **2000,** 300, 285.

[21] Nomiya, K.;Takahashi, M.;Widegren, J. A.;Aizawa, T.;Sakai, Y.;Kasuga, N. C. *Journal of the Chemical Society-Dalton Transactions* **2002,** 3679.

[22] Sakai, Y.;Yoza, K.;Kato, C. N.;Nomiya, K. *Dalton Transactions* **2003,** 3581.

[23] Hayashi, K.;Takahashi, M.;Nomiya, K. *Dalton Transactions* **2005,** 3751.

[24] Hayashi, K.;Murakami, H.;Nomiya, K. *Inorg. Chem.* **2006,** 45, 8078.

[25] Knoth, W. H.;Domaille, P. J.;Roe, D. C. *Inorg. Chem.* **1983,** 22, 198.

[26] Yamase, T.;Ozeki, T.;Motomura, S. *Bull. Chem. Soc. Jpn.* **1992,** 65, 1453.

[27] Domaille, P. J.; Knoth, W. H. *Inorg.Chem.* **1983,** 22, 818.

[28] Hayashi, K.;Kato, C. N.;Shinohara, A.;Sakai, Y.;Nomiya, K. *Journal of Molecular Catalysis A-Chemical* **2007,** 262, 30.

[29] Keana, J. F. W.; Ogan, M. D. *J. Am. Chem. Soc.* **1986,** 108, 7951.

[30] Wang, X. H.;Liu, J. F.;Chen, Y. G.;Liu, Q.;Liu, J. T.;Pope, M. T. *Journal of the Chemical Society-Dalton Transactions* **2000,** 1139.

[31] Tan, R. X.;Li, D. L.;Wu, H. B.;Zhang, C. L.;Wang, X. H. *Inorganic Chemistry Communications* **2008,** 11, 835.

[32] Nomiya, K.;Takahashi, M.;Ohsawa, K.;Widegren, J. A. *Journal of the Chemical Society-Dalton Transactions* **2001,** 2872.

[33] Lin, Y.;Weakley, T. J. R.;Rapko, B.;Finke, R. G. *Inorg. Chem.* **1993,** 32, 5095.

[34] Yamase, T.;Ozeki, T.;Sakamoto, H.;Nishiya, S.;Yamamoto, A. *Bull. Chem. Soc. Jpn.* **1993,** 66, 103.

[35] Hussain, F.;Bassil, B. S.;Bi, L. H.;Reicke, M.;Kortz, U. *Angewandte Chemie-International Edition* **2004,** 43, 3485.

[36] Qu, L. Y.;Shan, Q. J.;Gong, J.;Lu, R. Q.;Wang, D. R. *Journal of the Chemical Society-Dalton Transactions* **1997,** 4525.

[37] Sakai, Y.;Kitakoga, Y.;Hayashi, K.;Yoza, K.;Nomiya, K. *European Journal of Inorganic Chemistry* **2004,** 4646.

[38] Kortz, U.;Hamzeh, S. S.;Nasser, N. A. *Chemistry-a European Journal* **2003,** 9, 2945.

[39] Murakami, H.;Hayashi, K.;Tsukada, I.;Hasegawa, T.;Yoshida, S.;Miyano, R.;Kato, C. N.;Nomiya, K. *Bull.Chem.Soc.Jpn.* **2007,** 80, 2161.

[40] Yoshida, S.;Murakami, H.;Sakai, Y.;Nomiya, K. *Dalton Transactions* **2008,** 4630.

[41] Sakai, Y.;Yoza, K.;Kato, C. N.;Nomiya, K. *Chemistry-a European Journal* **2003,** 9, 4077.

[42] Sakai, Y.;Yoshida, S.;Hasegawa, T.;Murakami, H.;Nomiya, K. *Bull. Chem. Soc. Jpn.* **2007,** 80, 1965.

[43] Hussain, F.;Bassil, B. S.;Kortz, U.;Kholdeeva, O. A.;Timofeeva, M. N.;de Oliveira, P.;Keita, B.;Nadjo, L. *Chemistry-a European Journal* **2007,** 13, 4733.

[44] Clegg, W.;Elsegood, M. R. J.;Errington, R. J.;Havelock, J. *Journal of the Chemical Society-Dalton Transactions* **1996,** 681.

[45] Kholdeeva, O. A.;Maksimov, G. M.;Maksimovskaya, R. I.;Kovaleva, L. A.;Fedotov, M. A.;Grigoriev, V. A.;Hill, C. L. *Inorg. Chem.* **2000,** 39, 3828.

[46] Kholdeeva, O. A.;Donoeva, B. G.;Trubitsina, T. A.;Al-Kadamany, G.;Kortz, U. *European Journal of Inorganic Chemistry* **2009,** 5134.

[47] Gaunt, A. J.;May, J.;Collison, D.;Helliwell, M. *Acta Crystallographica Section C-Crystal Structure Communications* **2003,** 59, I65.

[48] Boglio, C.;Micoine, K.;Remy, P.;Hasenknopf, B.;Thorimbert, S.;Lacote, E.;Malacria, M.;Afonso, C.;Tabet, J. C. *Chemistry-a European Journal* **2007,** 13, 5426.

[49] Kato, C. N.;Shinohara, A.;Hayashi, K.;Nomiya, K. *Inorg. Chem.* **2006,** 45, 8108.

[50] Sokolov, M. N.;Chubarova, E. V.;Peresypkina, E. V.;Virovets, A. V.;Fedin, V. P. *Russian Chemical Bulletin* **2007,** 56, 220.

[51] Hou, Y.;Fang, X.;Hill, C. L. *Chemistry-a European Journal* **2007,** 13, 9442.

[52] Kholdeeva, O. A.;Maksimov, G. M.;Maksimovskaya, R. I.;Vanina, M. P.;Trubitsina, T. A.;Naumov, D. Y.;Kolesov, B. A.;Antonova, N. S.;Carbo, J. J.;Poblet, J. M. *Inorg. Chem.* **2006,** 45, 7224.

[53] Yamaguchi, S.;Kikukawa, Y.;Tsuchida, K.;Nakagawa, Y.;Uehara, K.;Yamaguchi, K.;Mizuno, N. *Inorg. Chem.* **2007,** 46, 8502.

[54] Bassil, B. S.;Dickman, M. H.;Kortz, U. *Inorg. Chem.* **2006,** 45, 2394.

[55] Kikukawa, Y.;Yamaguchi, S.;Tsuchida, K.;Nakagawa, Y.;Uehara, K.;Yamaguchi, K.;Mizuno, N. *J. Am. Chem. Soc.* **2008,** 130, 5472.

[56] Bassil, B. S.;Mal, S. S.;Dickman, M. H.;Kortz, U.;Oelrich, H.;Walder, L. *J. Am. Chem. Soc.* **2008,** 130, 6696.

[57] Finke, R. G.;Rapko, B.;Weakley, T. J. R. *Inorg. Chem.* **1989,** 28, 1573.

[58] Saku, Y.;Sakai, Y.;Shinohara, A.;Hayashi, K.;Yoshida, S.;Kato, C. N.;Yozac, K.;Nomiya, K. *Dalton Transactions* **2009,** 805.

[59] Villanneau, R.;Carabineiro, H.;Carrier, X.;Thouvenot, R.;Herson, P.;Lemos, F.;Ribeiro, F. R.;Che, M. *J Phys Chem B* **2004,** 108, 12465.

[60] Chauveau, F.;Eberle, J.;Lefebvre, J. *Nouveau Journal De Chimie-New Journal of Chemistry* **1985,** 9, 315.

[61] Errington, R. J.;Petkar, S. S.;Middleton, P. S.;McFarlane, W. *J. Am. Chem. Soc.* **2007,** 129, 12181.

[62] Kholdeeva, O. A.; Maksimovskaya, R. I. *Journal of Molecular Catalysis A-Chemical* **2007,** 262, 7.

[63] Kholdeeva, O. A.;Trubitsina, T. A.;Maksimov, G. M.;Golovin, A. V.;Maksimovskaya, R. I. *Inorg. Chem.* **2005,** 44, 1635.

[64] Kholdeeva, O. A.;Maksimovskaya, R. I.;Maksimov, G. M.;Kovaleva, L. A. *Kinetics and Catalysis* **2001,** 42, 217.

[65] Kholdeeva, O. A.;Maksimov, G. M.;Maksimovskaya, R. I.;Kovaleva, L. A.;Fedotov, M. A. *Reaction Kinetics and Catalysis Letters* **1999,** 66, 311.

[66] Kato, C. N.;Negishi, S.;Yoshida, K.;Hayashi, K.;Nomiya, K. *Applied Catalysis A-General* **2005,** 292, 97.

[67] Kato, C. N.;Hayashi, K.;Negishi, S.;Nomiya, K. *Journal of Molecular Catalysis A-Chemical* **2007,** 262, 25.

Chapter II

Experimental Details

Characterization of newly synthesized polyoxometalates requires the use of several analytical techniques, the single crystal X-ray diffractometry XRD being the most crucial of them all. The main challenge therefore is to obtain good quality crystals valid for XRD measurement. Infrared spectroscopy FTIR can then supply a "fingerprint" of the compound made showing the typical M-O bond vibration peaks, where M can be the addenda or the heteroatom. Thermogravimetry can provide information on the thermal stability of the compound in the solid state and the amount of crystal waters present.

Stability of POMs in solution is a completely different story where several species tend to exist in equilibrium and Nuclear magnetic resonance spectroscopy NMR, is one of the most commonly applied techniques for such analysis.

In the following sections, there will be a short description of the specific instruments used for the present work.

2.1 Instrumentation

2.1.1 Single crystal X-ray diffractometry

All crystals were mounted in Hampton cryoloops using light oil for data collection at 173 K. Indexing and data collection were performed using a Bruker X8 APEX II CCD diffractometer with κ geometry and Mo Kα radiation (λ=0.71073 Å). Data integration and routine processing were performed using the SAINT software suite. Further data processing, including multiscan absorption corrections, was performed using SADABS.[1] Direct method (SHELXS97) solutions successfully located the W atoms, and successive Fourier syntheses (SHELXL97) revealed the remaining atoms.[2] Refinements were full-matrix least-squares against F^2 using all data. All nondisordered heavy atoms were refined anisotropically, while the O atoms and disordered countercations were refined with fractional occupancies. No H or Li atoms were included in the models.

The degree of refinement is commonly expressed by the R factor, which is a measure of the degree of deviation of the predicted model (calculated) from the scattering amplitudes (observed):

$$R = \Sigma \| F(obs) | - | F(calc) \| / \Sigma | F(obs) |$$

2.1.2 Fourier transform infrared spectroscopy

Infrared spectra were recorded on a Nicolet Avatar 370 FT-IR spectrophotometer as KBr pellets. The following abbreviations were used to assign peak intensities: w: weak; m: medium; s: strong; vs: very strong; b: broad and sh: shoulder.

2.1.3 Thermogravimetry

Thermogravimetric analyses were performed on a Q 600 device from TA instruments for 10-30 mg of sample in alumina pans under 100mL/min nitrogen flow.

2.1.4 Nuclear magnetic resonance spectroscopy

NMR spectra were measured on a JEOL 400 ECP spectrometer operating at 9.39 T (400 MHz for ^{1}H) magnetic field. Chemical shifts were given relative to external standards, 2M solution of Na_2WO_4 in D_2O for ^{183}W-NMR, $Si(CH_3)_4$ in $CDCl_3$ for ^{1}H and ^{13}C-NMR and 10% H_3PO_4 in D_2O for ^{31}P-NMR.

2.2 Synthesis of POM precursors

Synthetic procedures of lacunary POM precursors that served as building blocks for all the compounds presented in this work are detailed in the following sections. They are categorized as trilacunary Keggin, lone-pair containing and hexavacant Wells-Dawson polyanions.

2.2.1 Trilacunary Keggin POM precursors

2.2.1.1 *Na$_{10}$[A-α-GeW$_9$O$_{34}$].23H$_2$O*

12 g of Na_2GeO_3 were dissolved in 200 mL of water, 182 g of $Na_2WO_4.2H_2O$ were then added. 130 mL of 6M HCl solution were added to the stirred solution, which was then boiled for 1hr until the final volume decreases to 300 mL. A solution of sodium carbonate (50 g of anhydrous Na_2CO_3 in 50 mL

water) was added, a white solid formed slowly and was then filtered off. For purification, the precipitate was stirred in 1 L of 4M NaCl solution, filtered again and air dried.[3]

2.2.1.2 $Na_9[A-\alpha-PW_9O_{34}].7H_2O$

120 g of $Na_2WO_4.2H_2O$ were dissolved in 150 g of water, 4 mL H_3PO_4 (85%) were then added dropwise while stirring. pH of the solution was then ~9. 22.5 mL of glacial acetic acid were added with vigorous stirring. Large quantities of white precipitate were formed during the addition. The final pH was 7.8, the solution was stirred for 1hr and the precipitate thus formed was filtered and air dried.[4]

2.2.2 Lone pair containing POM precursors

2.2.2.1 $Na_9[B-\alpha-AsW_9O_{33}].27H_2O$

11 g of As_2O_3 were added to a hot solution of 330 g $Na_2WO_4.2H_2O$ in 350 mL water. 83 mL of 11M HCl solution were added with vigorous stirring for 2 minutes. The resulting solution was then heated at 95°C for 10 minutes. The product was left to crystallize overnight, collected by filtration and air dried.[5]

2.2.2.2 $Na_9[B-\alpha-SbW_9O_{33}].27H_2O$

To a boiling solution of 40 g of $Na_2WO_4.2H_2O$ in 80 mL water, another solution of 1.96 g of Sb_2O_3 in 10 mL concentrated HCl (may or may not dissolve completely) was added dropwise. The resulting solution was refluxed for 1hr, cooled down. Crystals appeared almost immediately but the total

amount of product was collected after the solution reached the level of the crystals.[6]

2.2.2.3 *Na_9[B-α-BiW_9O_33].16H_2O*

To a hot solution (80°C) of 40 g of $Na_2WO_4.2H_2O$ in 80 mL water, another solution of 6.5 g of $Bi(NO_3)_3$ in 10 mL 6M HCl was added dropwise. The resulting solution was kept at 80°C for 1hr and then filtered off. The product was obtained upon slow evaporation.[7]

2.2.3 Hexavacant Wells-Dawson precursors

The hexavacant Wells-Dawson polyanion $K_{12}[α-H_2P_2W_{12}O_{48}].24H_2O$ is normally prepared from the plenary Wells-Dawson $K_6[α-$ or $β- P_2W_{18}O_{62}]$. The synthetic procedures of both are herein described.

2.2.3.1 *K_6[α-P_2W_18O_62]. 20H_2O*

A sample of $Na_2WO_4.2H_2O$ (300 g; 0.91 mol) dissolved in 350 mL water was acidified by fractional addition of HCl 4M (250 mL) under vigorous stirring. When the solution clears out, H_3PO_4 4M (250 mL) was added slowly. The pale yellow solution was refluxed for at least 24 h, after which the yellow color intensified. This solution was allowed to cool to room temperature and was then treated with 150 g KCl. The precipitate which appeared was filtered off and air-dried. This crude material was dissolved in 650 mL water, and the solution was, eventually, filtered to remove insoluble impurities. The limpid solution was then heated to ~80°C for at least 72 h. The solution was then allowed to cool to room temperature before being placed finally in a refrigerator at 4°C. After a few days, the yellow crystals were collected.[8]

2.2.3.2 $K_{12}[\alpha\text{-}H_2P_2W_{12}O_{48}].24H_2O$

83 g of $K_6[\alpha\text{- or }\beta\text{- }P_2W_{18}O_{62}]$ were dissolved in 300 mL of water. A solution of 48.4 g tris(hydroxymethyl)aminomethane in 200 mL water was then added. The mixture was stirred at room temperature for half an hour, then 80 g of KCl were added. After complete dissolution, another solution of 55.3 g of K_2CO_3 in 200 mL water was added. The solution was vigorously stirred for 15 minutes and the white precipitate that appeared was filtered on a sintered glass frit, and air dried overnight, washed with 50 mL ethanol, dried under suction. The washing process was done twice before the product was left to air dry for a few days.[9]

2.2.4 Eicosatungstodiarsenate Anion, $K_{14}[As_2W_{19}O_{67}(H_2O)].20H_2O$

To 50 mL of water at 80°C, 0.89 g of As_2O_3, 18.8 g of $Na_2WO_4.2H_2O$ and 0.67 g of KCl were added with stirring. After dissolution, the pH was adjusted to 6.3 by adding 12 M HCl solution dropwise. The solution was kept at 80°C for 10 minutes and then filtered. Finally, 15 g of KCl were added and the solution stirred for 15 minutes. The white precipitate was isolated by filtration and dried at 80°C resulting in 15.4 g product.[10]

2.3 References

[1] Sheldrick, G. M. SADABS; University of Göttingen: Göttingen, Germany, 1996.

[2] Sheldrick, G. M. SHELXS-97; University of Göttingen: Göttingen, Germany, 1997.

[3] Herve', G.; Teze', A. *Inorg. Chem.* **1977**, 16, 2115.

[4] Domaille, P. J. *Inorg. Synth.* **1990**, 27, 100.

[5] Kim, K. –C; Gaunt, A.; Pope, M. T. *J. Clust. Sci.* **2002**, 13, 423.

[6] Bösing, M.; Loose, I.; Pohlmann, H.; Krebs, B. *Chem. Eur. J.* **1997**, 3, 1232.

[7] Botar, B.; Yamase, T.; Ishikawa, E. *Inorg. Chem. Commun.* **2000**, 3, 579.

[8] Mbomekalle, I. M.; Lu Y. W.; Keita, B.; Nadjo, L. *Inorg. Chem. Commun.* **2004**, 7, **86.**

[9] Contant, R. *Inorg. Synth.* **1990**, 27, 108.

[10] Kortz, U.; Savelieff M. G.; Bassil, B. *Angew. Chem. Int. Ed.* **2001**, 40, **3384.**

Chapter III

Synthetic Results

This work was mainly focused on the incorporation of group 4 elements namely, titanium, zirconium and hafnium into various polyoxotungstate frameworks. Attempts were only successful with titanium, and the resulting structures are to be described along with the experimental conditions in a separate section each.

3.1 General synthetic approach

Lacunary polyoxotungstates that are deficient in one or more MO_6 octahedra are in most, but not all, cases stable and exist independently. Preparation methods were described in chapter II for the isolation of the precursors used in the synthetic procedures that will be introduced in this chapter. Lacunary POMs are known to act as ligands for electrophiles or metal ions. Binding normally occurs at the oxygens in the vacant sites.

Different titanium precursors were used as a source of Ti^{IV} in solution. These are $TiOCl_2.xHCl$, $TiOSO_4$ and $K_2TiO(C_2O_4)_2$ which are polymeric in nature and $Ti(SO_4)_2$ which is not.

$TiOSO_4.H_2O$ for example does not contain discrete MO^{2+} fragments, but rather contains chains of $-Ti-O-Ti-O-$ with each Ti being approximately octahedrally coordinated to 2 bridging oxygen atoms, 1 water molecule and an oxygen atom from each of three sulfates.[1] Dissolution in water is pH dependent, Ti precursors tend to form the soluble hydroxides and oxides (mainly TiO_2) under basic conditions (pH > 6).

$K_2TiO(C_2O_4)_2$ forms a solid tetrameric structure $K_8[Ti_4O_4(C_2O_4)_8]$ (**K-1**) (**Ti4**) when merely dissolved in water (Fig. 3.1). This appears as colorless crystals upon slow evaporation of water. **Ti4** was very frequently obtained as a by-product in synthesis reactions involving the $K_2TiO(C_2O_4)_2$ precursor. **Ti4** was however collected and used as a Ti^{IV} source itself.
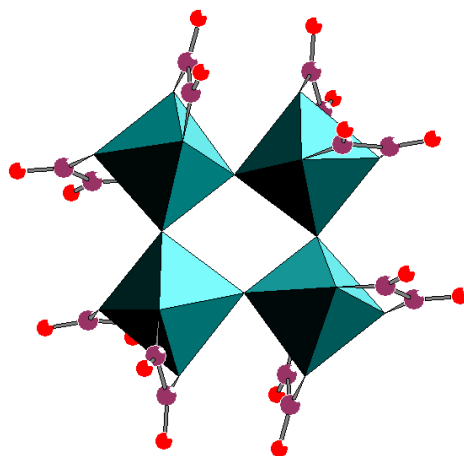
Fig. 3.1 polyhedral representation of $[Ti_4O_4(C_2O_4)_8]^{8-}$, **1**. Color code: TiO_6 octahedra (teal), carbon atoms (violet), oxygen atoms (red)

Due to the comparable sizes of the ionic radii of Ti^{IV} (0.75 Å) and W^{VI} (0.74 Å) and the fact that the coordination number of 6 is the most common for Ti^{IV}, Ti is expected to fit perfectly into the polytungstates framework. The substitution of W^{VI} with Ti^{IV} is particularly interesting because of the enhanced basicity which usually leads to oligomerization through the formation of the Ti-O-Ti bridging bonds.

Titanium has a high tendency to change its coordination in a reaction and it is able to form peroxo species with H_2O_2 without being extracted from its framework. This is what makes Ti-containing molecular sieves among the best catalysts for selective oxidation with H_2O_2. The above established facts were among the most prominent motivations for the synthesis of Ti-

containing POMs. They proved to deserve interest, not only because they serve as adequate probes to study the conventional titanium oxide catalysts or titanium silicates, but also because they, themselves show high potential as oxidation and photo catalysts.[2,3,4,5,6,7]

Several factors come into play in synthetic procedures which have to be taken into consideration. Discovery of novel species necessitates manipulation of these factors within the limitations that each system requires. The major factors are the stoichiometric ratios, temperature, pH, ionic strength and/or buffering capacity of the medium and the crystallizing agents such as alkali earth metal ions or others.

The newly synthesized Ti-containing polyanions are classified into three categories, Keggin based, lone pair containing and Wells-Dawson based. Every compound will be treated in a separate section and given a number code throughout this chapter for simplicity.

3.2 Keggin based Ti-POMs

3.2.1 Ti-{GeW$_9$} compounds, Polyanions **2, 3** and **4**

Structures of Ti^{IV}-germanotugnstates reported in literature are particularly few. The first was the dimeric Keggin-type $[a,a\text{-}Ge_2W_{18}Ti_6O_{77}]^{14-}$ discovered by Yamase *et al.* in 1993,[8] then Wang *et al.* reported on the tri-substituted monomers a- and β-$[(CpTi_3)GeW_9O_{37}]^{7-}$ in 2000.[9] In 2008, Tan *et al.* published the structure of the dimer[10] $[\{y\text{-}GeTi_2W_{10}O_{36}(OH)_2\}_2(\mu\text{-}O)_2]^{8-}$ based on the lacunary $[y\text{-}GeW_{10}O_{36}]^{8-}$ unit first synthesized in our group.[11] Two trimeric tri-substituted Keggin structures based on tetrahedral linkers were described by Ren *et al.* in 2008: $[(Ge(OH)O_3)(Ti_3GeW_9O_{38}H_2)_3]^{14-}$ and $[(SO_4)(Ti_3GeW_9O_{38}H_3)_3]^{10-}$. The two compounds were synthesized at a temperature of 98°C using $[y\text{-}GeW_{10}O_{36}]^{8-}$ as a precursor, where the high

temperature is supposed to be responsible for breaking the {GeW$_{10}$} down to the smaller {GeW$_9$} unit.[12]

Upon extensive investigation of the Ti^{IV}-[GeW$_9$O$_{34}$]$^{10-}$ system, three products have been constantly obtained, the already published dimer K$_9$H$_5$[a,a-Ge$_2$W$_{18}$Ti$_6$O$_{77}$] (**K-2**), the trimer Rb$_7$K$_3$Na$_7$[(α-Ti$_3$GeW$_9$O$_{37}$OH)$_3$(TiO$_3$(OH$_2$)$_3$)] (**Rb,K,Na-3**) and the novel tetramer K$_{14}$Na$_{14}$[(Ti$_3$GeW$_9$O$_{37}$)$_4$O$_6$] (**K,Na-4**).

It is noteworthy that the phosphorous and silicon analogues of the trimer were synthesized by our group and Cadot *et al.* respectively and reported jointly thereafter.[13] The cyclic Ti$_9$ Keggin trimers [(α-Ti$_3$PW$_9$O$_{38}$)$_3$(PO$_4$)]$^{18-}$ and [(α-Ti$_3$SiW$_9$O$_{37}$OH)$_3$(TiO$_3$(OH$_2$)$_3$)]$^{17-}$ are both composed of three (Ti$_3$XW$_9$O$_{37}$) units linked via three Ti-O-Ti bridges and a capping group, which is either tetrahedral PO$_4$ or octahedral TiO$_6$. The lacunary POM precursors used were K$_{14}$[P$_2$W$_{19}$O$_{69}$(H$_2$O)] for the phosphorous analogue and [{K(H$_2$O)$_2$}α-Si$_2$W$_{18}$O$_{66}$]$^{15-}$,[14] which was formed in situ by acidifying a solution of K$_{10}$[A-α-SiW$_9$O$_{34}$] to pH 6 for the silicon analogue.

Back to the {GeW$_9$} system, repeated trials with altered reaction conditions mainly led to various mixture combinations of the above mentioned compounds, namely the dimer, trimer and tetramer. Efforts were hence focused on establishing simple separate procedures, each producing the corresponding pure compound. The trimer, for example, was successfully synthesized in the pure form following a procedure completely different from that claimed by Ren *et al.*,[12] where the latter yielded mainly the plenary GeW$_{12}$O$_{40}$ Keggin type and the dimer [a,a-Ge$_2$W$_{18}$Ti$_6$O$_{77}$]$^{14-}$ crystals upon several trials to reproduce the work. The dimer on the other hand was made through another slightly simpler route than the one suggested by Yamase *et al.*[8]

Several synthetic parameters were therefore verified to play a major role in determining the identity and the purity of the product in this system and these are reaction medium, the counter cations present, the molar ratio and

temperature. The dimer seems to be favored by the presence of the potassium cation, where it has been the product or a by-product whenever (but not only) K^+ was there in the reaction medium. This also explains the formation of the dimer following the Ren *et al.*[12] proposed procedure where K^+ was the only available counter cation in solution. The trimer however is favored by Rb^+, but other parameters should come into play, namely the molar ratio, temperature and concentration.

3.2.1.1 *Synthetic procedures*

$K_9H_5[a,\alpha\text{-}Ge_2W_{18}Ti_6O_{77}].22H_2O$ (**K-2**)

0.6 g of $Na_{10}[A\text{-}\alpha\text{-}GeW_9O_{34}]$ (0.2 mmol) and 120 µL of titanium oxychloride hydrochloride acid solution $TiOCl_2.xHCl$ (d = 1.58) (0.8 mmol) were added to 20 mL of 1M potassium acetate buffer. The mixture was heated to 80°C for 1 hour, cooled down to room temperature, and then mixed with 1 mL of 1M KCl solution. The thin plate crystals appeared a few days later upon slow evaporation of the solvent, where they were subject to XRD and IR analysis. (20 % yield)

$Rb_7K_3Na_7[(TiO_3(H_2O)_3)(Ti_3GeW_9O_{37}OH)_3].23H_2O$ (**Rb,K,Na-3**)

0.5 g of $Na_{10}[A\text{-}\alpha\text{-}GeW_9O_{34}]$ (0.17 mmol) and 0.25 g of **Ti4** (0.19 mmol) were added to a mixture of 10 mL 0.5 M rubidium acetate buffer pH4.8 and 15 mL of 1M lithium acetate buffer pH4.8. The solution was heated at 60°C for 1 hour, cooled down to room temperature, and then left standing in open air. The rhombohedral crystals appeared a few days later upon slow evaporation of the solvent, where they were subject to XRD and IR analysis. (25 % yield)

$K_{14}Na_{14}[(Ti_3GeW_9O_{37})_4O_6].60H_2O$ (**K,Na-4**)

0.6 g of $Na_{10}[A\text{-}\alpha\text{-}GeW_9O_{34}]$ (0.2 mmol) and 120 μL of titanium oxychloride hydrochloride acid solution $TiOCl_2.xHCl$ (d = 1.58) (0.8 mmol) were added to 20 mL of 1M sodium acetate buffer. The mixture was heated to 80°C for 1 hour, cooled down to room temperature, and then left standing in open air. The needle-like crystals appeared upon slow evaporation of the solvent, where they were subject to XRD and IR analysis. X-ray diffraction of crystals produced via this synthetic route was reliable enough to reveal the structure of the compound but not strong enough to give the complete picture with the lighter atoms, e.g. oxygens. The well refined structure was however obtained by the diffraction of crystals collected through another synthetic route that unfortunately yielded a mixture of products. (25 %)

3.2.1.2 *FT-IR spectroscopy data*

IR spectra of the two compounds which are clearly different from that of the precursor are shown in Fig. 3.2. The following IR bands were detected for **K-2**, 456 (w), 520 (w), 630 (sh), 759 (m), 808 (w), 873 (m), 946 (m) and 1615 (s). While in the case of **Rb,K,Na-3**, the following peaks were detected: 457 (w), 490 (w), 525 (w), 715 (s), 810 (w), 885 (m), 949 (m), 1405 (w) and 1624 (s). As for **K,Na-4**, the spectrum showed absorption at the following wavenumbers, 462 (w), 729 (s), 810 (w), 883 (s), 952 (s) and 1617 (m) cm^{-1}.
Fig. 3.2 shows only the range between 400 and 1100 cm^{-1} in order to illustrate the area of difference between the three spectra that is between 700 and 800 cm^{-1}.
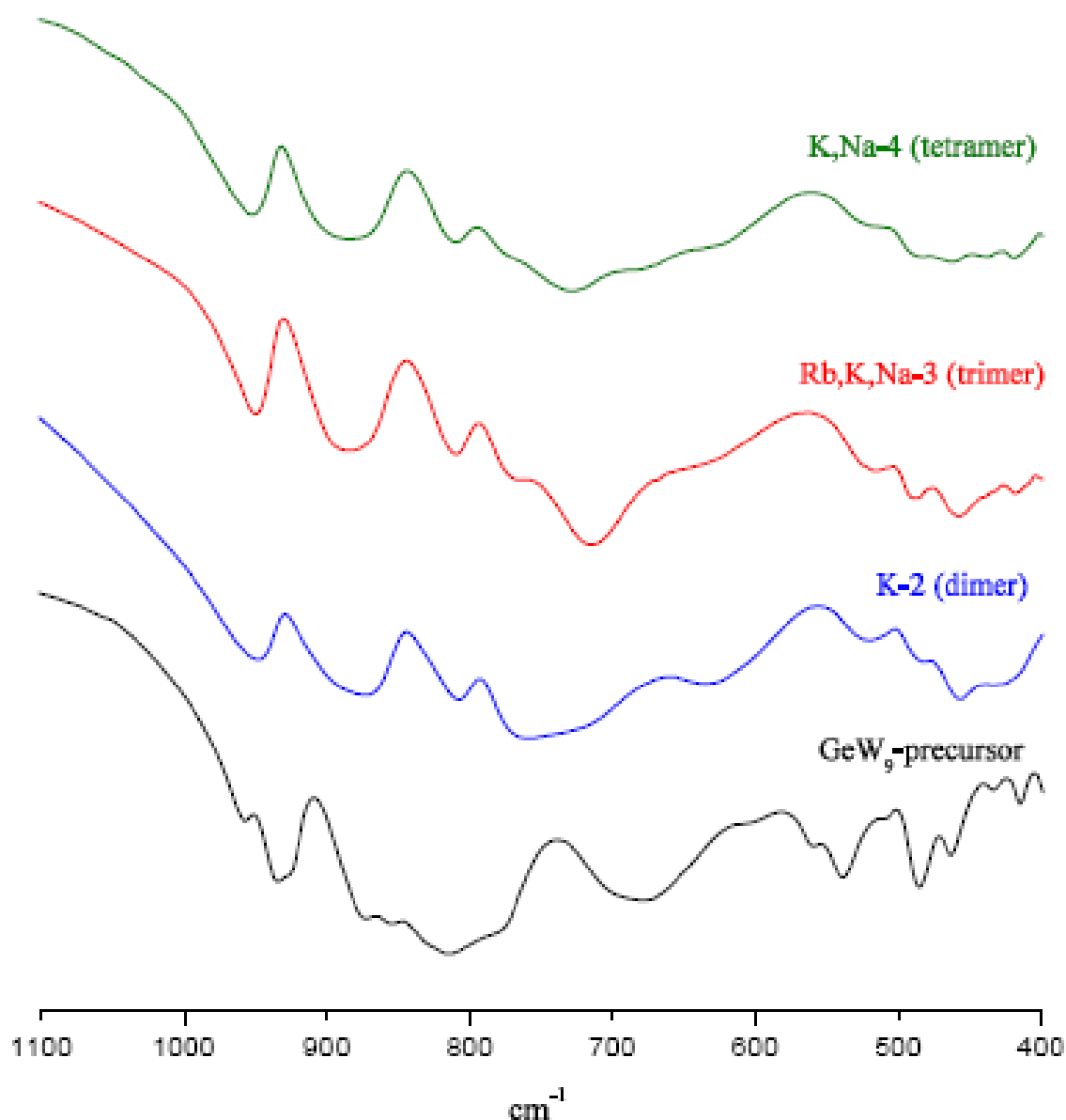
Fig. 3.2 Infra red spectra of the POM precursor {GeW$_9$}, the dimer (**K-2**) and the trimer (**Rb,K,Na-3**)

It is not unexpected that the spectra of the dimer, trimer and tetramer have similarities, the main determinant of the degree of agglomeration however seems to be the peak between 700 and 800 cm^{-1}; where it is at lower energy in the case of the trimer (715 cm^{-1}) than the case of the dimer (759 cm^{-1}) and tetramer (729 cm^{-1}). The 808 cm^{-1} peak in **2** and the 810 cm^{-1} peak in **3** and **4** are the "fingerprint" of the Ti-O-Ti bond stretching.

3.2.1.3 *Single crystal X-ray diffraction data*

Rb,K,Na-3 crystallizes in the space group R3m, while **K,Na-4** crystallizes in P$\bar{1}$. Significant crystallographic data are summed in Table 3.1.

Table 3.1 Crystallographic data of **Rb,K,Na-3** and **K,Na-4**

	Rb,K,Na-3	K,Na-4
Formula	Rb7 K3 Na7 Ge3 Ti10 W27 H69 O150	K14 Na14 Ge4 Ti12 W36 H50 O179
Formula weight (g/mol)	9006.79	11267.42
Crystal system	Trigonal	Triclinic
Space group (Nr.)	R3m (160)	P-1 (2)
a (Å)	29.6597(5)	21.897(3)
b (Å)	29.6597(5)	22.003(3)
c (Å)	16.0158(4)	22.225(3)
α (deg)	90	99.699(7)
β (deg)	90	115.374(7)
γ (deg)	120	92.252(9)
Volume (Å^3)	12201.5(4)	9462(2)
Z	3	2
D$_{calc}$ (g/cm^3)	3.677	3.955
Abs. Coeff. μ (mm^{-1})	22.289	23.328
Total reflections	107781	295507
Unique reflections	4902	31954
Final R1 *	0.0389	0.0540
wR2 *	0.1428	0.1889

$R1 = \Sigma \left| \left| F(obs) \right| - \left| F(calc) \right| \right| / \Sigma \left| F(obs) \right|$; $wR2 = \{ \Sigma[w(F_o^2 - F_c^2)^2] / \Sigma[w(F_o^2)^2] \}^{1/2}$

Polyanion **3** has nominal C$_{3v}$ symmetry with the main rotational axis passing through the capping Ti atom (Fig. 3.3). It consists of three (*A*-α-GeW$_9$O$_{34}$) Keggin units all substituted by three corner-shared TiO$_6$ octahedra and then linked to each other on one side by three Ti-O-Ti bridges and on the other side by an octahedral TiO$_6$ cap. Thereby, three O atoms of the TiO$_6$ moiety act as bridges to the Keggin units with Ti-O distances of 1.81(2) Å. BVS[15] calculations indicated that the three facial, terminal ligands of the octahedral

TiO$_6$ group pointing away from the center of the molecule are actually water molecules [Ti-Oaqua = 2.11(4) Å].
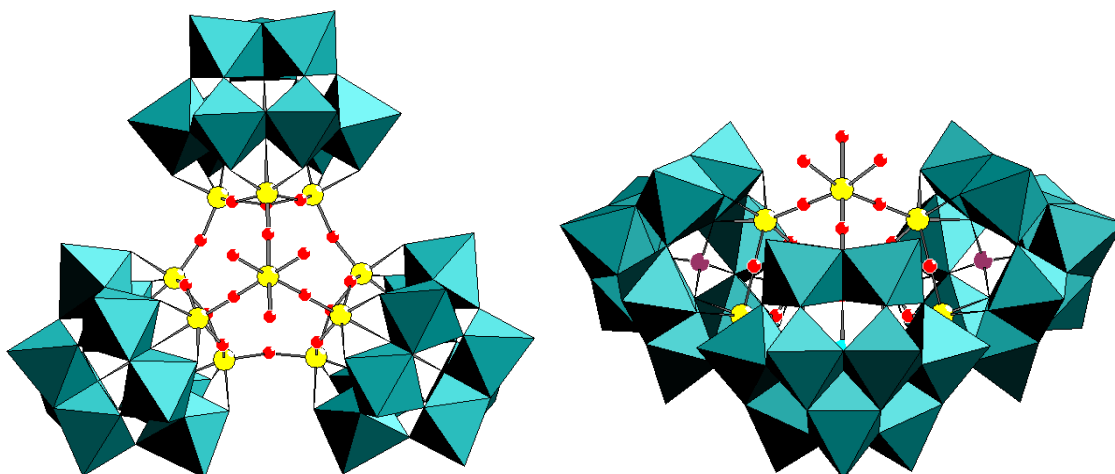
Fig. 3.3 Polyhedral/ball and stick representation of [(TiO$_3$(H$_2$O)$_3$)(Ti$_3$GeW$_9$O$_{37}$OH)$_3$]$^{17-}$ (**3**) from top view angle (left) and from side view angle showing the capping TiO$_6$ group (right). Color code: teal (WO$_6$ octahedra), yellow (Ti), red (O), violet (Ge)

In the solid state, **3** is stabilized by four Rb$^+$ countercations, which are closely associated with the polyanion (Fig 3.4). One of the Rb$^+$ ions is located on the 3-fold axis of **3** opposite the capping group. The other three Rb$^+$ ions occupy the space in between the neighboring Keggin units. The Rb-O bond lengths are in the range 2.898(14)- 3.610(15) Å.
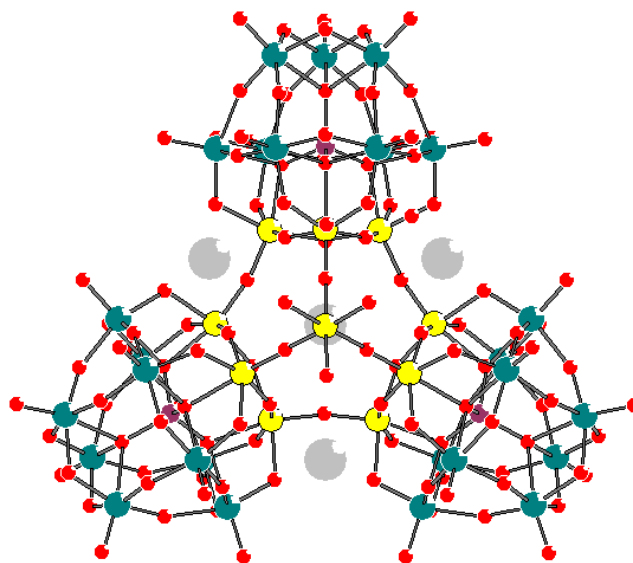
Fig. 3.4 Ball and stick representation of $[(TiO_3(H_2O)_3)(Ti_3GeW_9O_{37}OH)_3]^{17-}$ with three Rb cations between the three units and a fourth one at the main axis of rotation. Color code: teal (W), yellow (Ti), red (O), violet (Ge), grey (Rb)

Fig. 3.5 shows the ten titanium atoms of the trimer and the central rubidium in a more clear detailed fashion. Atoms which belong to the same {GeW$_9$} unit are displayed in the same color, and the tenth titanium in the cap is shown in violet. Ti1-Ti6 lie almost in the same plane, the oxygens that are connecting them are below the plane though, where the Ti-O-Ti angles are 153.9 and 140.1° alternatively. Ti7-Ti9 are not interconnected, but rather linked to the capping Ti10 through bonds that extend linearly at ~180° angles.
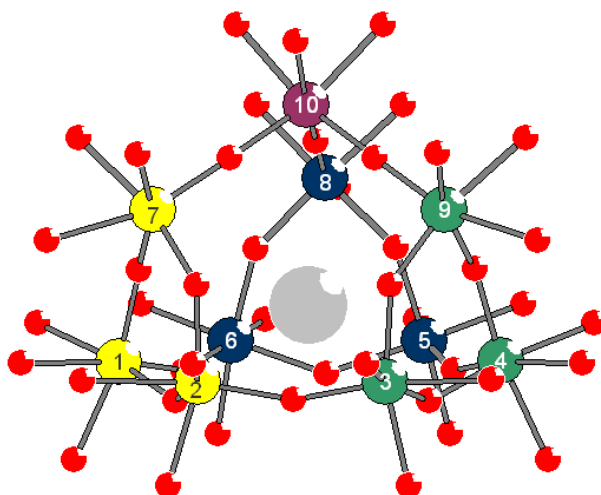
Fig. 3.5 Ball and stick representation of the ten titanium atoms (numbered) and the central rubidium (grey) of **Rb,K,Na-3**

Polyanion **4**, on the other hand, consists of four (A-α-GeW$_9$O$_{34}$) Keggin units all substituted by three corner-shared TiO$_6$ octahedra and then linked to each other via Ti-O-Ti bridges (Fig. 3.6) resulting in a T$_d$ nominal point group. BVS calculations[15] gave no indication of any mono or di-protonated oxygen in this polyanion. All Ti-O distances are within the normal range 1.805(16) to 2.227(14) Å. The longest Ti-O bonds are the ones that connect the titanium to the central heteroatom Ge, which usually is the case.

The same tetrameric assembly has been encountered before in polyoxometalate chemistry. Kortz *et al.* investigated the interaction of the trilacunary Wells-Dawson {P$_2$W$_{15}$} anion with titanium, one of the obtained products was the tetrameric [{Ti$_3$P$_2$W$_{15}$O$_{57.5}$(OH)$_3$}$_4$]$^{24-}$ structure.[16] Hill *et al.* reported on a niobium-substituted, Keggin-based tungstosilicate with T$_d$ symmetry, [Nb$_4$O$_6$(α-Nb$_3$SiW$_9$O$_{40}$)$_4$]$^{20-}$.[17] In this case the four (Nb$_3$SiW$_9$) Keggin fragments are linked to each other through a central Nb$_4$O$_6$ core.

In 2007, another iron-containing mixed valence tetrameric complex [{Fe^{II}Fe^{III} $_{12}$(µ$_3$-OH)$_{12}$(µ$_4$-PO$_4$)$_4$}(B-α-PW$_9$O$_{34}$)$_4$]$^{22-}$ composed of four {PW$_9$} units connected together in a tetrahedral fashion has been reported by Zhao *et al.*[18]
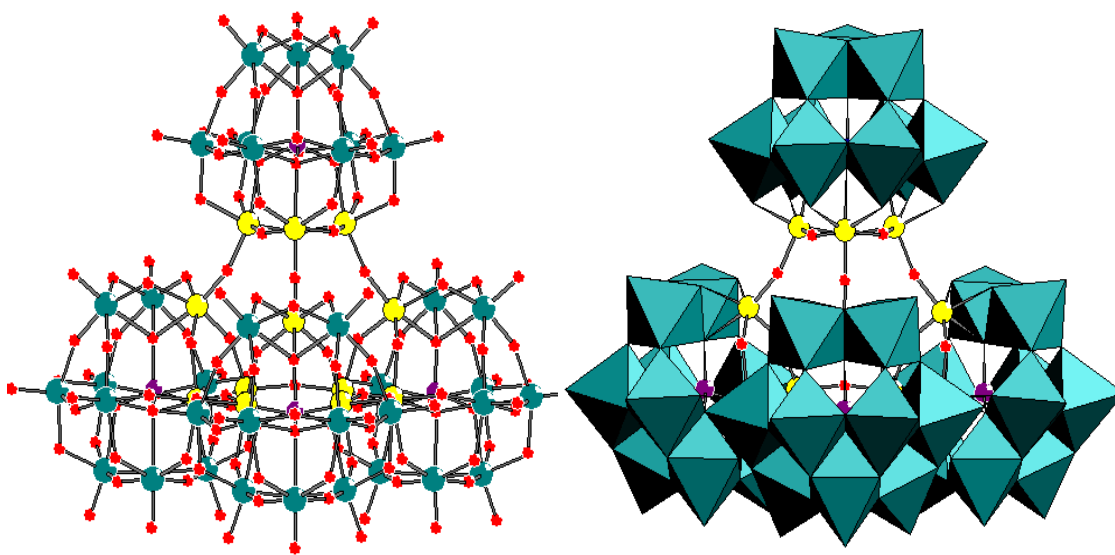
Fig. 3.6 Ball and stick (left) and polyhedral (right) representation of [(Ti$_3$GeW$_9$O$_{37}$)$_4$O$_6$]$^{28-}$ (**4**) Color code: teal (W or WO$_6$ octahedra), yellow (Ti), red (O), violet (Ge)

The connectivity of the twelve titanium atoms in polyanion **4** is more closely shown in Fig. 3.7. The core retains the T$_d$ symmetry of the whole molecule. Titanium atoms that belong to the same {GeW$_9$} unit are again given the same color. Taking a closer look at Ti1-Ti6 would point out the fact that they almost lie in the same plane, but unlike polyanion **3**, the oxygens that connect them to each other are not all below the plane, but they are alternately higher (Ti-O-Ti angle 159.1-160.3°) and lower (Ti-O-Ti angle 143.5-148.1°) than the plane.

Each titanium atom is basically linked to the other titanium atoms on the same {GeW$_9$} unit (like Ti10 is connected to Ti11 and Ti12) and to another titanium atom belonging to a neighboring {GeW$_9$} unit (like Ti10 is connected to Ti7).
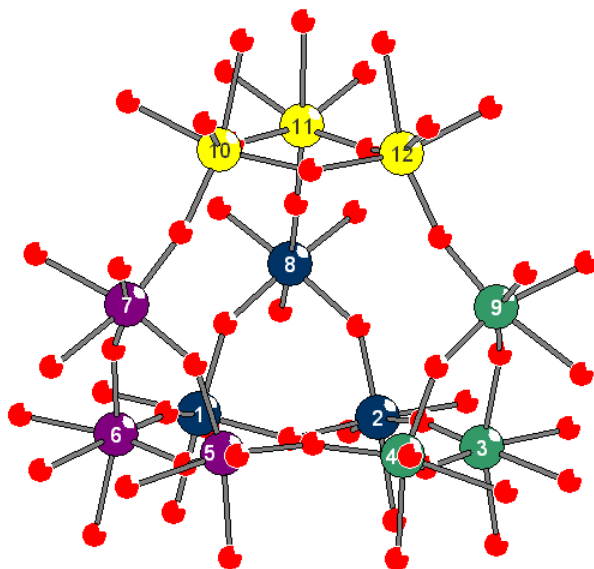
Fig. 3.7 Ball and stick representation of the twelve titanium atoms (numbered) of **K,Na-4**

3.2.1.4 *Thermogravimetric analysis data*

Thermogravimetric analysis mainly supplied information regarding the number of crystal waters associated with the polyanion. As for the dimer, **K-2** the crystal waters that are lost up to a temperature of 200°C make up ~6.8 % by weight, that is equivalent to 22 water molecules (Fig. 3.8). In the case of the trimer **Rb,K,Na-3**, the crystal waters seem to constitute ~4.7 % of the weight of the salt as depicted in Fig. 3.9. This is calculated to be equivalent to 23 water molecules. The number of crystal waters in **K,Na-4** were shown to be 60 which corresponds to ~9 % of the total weight of the crystalline solid. Decomposition of the compound started at around 400 degrees (Fig. 3.10).
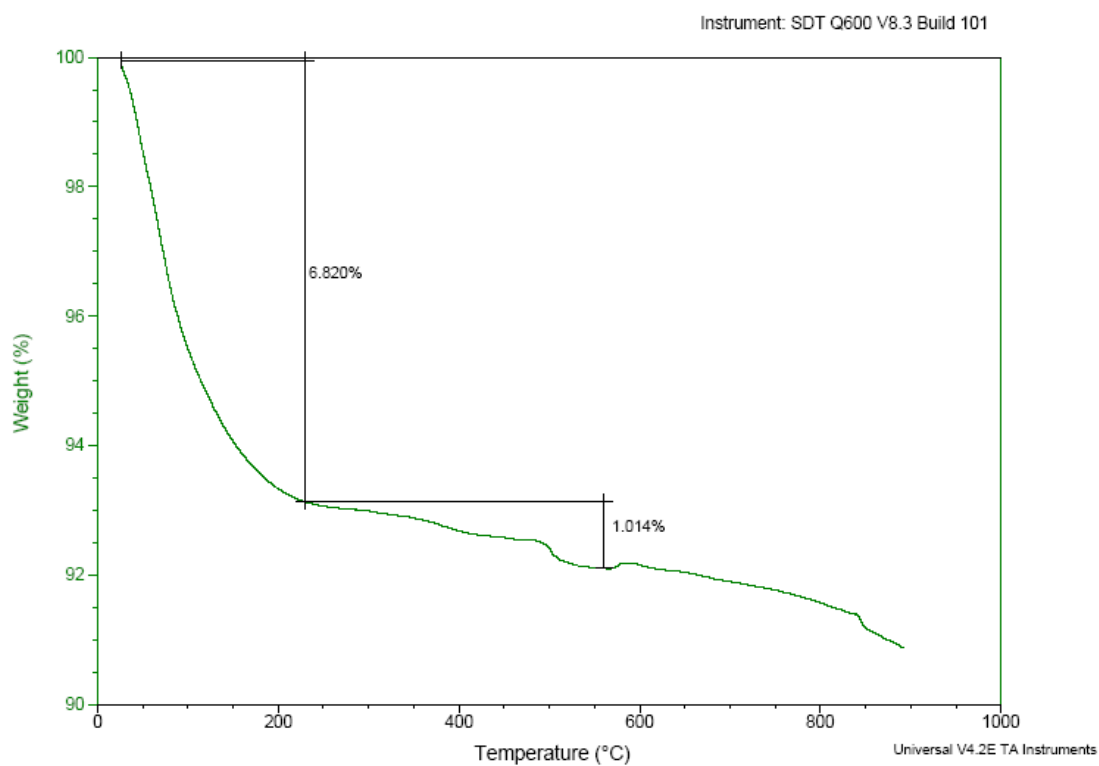
Fig. 3.8 Thermogram of **K-2**
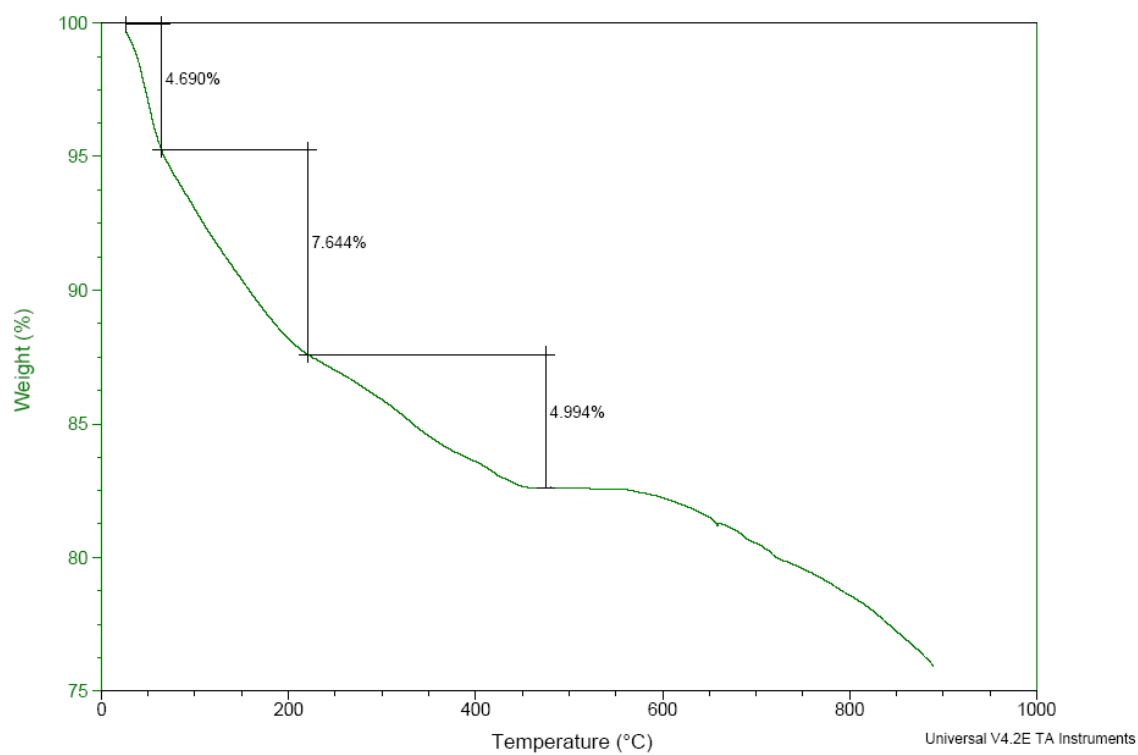
Fig. 3.9 Thermogram of **Rb,K,Na-3**
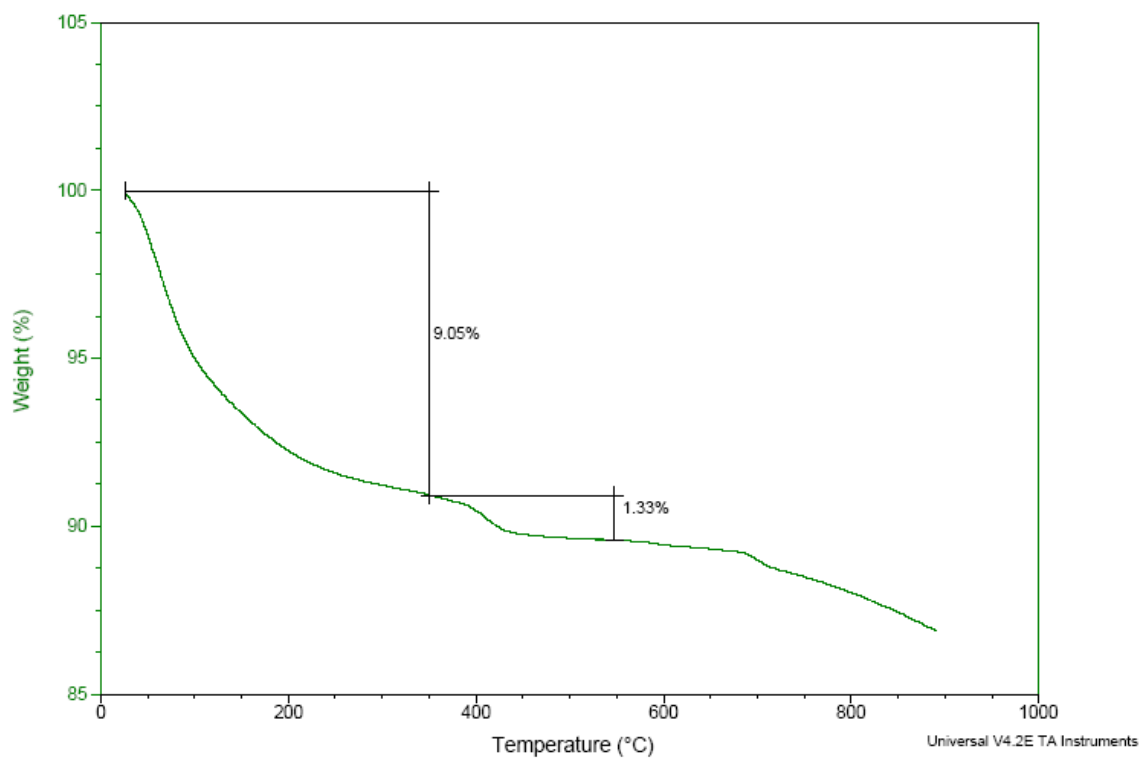
Fig. 3.10 Thermogram of **K,Na-4**

3.2.1.5 *Nuclear magnetic resonance studies*

[183]W is the only possible nucleus in the {GeW$_9$} compounds to be analyzed by NMR. Such experiment can offer a compelling evidence of the persistence of a structure under certain conditions in solution. **Rb,K,Na-3** was dissolved in 1M lithium acetate buffer pH 4.8 solution with the aid of sodium-exchange resin since rubidium salts tend to have very low solubility in water. The [183]W-NMR spectrum shows five peaks exactly as expected from the C$_{3v}$ symmetry of the molecule. The peaks showed at the following chemical shifts: -87.1, -93.7, -101.3, -131.5 and -134.1 ppm in a 2:2:2:2:1 ratio with the peak of small intensity being the most upfield (Fig. 3.11).
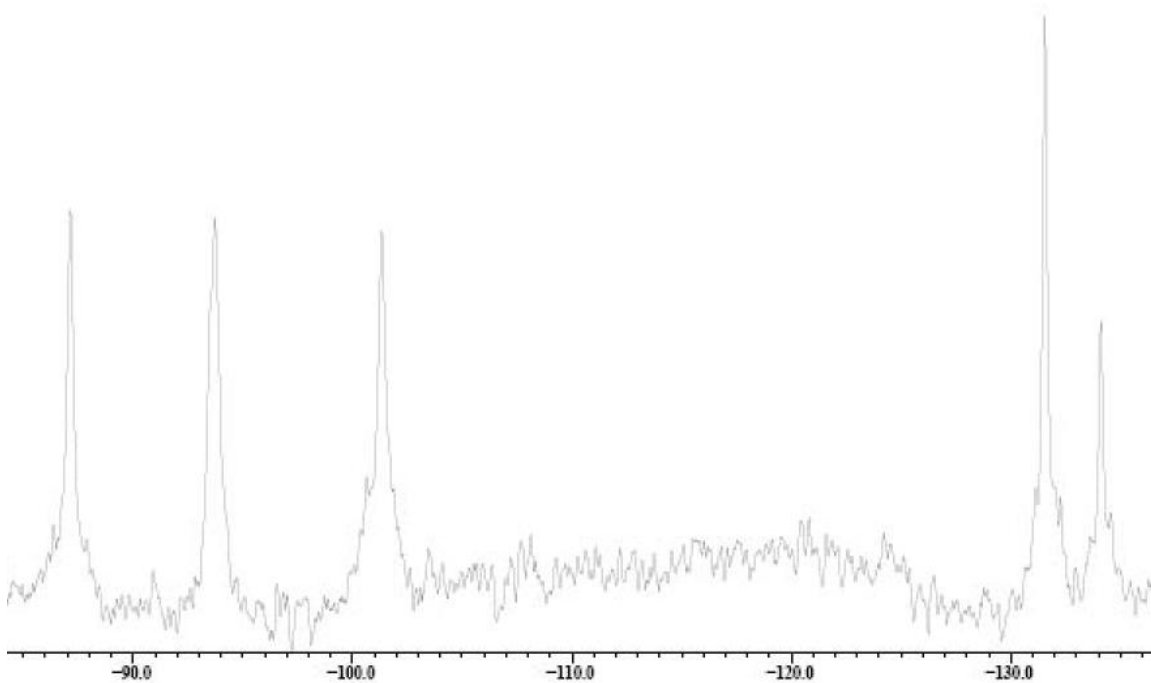
Fig. 3.11 [183]W-NMR spectrum of **Rb,K,Na-3** dissolved in 1M lithium acetate buffer pH 4.8

A very similar picture was produced for the W-NMR of the silicon analogue with three peaks closely spaced in the downfield region of intensities 2:2:2 and other two in the upfield region with 2:1 intensities. The peak of smallest intensity was also the most upfield.[13]

Interestingly, when lithium-exchange resin was used instead of sodium-exchange resin, two extra peaks appeared in the spectrum. This indicates that such a small counter cation like lithium can destabilize the polyoxoanion in solution.

3.2.1.6 *Conclusion*

Three compounds, a dimer, a trimer and a tetramer based on the same tri-Ti(IV) substituted GeW_9O_{34} unit were successfully purely synthesized. The structure of the dimer with all corresponding analytical data has been already reported by Yamase *et al.* in 1993. The procedure proposed there involves mixing the precursors α-$Na_{10}[GeW_9O_{34}]$ and $TiCl_4$ in water, refluxing for 30 minutes, adding KCl and then recrystallization twice in order to get the final product. We were able to obtain the same product **K-2** following a different procedure, where $TiOCl_2$ was used instead of $TiCl_4$. Starting materials were mixed in a 1M potassium acetate buffer medium, heated for 1 hour at 80°C, and then left for slow evaporation of the solvent.

The structure of the trimer has also been lately described by the group of Ren *et.al.* in 2008.[12] Two closely related polyanions based on the XW_9O_{34} (X = P or Si) unit and capped by a tetrahedral PO_4 or octahedral TiO_6 unit have been also reported by our group.[13] The synthetic procedure suggested by Ren *et al.* did not lead to the claimed product but rather to a mixture of the dimer and the plenary Keggin ions $[GeW_{12}O_{40}]^{4-}$. The trimer **3**, seems to be stabilized by the Rb^+ ion occupying the cavity underneath the cap. Interestingly, when the

Rb,K,Na-3 is filtered out of the solution, the dimer **K-2** comes out pure out of the same vial.

The novel tetramer **4** however, was made pure using sodium acetate buffer as a reaction medium instead of rubidium/lithium acetate used in the case of the trimer **3**.

3.2.2 Ti-{PW$_9$} compound, Polyanion 5

All the titanium containing phosphotungstates discovered to date are based either on the monolacunary and dilacunary Keggin, {PW$_{11}$} and {PW$_{10}$} or the monolacunary and trilacunary Wells-Dawson, {P$_2$W$_{17}$} and {P$_2$W$_{15}$} respectively. The only titanium-{PW$_9$} complex known to exist to date is the common sandwich type [α,α-P$_2$W$_{18}$Ti$_6$O$_{77}$]$^{12-}$ published by Nomiya *et al.* in 2001.[19] The latter was synthesized starting from Na$_9$[A-α-PW$_9$O$_{34}$] and Ti(SO$_4$)$_2$ mixed in a 3:1 molar ratio in an aqueous medium, followed by the addition of KCl and then recrystallization of the obtained solid from a pH 2.2 water solution. Nomiya *et al.* have further reacted the aforementioned dimer with an HCl-acidic solution of titanium(IV) sulfate and reported lately in 2010 on two novel polyanions based on the tetra-Ti(IV)-substituted α-PW9 subunits, the dimer [[{Ti(H$_2$O)$_3$}$_2$(μ-O)](α-PW$_9$Ti$_2$O$_{38}$)]$_2$$^{6-}$ and the monomer [{Ti$_4$(μ-O)$_3$(SO$_4$)$_2$(H$_2$O)$_8$}(α-PW$_9$O$_{34}$)]$^{3-}$.[20]

The compound to be described in this section is a new example of a {PW$_9$}-titanium product. Reaction of the Ti-precursor K$_2$TiO(C$_2$O$_4$)$_2$ with the sodium salt of the trilacunary Keggin species Na$_9$[A-α-P^{V}W$_9$O$_{34}$] resulted in a dimeric structure containing eight Ti atoms, each bearing an oxalate group exhibiting a non conventional dimeric structure. The compound was subject to solid state characterization using XRD, FT-IR and TGA.

3.2.2.1 *Synthetic procedure*

$K_{16}Na_2[P_2W_{18}Ti_8(C_2O_4)_8H_8O_{80}].20H_2O$ **K,Na-5**

0.5 g of $Na_9[A\text{-}\alpha\text{-}P^VW_9O_{34}]$ (0.2 mmol) were dissolved in 20 mL of 1M lithium acetate buffer pH 4.8. 0.37 g of $K_2TiO(C_2O_4)_2$ (1 mmol) were then added to the clear solution which was stirred for one hour at room temperature. Plate like colorless crystals appeared ~two weeks later upon slow evaporation of the solvent. (10 %)

3.2.2.2 *FT-IR spectroscopy data*

IR spectra of the POM precursor used in the reaction {PW$_9$} and the product, **K,Na-5** are shown in Fig. 3.12. The bands of the product are the following: 518 (w), 630 (w), 803 (s), 921 (w), 954 (m), 1019 (w), 1089 (s), 1268 (s), 1414 (s) and 1691 (s) cm^{-1}. Two prominent features in this spectrum are noteworthy, the 1268 and 1414 cm^{-1} bands on one hand which clearly imply the incorporation of oxalate groups into the polyoxotungstate framework and the 803 cm^{-1} band on the other which indicates the existence of Ti-O-Ti type of bonding in the structure which is definitely proven by single crystal X-Ray analysis.

Fig. 3.12 Infra red spectra of the POM precursor {PW$_9$} and the product (**K,Na-5**)

3.2.2.3 *Single crystal X-ray diffraction data*

K,Na-5 crystallizes in the triclinic space group P$\bar{1}$. Crystallographic data are detailed in Table 3.2.

Table 3.2 Crystallographic data of **K,Na-5**

	K,Na-5
Formula	K8 Na P Ti4 W9 C8 H24 O66
Formula weight (g/mol)	3389.15
Crystal system	Triclinic
Space group (Nr.)	P$\bar{1}$ (2)
a (Å)	14.0276(9)
b (Å)	14.1418(10)
c (Å)	19.3730(15)
α (deg)	76.531(5)
β (deg)	88.292(4)
γ (deg)	72.021(3)
Volume (Å^3)	3551.2(4)
Z	2
D_{calc} (g/cm^3)	3.379
Abs. Coeff. μ (mm^{-1})	15.186
Total reflections	74091
Unique reflections	12061
Final R1 *	0.0514
wR2 *	0.1774

$* R1 = \Sigma \|F(obs)| - |F(calc)\| / \Sigma |F(obs)| ;\ wR2 = \{ \Sigma[w(F_o^2 - F_c^2)^2] / \Sigma[w(F_o^2)^2] \}^{1/2}$

The structure of **K,Na-5** reveals some unusual dimerization of two PW$_9$ units each substituted with four Ti atoms instead of three which is the most common case, each bearing an oxalate group (Fig. 3.13). Two Ti atoms of each unit are linked to two from the other therefore leading to a skewed species if compared to the conventional sandwich-type structures. C$_{2h}$ point group can be assigned to polyanion **5** with the two-fold rotation axis passing through the two oxygens that connect the two half-units to each other.

Fig. 3.13 Polyhedral/ball and stick representation of $[P_2W_{18}Ti_8O_{76}(H_2O)_4(C_2O_4)_8]^{18-}$. Color code: teal ($WO_6$ octahedra), yellow (Ti), red (O), violet (C), pink (P)

Fig. 3.14 shows only one monomer of **K,Na-5** (left) and one monomer of the GeW_9-trimer **Rb,K,Na-3** (right) described in the previous section for the sake of clarification of the bonding description. The three Ti atoms in **5** occupying the lacuna are not interconnected via Ti-O-Ti bonds like the case of **3**, but are rather linked to a fourth capping Ti lying above their plane. Each of these three Ti atoms in **5** is attached to two oxygens of two edge shared octahedra in the tungstate entity instead of three as is the case in **3** where the third bond in the latter is to one oxygen atom of the tetrahedral GeO_4 moiety. This explains the significant difference in Ti-Ti distances where they are further apart in **5** (average of 5.85 Å) as compared to **3** (3.57Å).

Fig. 3.14 Polyhedral representation of one monomer of $[P_2W_{18}Ti_8O_{76}(H_2O)_4(C_2O_4)_8]^{18-}$ (**5**) (left) and $[(TiO_3(H_2O)_3)(Ti_3GeW_9O_{37}OH)_3]^{17-}$ (**3**) (right). Color code: teal (left) and dark red (right) (WO_6 octahedra), yellow (Ti), red (O), violet (C), blue (central PO_4, left, or GeO_4, right, group)

3.2.2.4 *Thermogravimetric analysis data*

Thermogravimetric analysis of **K,Na-5** as depicted in Fig. 3.15 shows in the first step the loss of crystal waters which correspond to 5.3 % of the total weight. This is equivalent to 20 water molecules. The thermogram might also suggest that disintegration of the compound starts at ~300 degrees.

Fig. 3.15 Thermogram of **K,Na-5**

3.2.2.5 *Nuclear magnetic resonance studies*

Several samples of **K,Na-5** were subject to ^{31}P-NMR measurements. All trials were however unsuccessful at obtaining a single peak as expected for such a compound given that it retains its structure in solution. The conclusion about instability of polyanion **5** in solution was thus arrived at. Interestingly, the decomposition products are different in different media. Upon dissolving the salt in water, two peaks were revealed at -10.6 and -14.7 ppm in a 1:1 ratio and a smaller one at -10.1 ppm with a relative intensity of 19 %. The -14.7 ppm can be assigned to the plenary $[PW_{12}O_{40}]^{3-}$ Keggin anion (Fig. 3.16).

If water is substituted by lithium acetate buffer, the medium used for crystallization, to dissolve the **K,Na-5** salt, two peaks appear again but at

different chemical shifts, -9.6 and -10.2 ppm (Fig. 3.17). The latter seems to be a common decomposition species since it showed up in water too (Fig. 3.16).

Fig. 3.16 ^{31}P-NMR spectrum of **K,Na-5** dissolved in water/D_2O

The number of peaks increased to six upon replacing lithium acetate by sodium acetate suggesting even further decomposition and thus more instability in such a medium.

Fig. 3.17 ^{31}P-NMR spectrum of **K,Na-5** dissolved in lithium acetate buffer/D_2O

3.2.2.6 *Conclusion*

Mainly solid state characterization has been conducted on the newly discovered PW_9O_{34}-based specie. The combination of XRD, TGA and EA analysis led to the full formula $K_{16}Na_2[P_2W_{18}Ti_8O_{76}(H_2O)_4(C_2O_4)_8].20H_2O$. The structure is constructed by peculiar dimerization in a skewed fashion aided by eight titanium atoms decorated by an oxalate group each.

3.3 Lone pair containing Ti-POMs

3.3.1 Ti-{AsW$_9$O$_{33}$} compounds, Polyanions **6** and **7**

Table 1.1 in chapter I contains an inventory of all titanium-containing POMs in literature to the best of my knowledge. The fact is revealed upon close inspection of the table entries that no titanium complex with a lone pair containing POM (like XW$_9$O$_{33}$, X = Sb^{III}, Bi^{III}, As^{III}) is known to date.

One exception is the {As$_2$W$_{19}$Ti$_2$} compound synthesized in our lab[21] and heavily studied catalytically in the lab of professor Kholdeeva in Russia.[22]

Various attempts to react lone pair containing trilacunary tungstates with titanium were unsuccessful. Using the K$_2$TiO(C$_2$O$_4$)$_2$ was however beneficial as a titanium(IV) source where reaction with {As$_2$W$_{19}$} and {As^{III}W$_9$} POM precursors yielded two different structures both based on the {AsW$_9$} unit.

Detailed description of the synthetic procedures and solid state characterization is presented in the following sections.

3.3.1.1 *Synthetic procedures*

K$_{14}$[As$_2$W$_{18}$Ti$_2$(C$_2$O$_4$)$_2$O$_{66}$].18 H$_2$O, **K-6**

0.5 g of K$_{14}$[As$_2$W$_{19}$O$_{67}$(H$_2$O)].20H$_2$O (0.1 mmol) and 0.07 g of K$_2$TiO(C$_2$O$_4$)$_2$ (0.2 mmol) were added to 20 mL of water. pH was then changed to 4 with 6M HCl solution. The solution was then heated at 80°C for one hour, cooled to room temperature. 1 mL of 1M KCl solution was then added dropwise, and the solution was left in open air for slow evaporation. Crystals appeared 2 weeks later (Yield 23 %).

$Rb_2K_5Na_{13}[As_2W_{18}Ti_8(C_2O_4)_8(H_2O)_2O_{75}].30H_2O$, **Rb,K,Na-7**

0.5 g of $Na_9[B\text{-}\alpha\text{-}AsW_9O_{33}].27H_2O$ (0.2 mmol) and 0.29 g of $K_2TiO(C_2O_4)_2$ (0.8 mmol) were added to 20 mL of water. pH was then changed to 3 with 6M HCl solution. The solution was then heated at 80°C for one hour, cooled to room temperature. 1 mL of 1M RbCl solution was then added dropwise, and the solution was left in open air for slow evaporation. Rod-shaped crystals appeared few weeks later (yield 34%).

3.3.1.2 *FT-IR spectroscopy data*

IR spectrum of **K-6** and that of the POM precursor $\{As_2W_{19}\}$ used in the reaction which are clearly distinct from each other are shown in Fig. 3.18. The following IR bands were detected for **K-6** : 461 (w), 516 (w), 667 (m), 758 (s), 820 (sh), 871 (m), 913 (w), 950 (m), 1265 (w), 1405 (w), 1684 (w) and 1711 (w) cm^{-1}.

The two bands at 1265 and 1405 cm^{-1} stick out in the product "fingerprint" spectrum as they correspond to the incorporated oxalate groups, whereas the absence of a strong peak around the area 800-810 cm^{-1} suggests that Ti-O-Ti type of bonding is not part of the structure which is actually the case according to single crystal X-Ray measurements.

Fig. 3.18 IR spectra of {As$_2$W$_{19}$} precursor and **K-6**

In the case of **Rb,K,Na-7**, on the other hand, the following peaks were detected: 449 (w), 518 (w), 608 (w), 645 (sh), 698 (w), 753 (sh), 802 (s), 904 (m), 964 (m), 1065 (sh), 1188 (w), 1275 (s), 1411 (s), 1690 (s) and 1718 (sh) cm^{-1} (Fig. 3.19).

Fig. 3.19 IR spectra of {AsW₉} precursor and **Rb,K,Na-7**

Same discussion applies here where the 1275 and 1411 cm⁻¹ peaks appear again to point to oxalate groups being part of the structure. But unlike the case of **K-6**, Ti-O-Ti bridging is suggested by the strong 802 cm⁻¹ peak in the **Rb,K,Na-7** spectrum.

3.3.1.3 *Single crystal X-ray diffraction data*

Detailed parameters related to the single crystal X-Ray measurements of **K-6** and **Rb,K,Na-7** are listed in Table 3.3. The first crystallizes in the triclinic space group P$\bar{1}$ while the second crystallizes in the higher symmetry orthorhombic space group Pmmn.

Table 3.3 Crystallographic data of **K-6** and **Rb,K,Na-7**

	K-6	Rb,K,Na-7
Formula	K14 As2 Ti2 W18 C4 H36 O92	Rb2 K5 Na13 As2 Ti8 W18 C16 H64 O139
Formula weight (g/mol)	5658.55	6988.32
Crystal system	Triclinic	Orthorhombic
Space group (Nr.)	P-1 (2)	Pmmn (59)
a (Å)	13.4859(9)	21.0722(16)
b (Å)	13.7389(8)	16.2435(15)
c (Å)	15.5526(11)	19.5073(17)
α (deg)	64.521(4)	90
β (deg)	89.161(5)	90
γ (deg)	89.466(4)	90
Volume (Å^3)	2601.1(3)	6677.1(10)
Z	1	4
D$_{calc}$ (g/cm^3)	3.705	1.738
Abs. Coeff. μ (mm^{-1})	21.260	8.714
Total reflections	98477	190899
Unique reflections	7422	7817
Final R1 *	0.0529	0.0760
wR2 *	0.1885	0.2687

$$* R1 = \Sigma \left\| F(obs) \right| - \left| F(calc) \right\| / \Sigma \left| F(obs) \right| ; \ wR2 = \{ \Sigma[w(F_o^2 - F_c^2)^2] / \Sigma[w(F_o^2)^2] \}^{1/2}$$
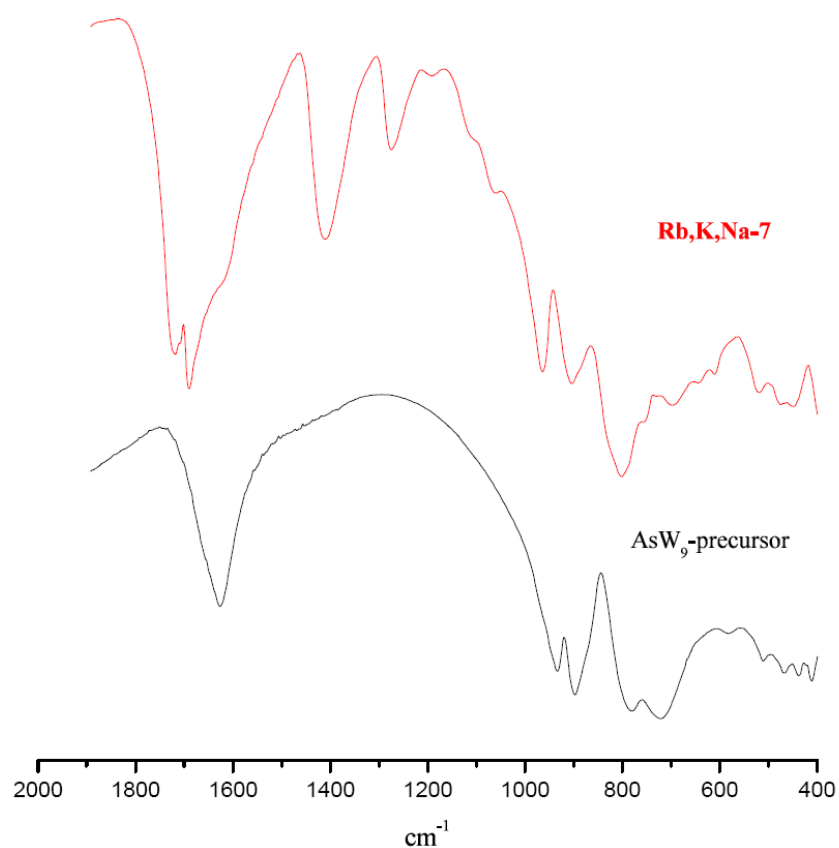
Polyanion **6** consists of two B-α-AsW$_9$O$_{33}$ units connected via two titanium atoms each bearing an oxalate group. The point group C$_{2h}$ is associated with this molecule, where the C$_2$ rotation axis passes through the two titanium atoms (Fig. 3.20).
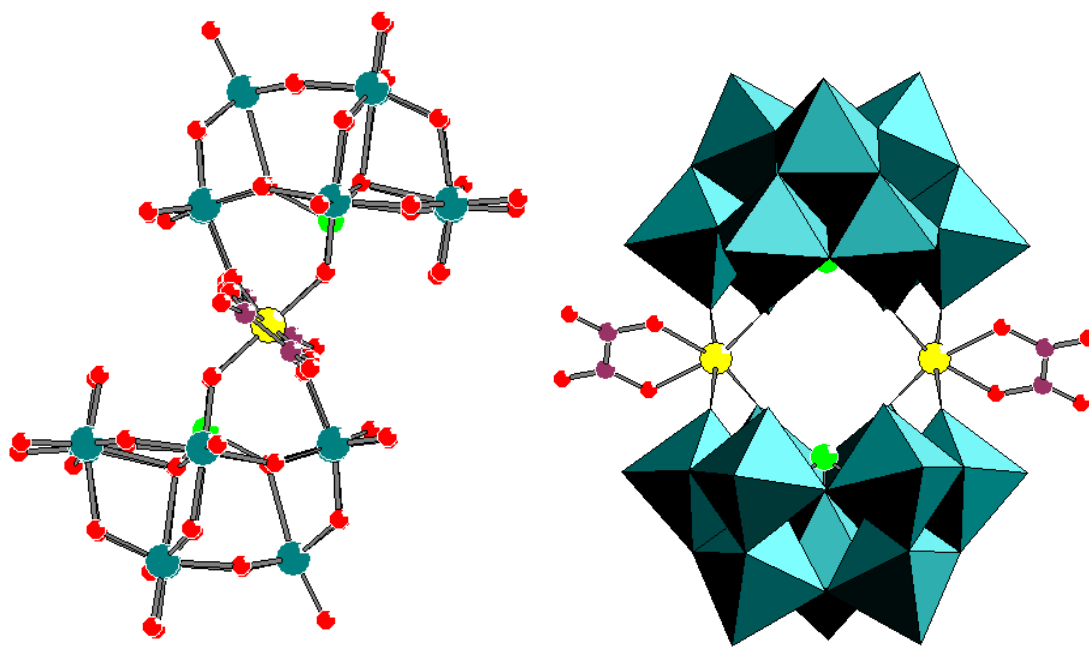
Fig. 3.20 Ball and stick representation of $[As_2W_{18}Ti_2(C_2O_4)_2O_{66}]^{14-}$, **6** in the side view (left) and a polyhedral representation of **6** in the front view (right). Color code: teal (W or WO_6 octahedra), yellow (Ti), red (O), violet (C), green (As)

The molecule can be described as having a chair-like conformation that clearly shows in the side view (Fig. 3.20, left). This dimerization fashion can be rationalized based on the repulsion exerted by the lone pair on the central As^{III} atom, and this is not unusual in the chemistry of such lone pair containing POMs. A class of sandwich-type POMs based on two lone-pair containing, β-Keggin fragments, e.g. $[\beta\text{-}Sb^{III}W_9O_{33}]^{9-}$ and $[\beta\text{-}Bi^{III}W_9O_{33}]^{9-}$ have been long known. The first members of this class, $([M_2(H_2O)_6(WO_2)_2(\beta\text{-}SbW_9O_{33})_2]^{(14-2n)-}$ ($M^{n+} = Mn^{2+}$, Fe^{3+}, Co^{2+}, Ni^{2+}), were reported by Krebs *et al.* in 1997.[23] Krebs-type molecules are similar to **6** in the sense that the two units are not "head-on" dimerized, but they are nevertheless different. **6** is composed of α-type units instead of β without the extra tungstens that usually serve to connect the two β-fragments in Krebs type structures.

In addition to the two oxygens of the oxalate group each titanium atom is connected to four other oxygens, two from each {AsW$_9$} unit resulting in the usual octahedral geometry.

What draws the attention here about the synthetic procedure is that the starting lacunary precursor {As$_2$W$_{19}$} is not retained as a fragment in the product but rather falls apart to two {AsW$_9$} units. Polyanion **7** is however made starting with {AsW$_9$} precursor itself and with a higher molar ratio of titanium. It similarly consists of two B-α-AsW$_9$O$_{33}$, but sandwiches a larger titanium core with eight atoms as compared to the core of polyanion **6** with only two (Fig. 3.21).
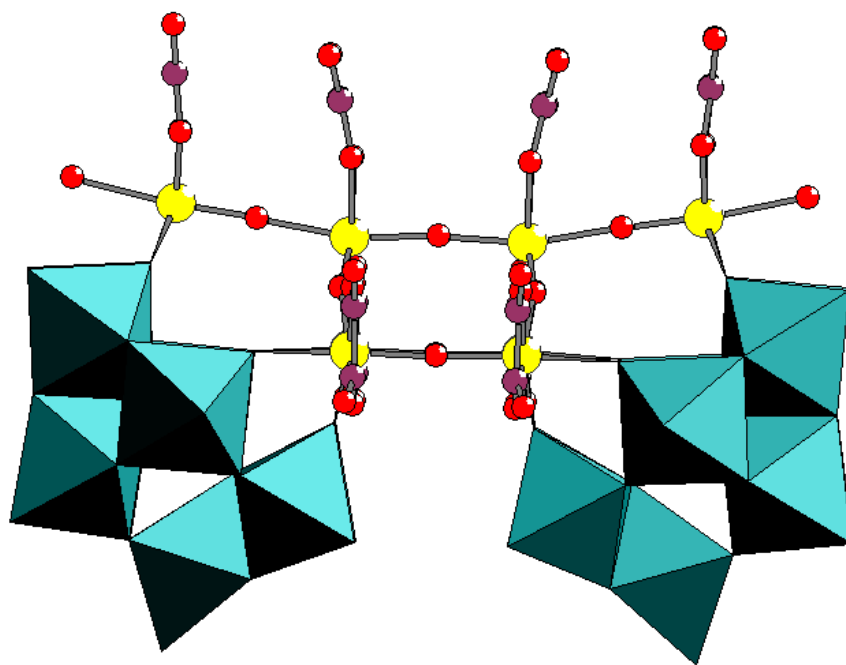
Fig. 3.21 Polyhedral representation of a side view of [As$_2$W$_{18}$Ti$_2$(C$_2$O$_4$)$_8$(H$_2$O)$_2$O$_{75}$]$^{20-}$, **7**. Color code: teal (WO$_6$ octahedra), yellow (Ti), red (O), violet (C)

The symmetry elements in the anionic molecule correspond to the C_{2v} point group. The oxygen through which the C_2 rotational axis passes is depicted in blue in Fig. 3.22 that provides a top view of the molecule, the axis is perpendicular to the plane of the paper.
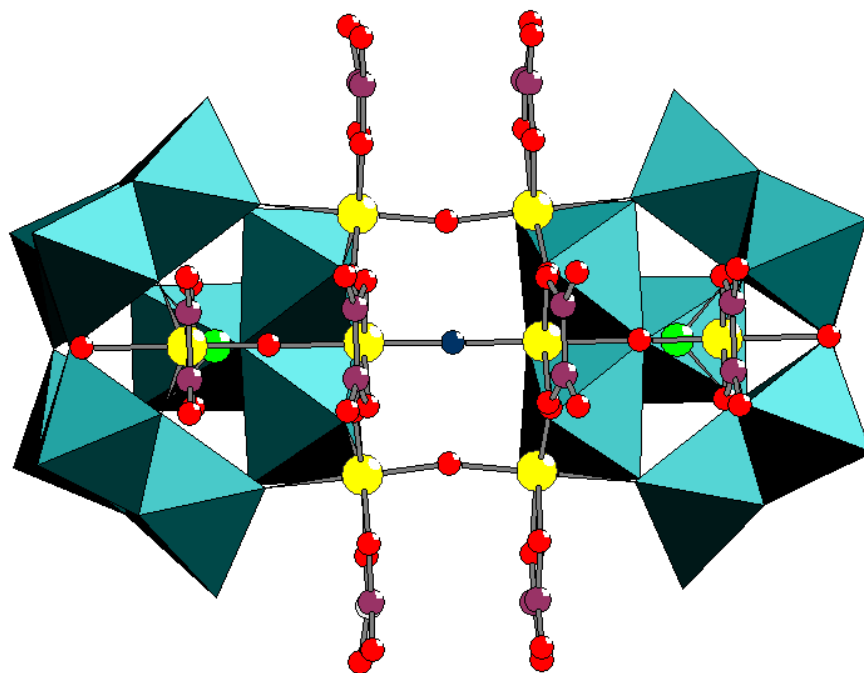
Fig. 3.22 Polyhedral representation of a top view of $[As_2W_{18}Ti_8(C_2O_4)_8(H_2O)_2O_{75}]^{20-}$, **7**. Color code: teal (WO_6 octahedra), yellow (Ti), red (O), violet (C), green (As^{III}) and blue (the O through which C_2 passes)
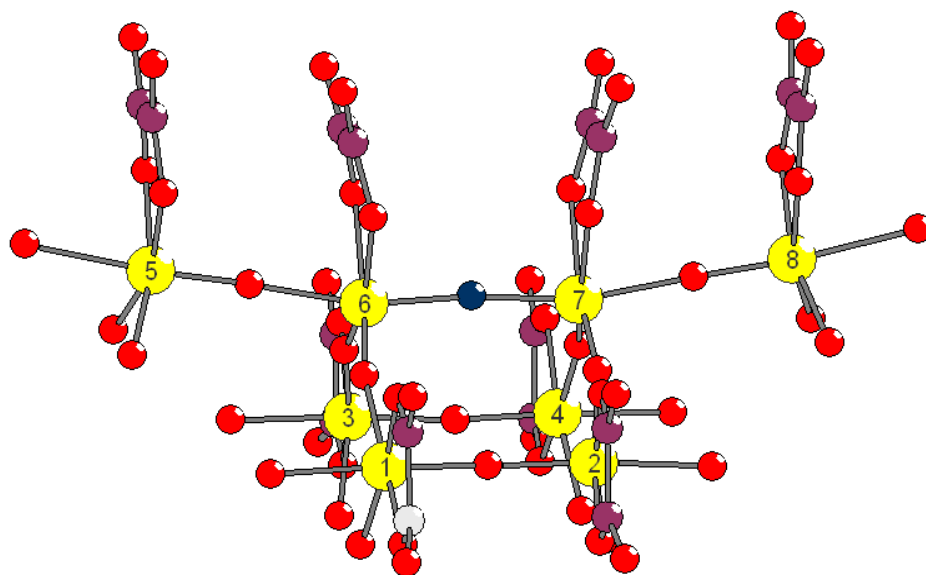
Fig. 3.23 Ball and stick representation of the eight titanium atoms (numbered) of **Rb,K,Na-7**

The core of eight titanium atoms of polyanion **7** is shown in Fig. 3.23 for a clearer picture of the bonding. Ti1 is connected to Ti2 via an oxide bridge, same for Ti3 and Ti4 and the four of them lie in one plane. Ti1 and Ti3 are then connected to Ti6 while Ti2 and Ti4 are connected with Ti7 again through oxide bridges. Ti5 and Ti8 are more to the sides of the "seesaw-shaped" titanium core with terminal diprotonated oxygen each (Ti-OH$_2$ distance of 2.243 Å).

One interesting aspect worth mentioning here is the fact that the monomer of **7** is in very close resemblance to that of **5** (Fig. 3.24).
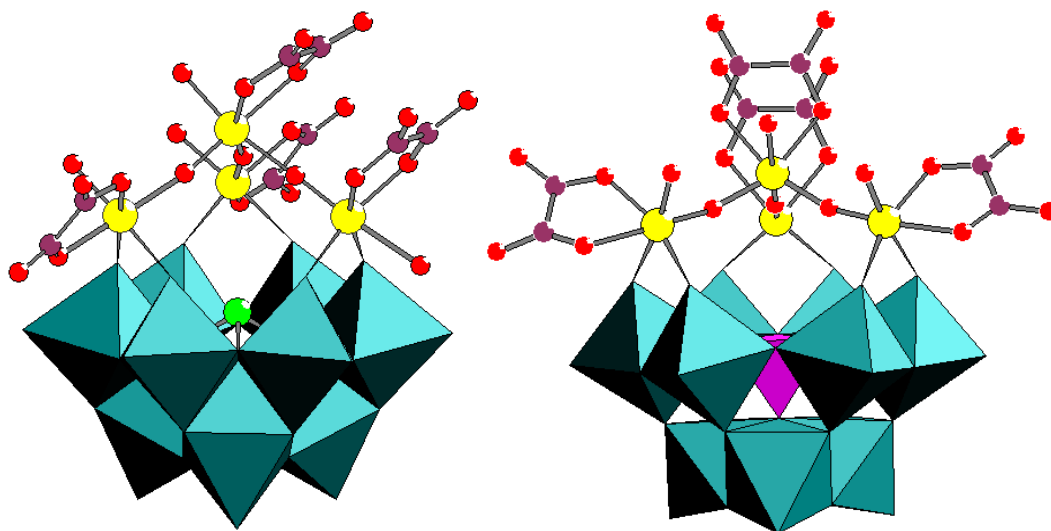
Fig. 3.24 Polyhedral representation of one monomer of $[P_2W_{18}Ti_8O_{76}(H_2O)_4(C_2O_4)_8]^{18-}$ (**5**) (right) and $[(TiO_3(H_2O)_3)(Ti_3GeW_9O_{37}OH)_3]^{17-}$ (**7**) (left). Color code: teal (WO_6 octahedra), yellow (Ti), red (O), violet (C), blue (PO_4 tetrahedron), green (As^{III})

Striking similarities are noticed in the connection fashion of the four titanium atoms to each other in **5** and **7**. One distinction however is to be pointed out; that is each titanium atom out of the three in the lacuna of **7** (left) is connected to two corner shared octahedra of the tungstate entity, B-α-AsW_9O_{33} in this case, while the connection is to two edge shared octahedra of the A-α-PW_9O_{34} unit to the right. This is more realized in the larger Ti-Ti distances for the three atoms directly engrafted into the lacuna in **7** as compared to **5** (5.51 Å and 5.85 Å on average for **7** and **5** respectively). The orientation of the oxalate groups in space is also different, where they all align in almost parallel planes in **7** while they do not in **5** as evident in Fig. 3.24 in a way that relates to the different dimerization modes which then led to dissimilar structures. Three titanium atoms from each monomer of **7** were engaged in dimerization, while two only from each monomer of **5** were available for bridging.

This is a demonstration of how the lone pair on the heteroatom can affect the chemistry involved for such polyanions.

3.3.1.4 *Thermogravimetric analysis data*

Thermogravimetric analysis of **K-6** as depicted in Fig 3.25 shows in the first step the loss of crystal waters which correspond to 5.6 % of the total weight. This is equivalent to 18 water molecules. The thermogram might also suggest that the compound starts to disintegrate at ~300°C. Fig. 3.26, on the other hand, is the thermogram of **Rb,K,Na-8** and it shows the first step that normally corresponds to crystal waters which in this case amount to 7.5 % of the total weight, this can be translated to 30 water molecules given the molecular weight of the compound. The structure seems to fall apart beyond a temperature of ~250°C.
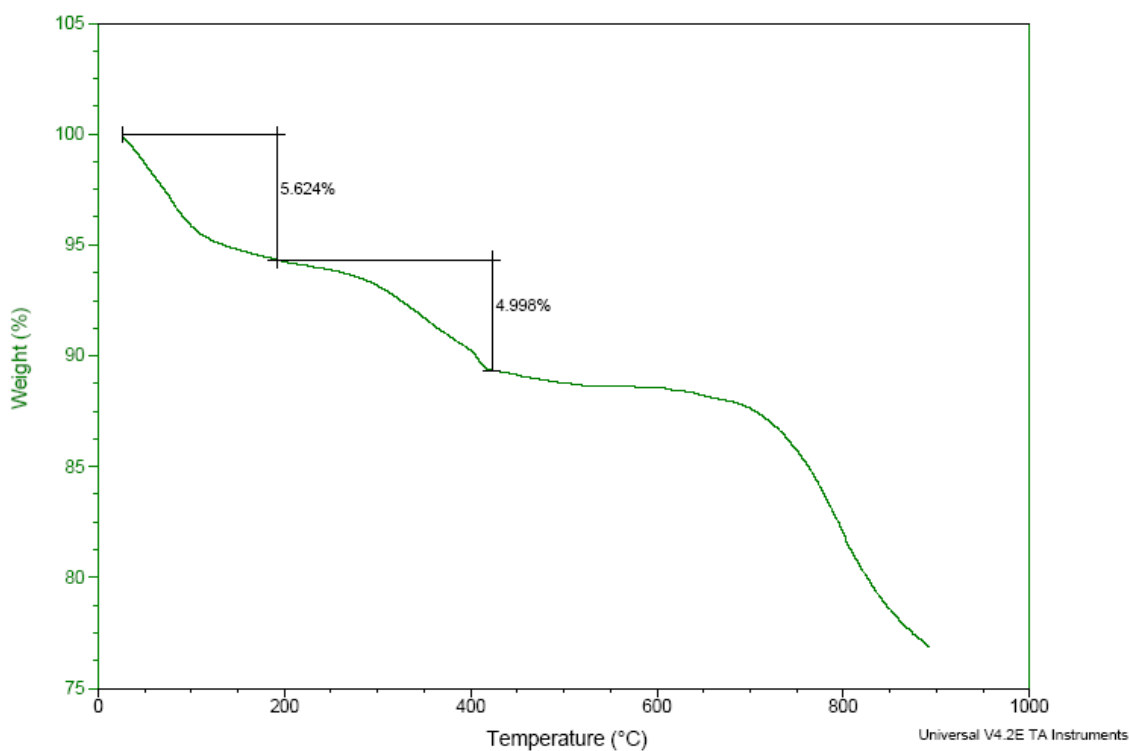
Fig. 3.25 Thermogram of **K-6**
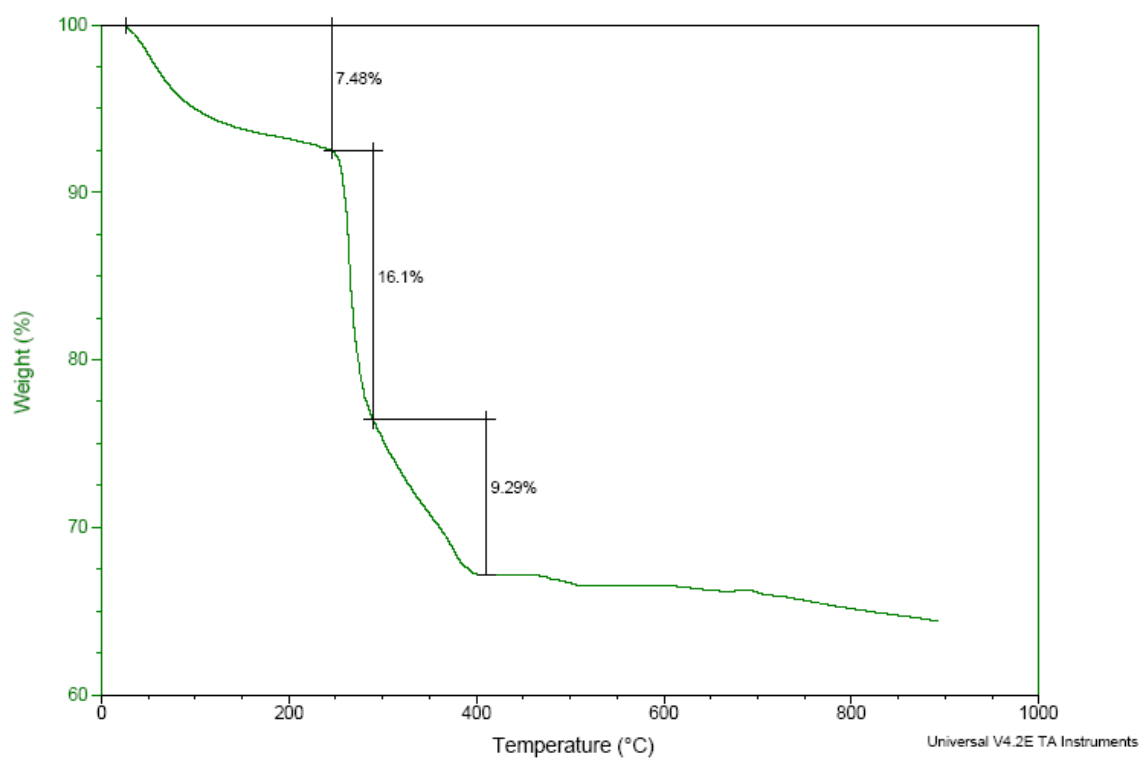
Fig. 3.26 Thermogram of **Rb,K,Na-7**

3.4 Wells-Dawson based Ti-POMs

3.4.1 Ti-$\{P_2W_{16}\}$ compound, Polyanion **8**

Synthesis and isolation of the mono- $\{P_2W_{17}\}$, tri- $\{P_2W_{15}\}$ and hexavacant $\{P_2W_{12}\}$ derivatives of the Wells-Dawson anion were known since the 70's though the question of purity, solution transformations and interconversions between these compounds was later revisited and thoroughly investigated.[24,25]

Contant and Tézé for instance in their 1985 publication[25], which opened the door later for further exploration of the system by other research groups, discussed mainly the condensation routes of the $\{P_2W_{12}\}$ fragment into the dimeric $\{P_4W_{24}\}$ and then the cyclic tetrameric $\{P_8W_{48}\}$ species on one hand and the α_1 and α_2 isomers of the monovacant $\{P_2W_{17}\}$ fragment on the other.

Polyanions synthesized starting from $\{P_2W_{12}\}$ lacunary species are known in literature, some of which retained the $\{P_2W_{12}\}$ tungstate framework such as the polyperoxo $[P_2W_{12}(NbO_2)_6O_{56}]^{12-}$ monomer[26], the iron substituted $[H_4P_2W_{12}Fe_9O_{56}(OAc)_7]^{6-}$ monomer and $[H_{55}P_8W_{49}Fe_{27}O_{248}]^{26-}$ tetramer[27] and the different trimeric species with different transition metals and mixed 3d-4f metals engrafted, all containing the crown type polyoxoanion shell $[\{WO(H_2O)\}_3(P_2W_{12}O_{48})_3]^{30-}$ ($\{P_6W_{39}\}$) as referred to by the authors[28,29]. Other synthetic procedures led to higher condensation tungstate frameworks such as the Co-containing $\{P_4W_{24}\}$-based anion[30] $[\{W_2Co_2O_8(H_2O)_2\}(P_2W_{12}O_{46})_2]^{20-}$, the iron(III) and the disordered Mn(II) complexes derived from the $\{P_2W_{14}O_{54}\}$ fragment[31] $[H_{12}P_4W_{28}Fe_8O_{120}]^{16-}$ and $[W_4Mn_4O_{12})(P_2W_{14}O_{54})_2]^{20-}$ and the La and Nd substituted $\{\alpha_2$- $P_2W_{17}\}$ dimers $[\{La(CH3COO)(H_2O)_2(\alpha_2$-$P_2W_{17}O_{61})\}_2]^{16-}$ and $[\{Nd(H_2O)_3(\alpha_2$- $P_2W_{17}O_{61})\}_2]^{14-}$.[32,33] Another study reported on the transformation of $\{P_2W_{12}\}$ into a $\{P_2W_{16}\}$ fragment yielding the heteropolytungstotetracerate(III) $[Ce_4(OH_2)_9(OH)_2(P_2W_{16}O_{59})_2]^{14-}$.[34] Both

vacant sites of $\{P_2W_{16}\}$ in this specific example lay in adjacent α_1 (belt) positions on either side of the anion's equator on top of each other looking down the axis that passes through the two P atoms.

The second example is to be herein reported, a novel dimeric Ti-substituted $\{P_2W_{16}\}$ based structure, the two vacant sites of which lie also in α_1 (belt) positions on either side of the anion's equator, they are however not adjacent but rather diagonally located with respect to each other. The exact same fragment was previously reported[35] in 2009, in a trimeric aggregate $[K \subset (P_2W_{16}Co_2O_{60})_3]^{23-}$ interlinked via W-O-Co bonds. Nevertheless, the synthetic route in the 2009 report[35] starts from the plenary $\{P_2W_{18}\}$ Wells-Dawson anion rather than the metastable hexavacant $\{P_2W_{12}\}$ like our case is.

Two other isostructural $\{P_2W_{16}\}$ dimers are known in literature, both formed starting from the tri-vacant $\{P_2W_{15}\}$, where the Zr-containing compound $[Zr_4(\mu_3\text{-}O)_2(\mu_2\text{-}OH)_2(H_2O)_4(P_2W_{16}O_{59})_2]^{14-}$ was first reported[36] in 2003 and then the Hf analogue $[Hf_4(\mu_3\text{-}O)_2(\mu_2\text{-}OH)_2(H_2O)_4(P_2W_{16}O_{59})_2]^{14-}$ made by another group in 2009.[37] What distinguish those two compounds are the two lacunae lying in adjacent α_2 (cap) positions, a fact probably dictated by the different coordination chemistry involved in the case of zirconium and hafnium.

The same P_2W_{16} fragment was published in 1996 by Crano *et al.*[38] for a structure $[P_4Ti_6W_{32}O_{132}]^{28-}$ closely related to the one here reported. It consists of a dimer of two P_2W_{16} units substituted by two titanium atoms each, in the α_2 vacant adjacent sites and linked from the sides via two extra titanium atoms. It is noteworthy though that later in 2000, in a thorough review by Nomiya *et al.*[39], the unreliability of the experimental procedure was clearly pointed at, and the adduct of the indicated reaction between the $\{P_2W_{15}\}$ precursor and the Ti^{IV} source $K_2Ti(O)(C_2O_4)_2$ was shown to be some oligomeric form of the tri titanium-substituted $\{P_2W_{15}\}$ instead of the claimed $[P_4Ti_6W_{32}O_{132}]^{28-}$.

This section is therefore dedicated to describe the structure of $K_{15}Li_5[P_4W_{32}Ti_6(C_2O_4)_4O_{124}].53H_2O$, (**K,Li-8**) the detailed synthetic procedure, the solid state structural characterization (XRD, IR, TGA) and solution studies (P and W-NMR).

3.4.1.1 *Synthetic procedure*

$K_{15}Li_5[P_4W_{32}Ti_6(C_2O_4)_4O_{124}].53H_2O$ **K,Li-8**

0.5 g of $K_{12}[H_2P_2W_{12}O_{48}]$ (0.12 mmol) were dissolved in 20 mL of 1M LiCl solution, then 0.5 g of $K_2Ti(O)(C_2O_4)_2$ (1.4 mmol) were added. Using concentrated HCl, pH of the resulting clear solution was adjusted to 1 and it was left to stir overnight. 1 mL of 1M KCl solution was then added, and the solution was left to evaporate slowly leading to the formation of colorless cubic crystals. Yield (20 %)

It should be noted that **K,Li-8** crystals have to be collected early enough (after 2 weeks) before **Ti4** starts to come out as a by-product. The two types of crystals are luckily perfectly distinguishable by shape and color, where our desired product forms in pale yellow big chunks while **Ti4** appears as colorless very shiny thin plates.

3.4.1.2 *FT-IR Data*

IR spectra shown in Fig. 3.27 show an obvious difference between the POM precursor used for this reaction {P_2W_{12}} and the product obtained **K,Li-8** and the byproduct **Ti4**. The following peaks were detected for **Ti4**: 529 (s), 808 (s), 1254 (s), 1385 (s), 1695 (sh) and 1720 (s) cm^{-1}. As for **K,Li-8**, absorption at the following wave numbers occurred: 521 (w), 592 (w), 782 (s), 909 (w), 959 (w),

1090 (s), 1245 (w), 1385 (m), 1622 (m) and 1701 (m) cm^{-1}. The stretching bands that correspond to the oxalate group are found in both the product and the byproduct in the range extending between 1200 and 1400 cm^{-1}. Another band that can be attributed to the Ti-O-Ti bonds shows around 780-810 cm^{-1}.
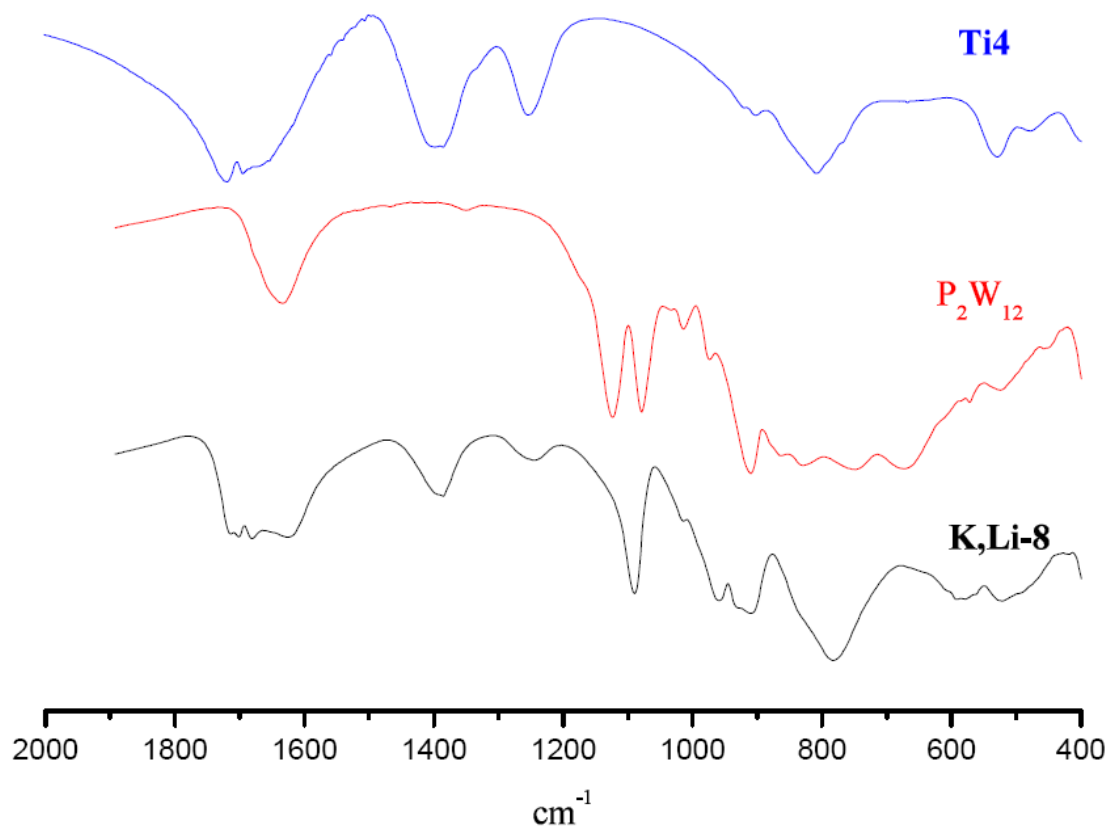
Fig. 3.27 Infra red spectra of the POM precursor {P$_2$W$_{12}$}, the product (**K,Li-8**) and the byproduct (**Ti4**)

3.4.1.3 *Single crystal X-ray data*

K,Li-8 crystallizes in the rhombohedral space group R-3c. Detailed crystallographic data are presented in Table 3.4.

<p align="center">Table 3.4 Crystallographic data of K,Li-8</p>

	K,Li-8
Formula	K20 P4 Ti6 W32 C8 H106 O193
Formula weight (g/mol)	10367.41
Crystal system	Rhombohedral
Space group (Nr.)	R-3c (167)
a (Å)	48.442(8)
b (Å)	48.442(8)
c (Å)	50.008(8)
Volume (Å^3)	101627(28)
Z	24
D_{calc} (g/cm^3)	4.066
Abs. Coeff. μ (mm^{-1})	22.563
Total reflections	596416
Unique reflections	11790
Final R1 *	0.0993
wR2 *	0.3196

$* R1 = \Sigma ||F(obs)| - |F(calc)|| / \Sigma |F(obs)| ; \; wR2 = \{ \Sigma[w(F_o^2 - F_c^2)^2] / \Sigma[w(F_o^2)^2] \}^{1/2}$

The molecule has an inversion center, where a K$^+$ ion exactly sits and two C$_2$ rotation axes perpendicular to each other, thus making D$_2$ the point group the molecule belongs to. The polyanion shows a unique structure composed of two {P$_2$W$_{16}$} units substituted by two titanium atoms each as shown in Fig. 3.29 in which only one subunit of the molecule is shown. Ti-O distances in the respective TiO$_6$ octahedra occupying the vacant sites of the Wells-Dawson entity range between 1.818 and 2.295 Å, the latter connects the Ti to the nearby central tetrahedral PO$_4$ through a Ti-O-P bond. The two vacant sites lie in α$_1$ (belt) positions on either side of the anion's equator, they are however not adjacent but rather diagonally located with respect to each other. The two {P$_2$W$_{16}$} are almost perpendicular to each other; the two lines formed by the

two phosphorous atoms of each subunit lie at an angle of 86 deg. The two units are connected to each other via two bridging titanium atoms bearing two oxalate groups each through which one of the C_2 rotational axes passes. Bottom picture in Fig. 3.28 shows the molecule along this C_2 axis being perpendicular to the plane of the page.
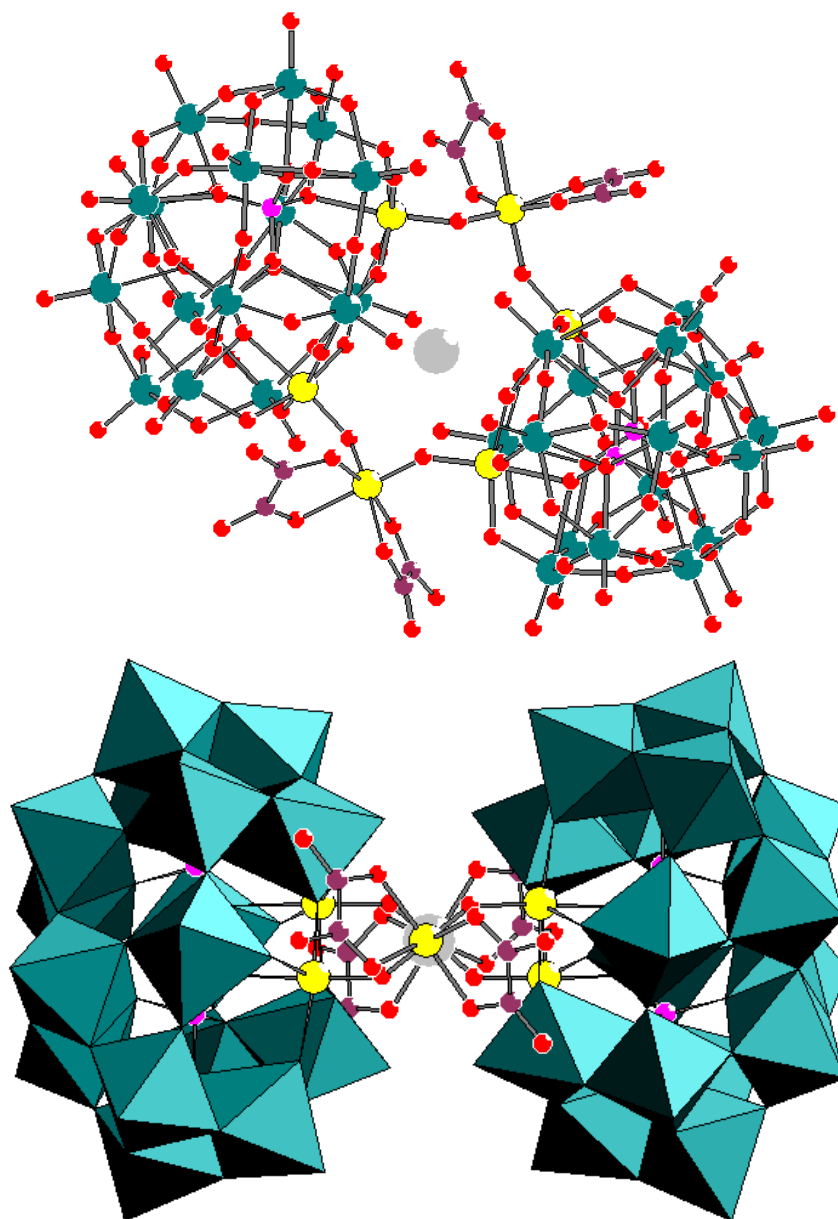
Fig. 3.28 Ball and stick and polyhedral representation of $[P_4W_{32}Ti_6(C_2O_4)_4O_{124}]^{20-}$ (**8**) showing the two subunits connected to each other by two outer titanium atoms and a potassium ion sitting at the inversion center from two different sides. Color code: teal (W), yellow (Ti), red (O), violet (C), pink (P), grey (K)
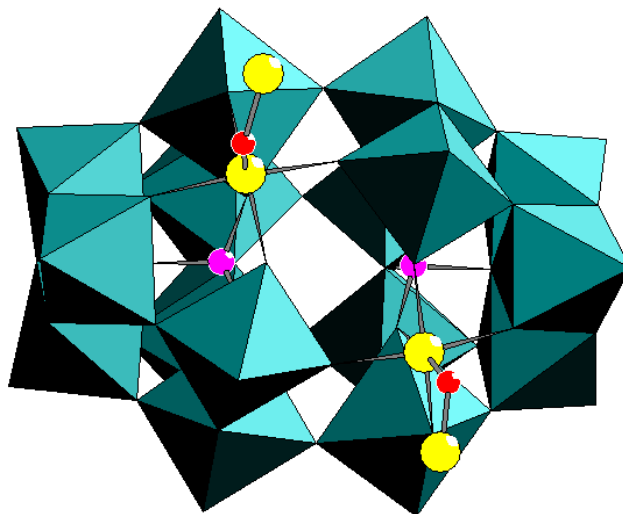
Fig. 3.29 Polyhedral/Ball and stick representation of one portion of **8** showing one of the {P$_2$W$_{16}$} subunits substituted with two titanium atoms and the two bridging ones. Color code: teal (W), yellow (Ti), red (O), pink (P)

The Ti-O distances in the Ti-O-C bonds that serve as the link to the oxalate are between 2.000 and 2.127 Å. BVS calculations[15] showed no protonation sites, not even on the oxygens linking two titanium atoms or a titanium and a tungsten atom as to be expected.

3.4.1.4 *Thermogravimetric analysis data*

Thermogravimetric analysis of **K,Li-8** as depicted in Fig. 3.30 shows in the first step the loss of crystal waters which correspond to 9.1 % of the total weight. This is equivalent to 53 water molecules. The thermogram might also suggest that the compound starts to disintegrate at ~250°C.
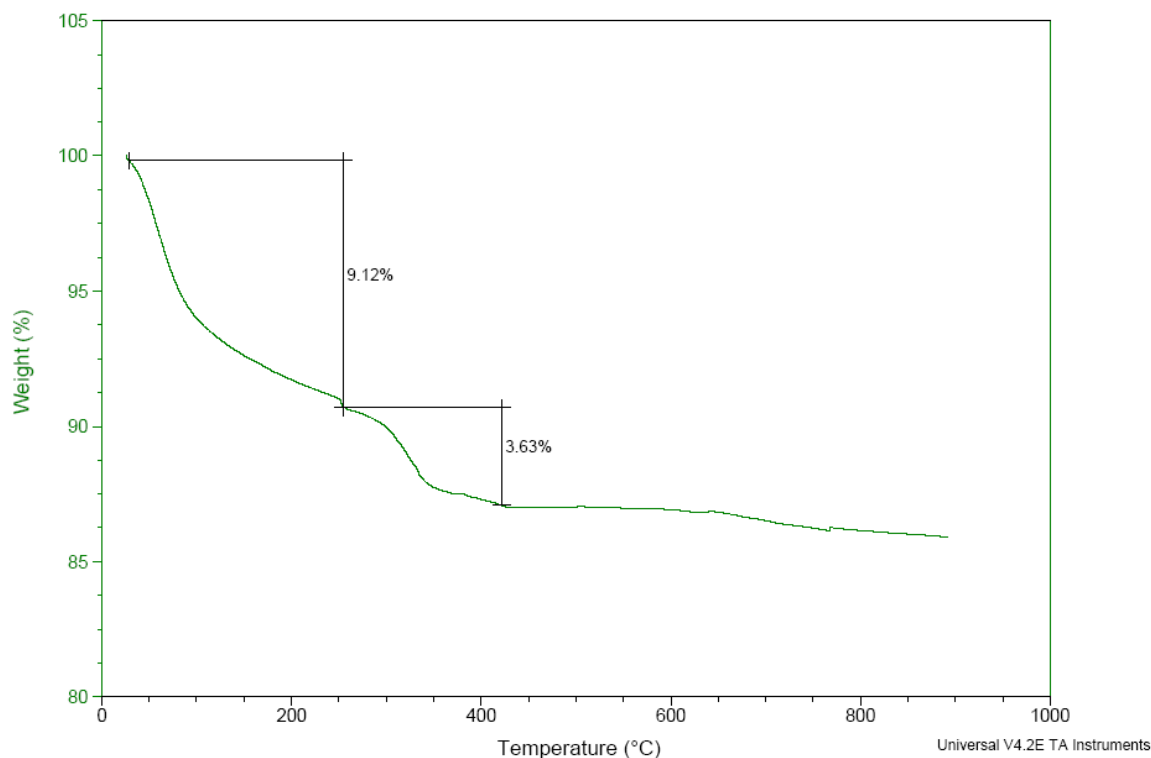
Fig. 3.30 Thermogram of **K,Li-8**

3.4.1.5 *Nuclear magnetic resonance studies*

An ideal technique to examine the behavior and stability and to check for bulk purity of certain specie in solution is NMR spectroscopy. This analytical technique like any other has its limits and drawbacks. **K,Li-8** was redissolved in the same medium it was crystallized out of, a 1M lithium chloride solution at pH 1 changed using concentrated HCl solution 37%. ^{31}P-NMR and [183]W-NMR spectra clearly confirm the symmetry suggested by the solid state structure unraveled by XRD analysis. One question stays however unanswered on whether the dimeric unit stays intact in solution or breaks apart into two identical species, since the spectra would fit in both cases. Nevertheless, the Ti-O-Ti bridges holding the whole entity together in the

solid state are highly suspected not to be able to withstand hydrolysis in solution.

^{31}P-NMR shows a singlet at -10.8 ppm (Fig. 3.31), that is far away from the chemical shift that the precursor $\{P_2W_{12}\}$ would show (-8.6 ppm) or its possible solution transformation products that may show one peak in P-NMR, $\{P_8W_{48}\}$ (-6.6 ppm) or $\{P_2W_{18}\}$ (-12.5 ppm).[34] Another control experiment was performed to rule out the last possibility where a salt of $[\alpha\text{-}P_2W_{18}O_{62}]^{6-}$ was added to the NMR sample that was subsequently measured again, then two peaks appeared next to each other instead of one intensified signal that would have showed had the species existing upon dissolution of our product was actually $\{P_2W_{18}\}$.

Interestingly, when **K,Li-8** was dissolved in water instead of 1M LiCl, two peaks appeared in the P-NMR spectrum at -10.8 and -11.1 ppm chemical shifts in a 1:1 ratio suggesting further decomposition into some unidentified species in water (Fig. 32).
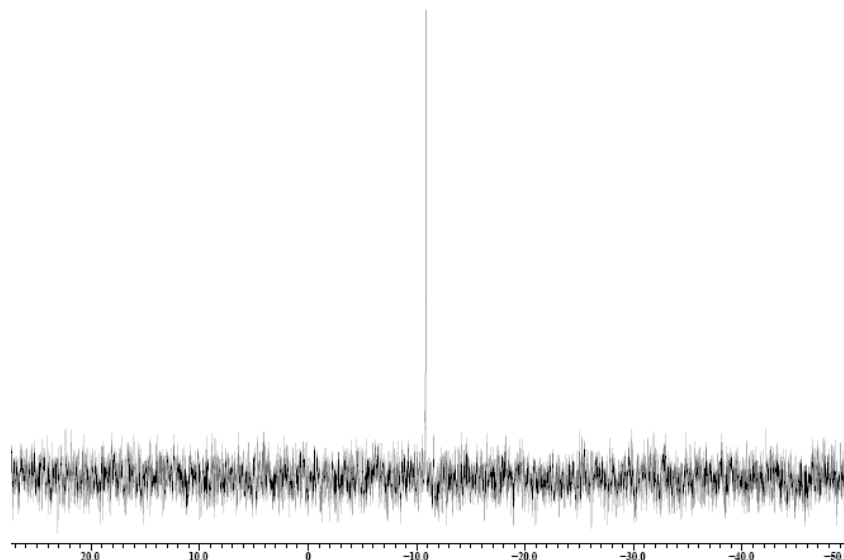
Fig. 3.31 ^{31}P-NMR spectrum of **K,Li-8** dissolved in 1M LiCl solution at pH1
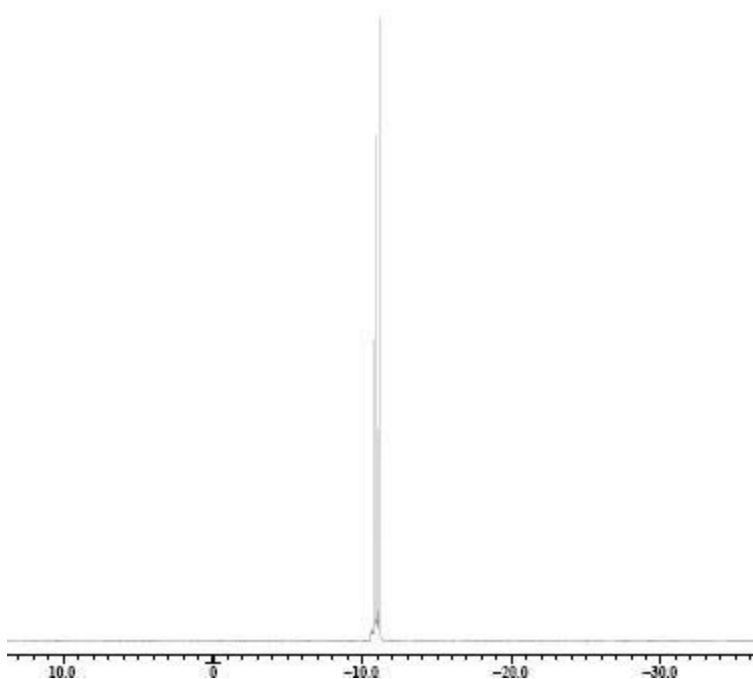
Fig. 3.32 ^{31}P-NMR spectrum of **K,Li-8** dissolved in water/D$_2$O

^{183}W-NMR provided another evidence to the existence of the monomeric or dimeric Ti-substituted {P$_2$W$_{16}$} specie in solution. The solid crystals were dissolved in the same solution above described; the spectrum measured showed eight peaks in a ratio close to the expected 1:1:1:1:1:1:1:1 at the chemical shifts -127.1, -136.2, -142.3, -172.6, -175.1, -184.2, -185.8 and -224.7 ppm. (Fig. 3.33)
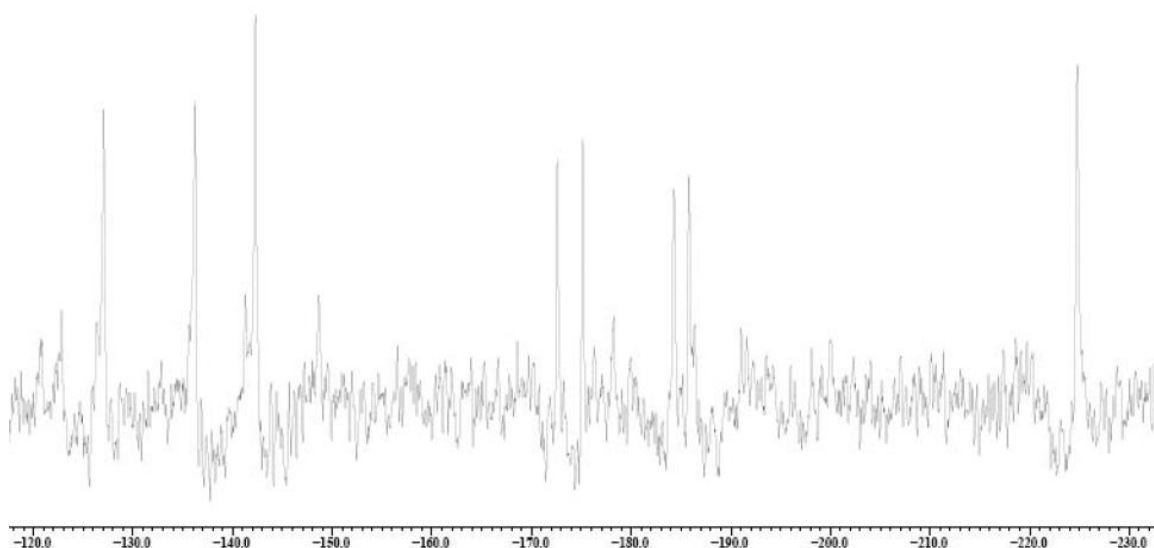
Fig. 3.33 ^{183}W-NMR spectrum of **K,Li-8** dissolved in 1M LiCl solution at pH1

3.4.1.6 *Conclusion*

A new dimeric compound based on the Wells-Dawson anion was synthesized starting from $\{P_2W_{12}\}$ as a POM precursor and $K_2Ti(O)(C_2O_4)_2$ as titanium precursor. The resulting structure revealed by X-Ray analysis is composed of two subunits constituting of a di-titanium substituted $\{P_2W_{16}\}$ moiety each. The two subunits are connected via two external titanium atoms bearing two oxalate groups each. The full formula arrived at through multiple analytical techniques, XRD, TGA and EA, is $K_{15}Li_5[P_4W_{32}Ti_6(C_2O_4)_4O_{124}].53H_2O$. ^{31}P- and ^{183}W-NMR studies showed that the compound stays monomerically or dimerically intact in solution. What the NMR spectra indicate definitively is that the species that exist, in case the compound really falls apart, are equivalent in a way to result in similar ^{31}P- and ^{183}W-NMR spectra.

3.5 Disordered structures

Solid crystalline products with crystallographic defects are very likely to form. I will herein introduce two examples. The first is a hexameric structure of Ti-containing AsW_9 species and will be referred to as polyanion **9**, while the second results from the attachment of four titanium atoms disordered over eight positions on both sides of a $\{P_8W_{48}\}$ ring. The latter will be referred to as polyanion **10**.

3.5.1 $[Ti_{9.3} As_6 W_{59.7} O_{244} (H_2O)_4]^{82-}$, Polyanion **9**

1g of the precursor $Na_9[B\text{-}\alpha\text{-}AsW_9O_{33}].27H_2O$ was mixed with 130 μL of $TiOCl_2.xH_2O$ (d = 1.58 g.mol^{-1}) in a 2:1 molar ratio in 20 mL of water. The pH of the resulting mixture was adjusted to 3 and then the solution was heated for 1 hour at 80°C. After cooling, few drops of 1M CsCl solution were added, and the crystals appeared in a few weeks upon the slow evaporation of the solvent.

The resulting compound crystallizes in the triclinic P$\bar{1}$ space group with the following unit cell parameters: (a= 19.9280(15) Å, b= 21.2079(14) Å, c= 24.4760(26) Å, α= 105.934(4)°, ß= 102.918(4)°, γ= 111.309(3)°).

Based on single-crystal XRD analysis, it was explicitly modeled as a hexamer that consists of six units of $\alpha\text{-}AsW_9O_{33}$ linked to each other by extra tungsten and titanium atoms via Ti-O-Ti and Ti-O-W bonds as shown in Fig. 3.34.

This compound is closely related to $[As^{III}_6W_{65}O_{217}(H_2O)_7]^{26-}$ $\{As_6W_{65}\}$ reported by Kortz *et al.* in 2001[40] which consists of four inner ($\beta\text{-}AsW_9O_{33}$) and two outer ($\alpha\text{-}AsW_9O_{33}$) fragments, which are linked together by a total of eleven corner-sharing WO_6 octahedra. The eleven Ti atoms in **9** are arranged in a different way in the core since unlike $\{As_6W_{65}\}$ all six $\{AsW_9\}$ units are alpha

isomers. The two structures however have the chair confirmation resembling that of cyclohexane (Fig. 3.35) and both have the same point group C_{2h}.
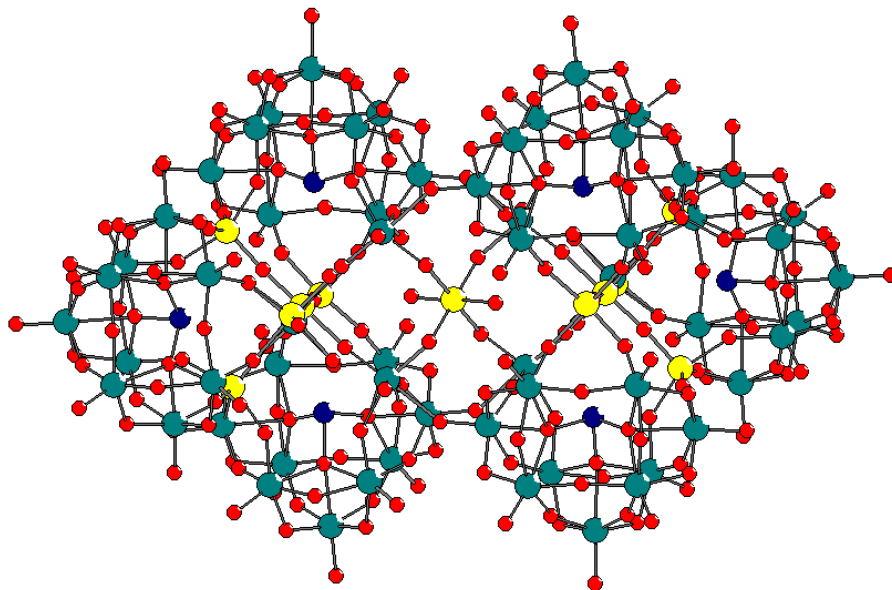
Fig. 3.34 Ball and stick representation of **9**. Color code: teal (W), yellow (Ti), red (O) and dark blue (As)
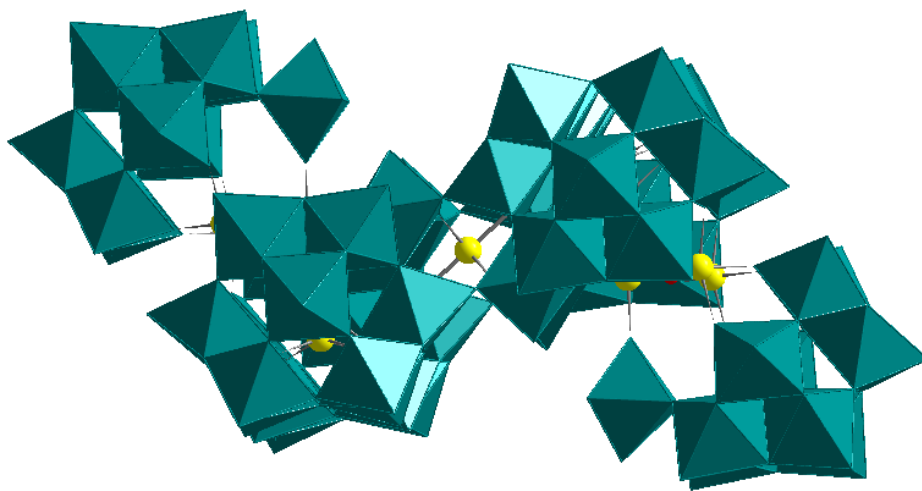
Fig. 3.35 Polyhedral representation of **9** showing the chair confirmation

The formula of this compound based on the XRD analysis is $[Ti_{9.3} As_6 W_{59.7} O_{244} (H_2O)_4]^{82-}$ since three out of the eleven titanium atoms are disordered with tungsten, the one at the center of symmetry and two others related by symmetry.

3.5.2 {Ti₄P₈W₄₈}, Polyanion 10

The reaction of 0.2 g of $K_{28}Li_5[H_7P_8W_{48}O_{184}].92H_2O$ (0.013 mmol) and 0.1 g of **Ti4** (0.08 mmol) led to the formation of big crystals after one week of slow evaporation of the solvent. The reagents were dissolved in 20 mL of 1M LiCl solution at room temperature; pH was changed from ~4 to 2 using concentrated HCl solution.

The crystal belongs to the tetragonal space group I4/m with $\alpha = \beta = \gamma = 90°$. The unit cell edge lengths are a = 27.3210(15), b = 27.3210(18) and c = 21.1015(22) Å.
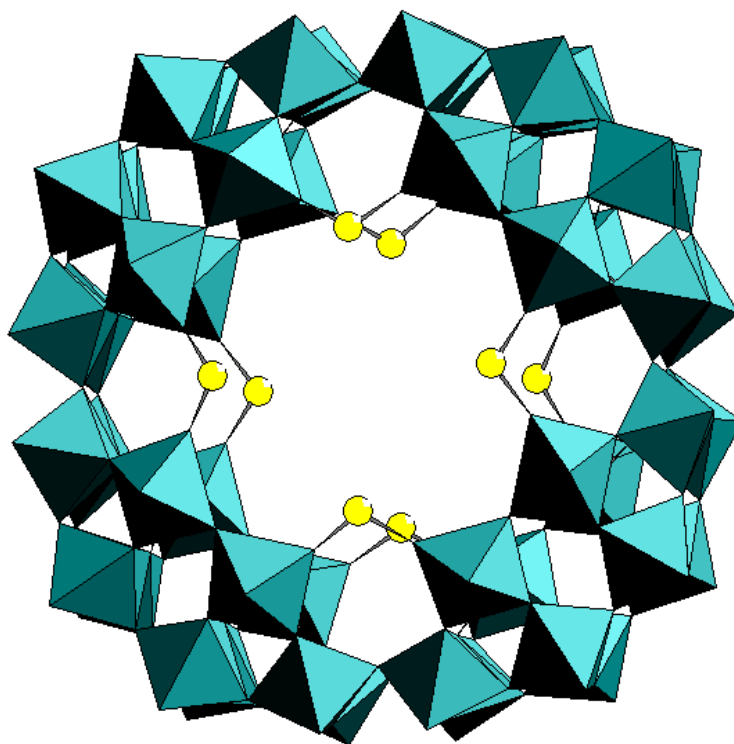
Fig. 3.36 Polyhedral representation of **10** showing the eight disordered titanium atoms with missing oxygens

The single crystal XRD measurement, though repeated multiple times, could not print an unequivocal image of the structure of the crystal (Fig. 3.36).

The complete coordination spheres of the Ti atoms were not spotted. Each titanium seems to miss four other oxygens. Moreover, each is 50 % disordered over its own position. The eight Ti atoms are actually four in each molecule at alternating positions above and below the ring.

3.6 References

[1] Greenwood, N. N.; Earnshaw, A. *Chemistry of the elements, second edition* Butterworth-Heinemann, Elsevier Science ltd, 1997.

[2] Kholdeeva, O. A.; Maksimovskaya, R. I. *Journal of Molecular Catalysis A: Chemical* **2007**, 262, 7.

[3] Kholdeeva, O. A.; Trubitsina, T. A.; Maksimov, G. M; Golovin, A.V.; Maksimovskaya, R. I. *Inorg. chem* **2005**, 44, 1635.

[4] Kholdeeva, O. A.; Maksimov, G.M.; Maksimovskaya, R. I.; Kovaleva, L.A.; Fedotov, M.A. *React. Kinet. Catal. Lett* **1999**, 66, 311.

[5] Kholdeeva, O.A.; Mel'gunov, M.S.; Shmakov, A.N.; Trukhan, N.N.; Kriventsov, V.V.; Zaikovskii, V.I.; Malyshev, M.E.; Romannikov, V.N. *Catalysis Today* **2004**, 91-92, 205.

[6] Fierro, J. L. G. *Metal Oxides, Chemistry and Applications.* s.l. : CRC Press, Taylor and Francis Group, 2006.

[7] Yamaze, T.; Cao, X.; Yazaki, S. *Journal of Molecular Catalysis A: Chemical* **2007**, 262, 119.

[8] Yamase, T.; Ozeki, T.; Sakamoto, H.; Nishiya, S.; Yamamoto, A. *Bull. Chem. Soc. Jpn.* **1993,** 66, 103.

[9] Wang, X. H.; Liu, J. F.; Chen, Y. G.; Liu, Q.; Liu, J. T.; Pope, M. T. *Journal of the Chemical Society-Dalton Transactions* **2000,** 1139.

[10] Tan, R. X.; Li, D. L.; Wu, H. B.; Zhang, C. L.; Wang, X. H. *Inorganic Chemistry Communications* **2008,** 11, 835.

[11] Nsouli, N. H.; Bassil, B. S.; Dickman, M. H.; Kortz, U.; Keita, B.; Nadjo, L. I*norg. Chem.* **2006,** 45, 3858.

[12] Ren, Y. H.; Liu, S. X.; Cao, R. G.; Zhao, X. Y.; Cao, J. F.; Gao, C. Y. *Inorganic Chemistry Communications* **2008,** 11, 1320.

[13] Al-Kadamany, G. A.; Hussain, F.; Mal, S. S.; Dickman, M. H.; Leclerc-Laronze, N.;Marrot, J.; Cadot, E.; Kortz, U. *Inorg. Chem.* **2008,** 47, 8574.

[14] Laronze, N.; Marrot, J.; Herve´, G. *Chem. Commun.* **2003**, 2360.

[15] Brown, I. D.; Altermatt, D. *Acta Crst.* **1985**, B41, 244.

[16] Kortz, U.; Hamzeh, S. S.; Nasser, N. A. *Chemistry-a European Journal* **2003,** 9, 2945.

[17] Kim, G. S.; Zeng, H.; VanDerveer, D.; Hill, C. L. *Angew. Chem.* **1999**, 111, 3413; *Angew. Chem. Int. Ed.* **1999**, 38, 3205.

[18] Zhao, J. W.; Zhang, J.; Zheng, S. T.; Yang G. Y. *Inorg. Chem* **2007**, 46, 10944.

[19] Nomiya, K.; Takahashi, M.; Ohsawa, K.; Widegren, J. A. *Journal of the Chemical Society-Dalton Transactions* **2001,** 2872.

[20] Mouri, Y.; Sakai, Y.; Kobayashi, Y.; Yoshida, S.; Nomiya, K. *Materials* **2010**, 3, 503.

[21] Hussain, F.; Bassil, B. S.; Kortz, U.; Kholdeeva, O. A.; Timofeeva, M. N.; de Oliveira, P.; Keita, B.; Nadjo, L. *Chemistry-a European Journal* **2007,** 13, 4733.

[22] Kholdeeva, O. A.; Donoeva, B. G.; Trubitsina, T. A.; Al-Kadamany, G.; Kortz, U. *European Journal of Inorganic Chemistry* **2009,** 5134.

[23] Bösing, M.; Loose, I.; Pohlmann, H.; Krebs, B. *Chem. Eur. J.* **1997**, *3*, 1232.

[24] Hornstein, B. J.; Finke, R. G. *Inorg. Chem.* **2002,** 41, 2720.

[25] Contant, R.; Teze, A. *Inorg. Chem.* **1985,** 24, 4610.

[26] Judd, D. A.; Chen, Q.; Campana, C. F.; Hill, C. L. *J. Am. Chem. Soc.* **1997,** 119, 5461.

[27] Godin, B.; Chen, Y. G.; Vaissermann, J.; Ruhlmann, L.; Verdaguer, M.; Gouzerh, P. *Angewandte Chemie-International Edition* **2005,** 44, 3072.

[28] Zhang, Z. M.; Yao, S.; Li, Y. G.; Wang, Y. H.; Qi, Y. F.; Wang, E. B. *Chemical Communications* **2008,** 1650.

[29] Yao, S.; Zhang, Z.; Li, Y.; Lu, Y.; Wang, E. B.; Su, Z.*Crystal Growth and Design* **2010**, 10, 135.

[30] Zhang, Z. M.; Yao, S.; Qi, Y. F.; Li, Y. G.; Wang, Y. H.; Wang, E. *Dalton Transactions* **2008,** 3051.

[31] Godin, B.; Vaissermann, J.; Herson, P.; Ruhlmann, L.; Verdaguer, M.; Gouzerh, P. *Chemical Communications* **2005,** 5624.

[32] Yao, S.; Zhang, Z. M.; Li, Y. G.; Wang, E. *Dalton Transactions* **2009,** 1786.

[33] Kortz, U. *Journal of Cluster Science* **2003,** 14, 205.

[34] Ostuni, A.; Pope, M. T. *Comptes Rendus De L Academie Des Sciences Serie Ii Fascicule C-Chimie* **2000,** 3, 199.

[35] Mitchell, S. G.; Khanra, S.; Miras, H. N.; Boyd, T.; Long, D. L.; Cronin, L. *Chemical Communications* **2009,** 2712.

[36] Gaunt, A. J.; May, I.; Collison, D.; Holman, K. T.; Pope, M. T. *J. Mol. Struct.* **2003,** 656, 101.

[37] Saku, Y.; Sakai, Y.; Nomiya, K. *Inorganic Chemistry Communications* **2009,** 12, 650.

[38] Crano, N. J.; Chambers, R. C.; Lynch, V. M.; Fox, M. A. *Journal of Molecular Catalysis A-Chemical* **1996,** 114, 65.

[39] Nomiya, K.; Arai, Y.; Shimizu, Y.; Takahashi, M.; Takayama, T.; Weiner, H.; Nagata, T.; Widegren, J. A.; Finke, R. G. *Inorg. Chim. Acta* **2000,** 300, 285.

[40] Kortz, U.; Savelieff M. G.; Bassil, B. *Angew. Chem. Int. Ed.* **2001**, 40**,** 3384.

Chapter IV

Catalytic Results

4.1 Heterogeneous catalysis with Ru-POMs

The catalytic efficiency of ruthenium complexes for various organic transformations[1] has triggered attempts to synthesize ruthenium-containing POMs. Their high reactivity and selectivity toward the catalytic oxidation of a variety of organic substrates by O_2 and H_2O_2 were confirmed in the past few years.[2] Neumann and Dahan in 1997 described the use of the polyoxometalates $\{[WZnRu_2(OH)(H_2O)](ZnW_9O_{34})_2\}^{11-}$ as a catalyst for non-radical molecular oxygen activation and alkene epoxidation. The polyoxometalate that acts as a dioxygenase catalyst has the advantages of being stable against decomposition by self-oxidation.[2b] Other more detailed studies were published by the same group on the same sandwich-type ruthenium-containing compounds used as catalysts for hydroxylation of adamantane[2c] and oxidation of allylic alcohols with organic hydroperoxides as oxygen sources.[2f] All above mentioned findings of Neumann concerning the mechanism of reaction were reinvestigated by Finke in a thorough report in 2005.[2g] In 2002, Mizuno *et.al* published the results of the catalytic study conducted on the TBA-salt of the ruthenium substituted silicotungstate $[SiW_{11}Ru^{III}(H_2O)O_{39}]^{5-}$. It was shown that it can act as an efficient heterogeneous catalyst for the oxidation of a wide range of alkanes and alcohols using 1 atm of molecular oxygen as the sole oxidant.[2e] These were just examples, but we can find many other reports published in this area.

A class of sandwich-type POMs based on two lone-pair containing, β-Keggin fragments, e.g. $[\beta\text{-}Sb^{III}W_9O_{33}]^{9-}$ and $[\beta\text{-}Bi^{III}W_9O_{33}]^{9-}$ has emerged. The first

members of this class, $([M_2(H_2O)_6(WO_2)_2(\beta\text{-}SbW_9O_{33})_2]^{(14\text{-}2n)\text{-}}$ (M^{n+} = Mn^{2+}, Fe^{3+}, Co^{2+}, Ni^{2+}), were reported by Krebs *et al.* in 1997.[3] Since then some more isostructural derivatives have been characterized.[4]

Other examples of Ru-containing POMs, $[O\{Ru^{IV}Cl(\alpha_2\text{-}P_2W_{17}O_{61})\}_2]^{16\text{-}}$, $[WZnRu^{III}_2(OH)(H2O)(ZnW_9O_{34})_2]^{11\text{-}}$, $[SiW_{11}Ru^{III}O_{39}(H_2O)]^{5\text{-}}$ and $\{Ru_4O_4(OH)_4(H_2O)_4\}(\gamma\text{-}SiW_{10}O_{36})_2]^{10\text{-}}$ have been reported.[5] In 2004, our group published the structures of several $Ru^{II}(dmso)_3$-supported heteropolytungstates.[6] We also discovered that dmso inhibits the desired redox liability of the ruthenium centers. Thus we moved to organo-ruthenium precursors (e.g., $[(benzene)RuCl_2]_2$, $[(p\text{-}cymene)RuCl_2]_2$) and reacted those with a large variety of lacunary polytungstates. We successfully synthesized organo-Ru(II)-supported lacunary tungstosilicates and -germanates, $[(RuC_6H_6)_2XW_9O_{34}]^{6\text{-}}$ (X = Si, Ge) and $[\{Ru(C_6H_6)(H_2O)\}\{Ru(C_6H_6)\}(\gamma\text{-}XW_{10}O_{36})]^{4\text{-}}$ (X = Si, Ge), lacunary tungstoarsenate and tungstophosphate $[(Ru\text{-}C_6H_6)XW_9O_{34}]^{7\text{-}}$ (X = P, As), zinc-substituted tungstoarsenate, and a derivative of the cyclic $[H_7P_8W_{48}O_{184}]^{33\text{-}}$ anion, $[\{K(H_2O)\}_3\{Ru(p\text{-}cymene)(H_2O)\}_4P_8W_{49}O_{186}(H_2O)_2]^{27\text{-}}$.[8] Before us some other groups reported on organometallic ruthenium POMs structures, most of them being characterized by elemental analysis, IR, and multinuclear NMR.[8] In 2005, Proust and co-workers reported on the Keggin-based (arene)Ru^{2+} derivatives $[PW_{11}O_{39}\{Ru(arene)(H_2O)\}]^{5\text{-}}$ and $[\{PW_{11}O_{39}\{Ru(arene)\}\}_2\{WO_2\}]^{8\text{-}}$ (arene = benzene, toluene, p-cymene, hexamethylbenzene),[9] and also the first Ru-derivative with the Krebs-type structure, $[Sb_2W_{20}O_{70}\{Ru(p\text{-}cymene)\}_2]^{10\text{-}}$.[10] In 2006, Sakai *et al.* reported on the Wells-Dawson derivatives $[\{(benzene)Ru(H_2O)(\alpha_2\text{-}P_2W_{17}O_{61})]^{8\text{-}}$ and $[\{(pcymene)Ru(H_2O)\}(\alpha_2\text{-}P_2W_{17}O_{61})]^{8\text{-}}$,[11] and they also showed that these species can act as homogeneous catalyst precursors for the selective oxidations of a wide variety of alcohols with 1 atm molecular oxygen in water-alcohol biphasic media without any additives.[12]

The synthesis, structure and catalytic properties of four (arene)Ru^{2+} derivatives of the Krebs type $[X_2W_{22}O_{74}(OH)_2]^{12-}$ (X = Sb^{III}, Bi^{III}) structure will be here presented.

4.1.1 Synthetic procedures, FT-IR and nuclear magnetic resonance spectroscopy data

$K_5Na_5[Sb_2W_{20}O_{70}(RuC_6H_6)_2].22H_2O$ **K,Na-11**

$[(C_6H_6)RuCl_2]_2$ (0.04 g; 0.08 mmol) and $Na_{12}[Sb_2W_{22}O_{74}(OH)_2]$ (0.5 g; 0.08 mmol) were dissolved with stirring and heating to 50°C for 30 min in 20 mL of 0.5 M sodium acetate buffer (pH 6.0). The solution was cooled and then filtered. Then 0.5mLof 1.0M KCl solution was added to the filtrate which was left for slow evaporation. A dark red-brown crystalline product was collected by filtration (yield 0.22 g, 47%).

IR of **K,Na-11**: 480 (w), 560 (sh), 601 (m), 768 (s), 841 (m), 882 (sh), 931 (s), 1436 (w), 1618 (m), 1638 (m) cm^{-1}.

Anal. Calcd (Found) for **K,Na-11**: K 3.2 (2.6), Na 1.9 (1.9), W 60.2 (59.5), Ru 3.3 (2.9), Sb 4.0 (4.2), C 2.4 (2.4), H 0.9 (1.0).

NMR of **K,Na-11** in D$_2$O at 293 K: ^{1}H: 6.1 ppm; ^{13}C: 80.8 ppm; ^{138}W: -58.4, -103.1, -115.8, -125.4, -157.3, and -334.1 ppm.

$Cs_2Na_8[Bi_2W_{20}O_{70}(RuC_6H_6)_2].30H_2O$ **Cs,Na-12**

$[(C_6H_6)$- $RuCl_2]_2$ (0.04 g; 0.08 mmol) and $Na_{12}[Bi_2W_{22}O_{74}(OH)_2]$ (0.5 g; 0.08 mmol) were dissolved with stirring and heating to 50°C for 30 min in 20 mL of 0.5 M sodium acetate buffer (pH 6.0). The solution was cooled and then filtered. Then 0.5 mL of 1.0 M CsCl solution was added to the filtrate which

was left for slow evaporation. A dark red crystalline product was collected by filtration (yield 0.23 g, 47%).

IR of **Cs,Na-12**: 459 (w), 518 (sh), 609 (sh), 647 (m), 745 (s), 800 (vs), 843 (sh), 943 (s), 1430 (w), 1630 (m) cm^{-1}.

Anal. Calcd (Found) for **Cs,Na-12**: Na 2.8 (2.8),W 56.0 (54.8), Ru 3.1 (2.8), Bi 6.4 (6.0), C 2.2 (2.6), H 1.1 (1.3).

NMR of **Cs,Na-12** in D2O at 293K: ^{1}H: 6.1ppm; ^{13}C: 81.0 ppm; ^{138}W: -31.1, -88.8, -111.8, -125.1, -154.7, and -336.1 ppm.

$Cs_3Na_7[Sb_2W_{20}O_{70}(RuC_{10}H_{14})_2].27H_2O$ **Cs,Na-13**

A 0.05 g (0.08 mmol) sample of $[(C_{10}H_{14})RuCl_2]_2$ was dissolved with stirring in 20 mL of 0.5Msodium acetate buffer (pH 6.0). Then 0.5 g (0.08 mmol) of $Na_{12}[Sb_2W_{22}O_{74}(OH)_2]$ was added. The solution was stirred at room temperature for 2 h and filtered. Then 0.5 mL of 1.0 M CsCl solution was added to the filtrate which was left for slow evaporation. An orange crystalline product was collected by filtration (yield 0.18 g, 39%).

IR of **Cs,Na-13**: 457 (w), 667 (w), 703 (w), 769 (s), 807 (s), 845 (sh), 948 (s), 1642 (m) cm^{-1}.

Anal. Calcd (Found) for **Cs,Na-13**: Cs 6.1 (5.4), Na 2.5 (2.3), W56.1 (55.3), Ru 3.1 (2.9), Sb 3.7 (3.8), C 3.7 (3.6), H 1.3 (1.3).

NMR of **Cs,Na-13** in D$_2$O at 293 K: ^{1}H: 1.38, 1.40, 2.34, 3.07, 5.61, 5.63, 6.18, 6.20 ppm; ^{13}C: 16.98, 17.05, 22.15, 30.55, 31.06, 75.79, 76.36, 83.22, 96.47, 99.05 ppm; ^{138}W: -71.9, -103.1, -118.8, -165.7, and -327.6 ppm.

$Na_{10}[Bi_2W_{20}O_{70}(RuC_{10}H_{14})_2].35H_2O$ **Na-14**

$[(C_{10}H_{14})\text{-} RuCl_2]_2$ (0.05 g; 0.08 mmol) and $Na_{12}[Bi_2W_{22}O_{74}(OH)_2]$ (0.5 g; 0.08 mmol) were dissolved with stirring and heating to 50°C for 30 min in 20 mL of 0.5 M sodium acetate buffer (pH 6.0). The solution was cooled and then filtered. Then 0.5mLof 1.0MKCl solution was added to the filtrate which was left for slow evaporation. An orange crystalline product was collected by filtration (yield 0.18 g, 39%).

IR of **Na-14**: 645 (vw), 735 (vw), 797 (w), 820 (sh), 947 (m), 1380 (vw), 1454 (w), 1625 (s) cm^{-1}.

Anal. Calcd (Found) for **Na-14**: Na 3.5 (3.1),W 56.2 (55.5), Ru 3.1 (2.7), Bi 6.4 (6.1), C 3.7 (4.0), H 1.5 (1.3).

NMR of **Na-14** in D_2O at 293 K: ^{1}H: 1.39, 1.41, 2.36, 3.07, 5.63, 5.64, 6.21, 6.22 ppm; ^{13}C: 16.86, 17.05, 22.52, 30.91, 31.06, 76.13, 76.36, 84.11, 96.26, 98.43 ppm; ^{138}W:-43.8,-88.9, -113.6, -117.8, -159.9, and -330.8 ppm.

^{183}W-NMR , ^{1}H-NMR and ^{13}C-NMR of the four compounds are shown in Fig. 4.1, Fig. 4.2 and Fig. 4.3 respectively.
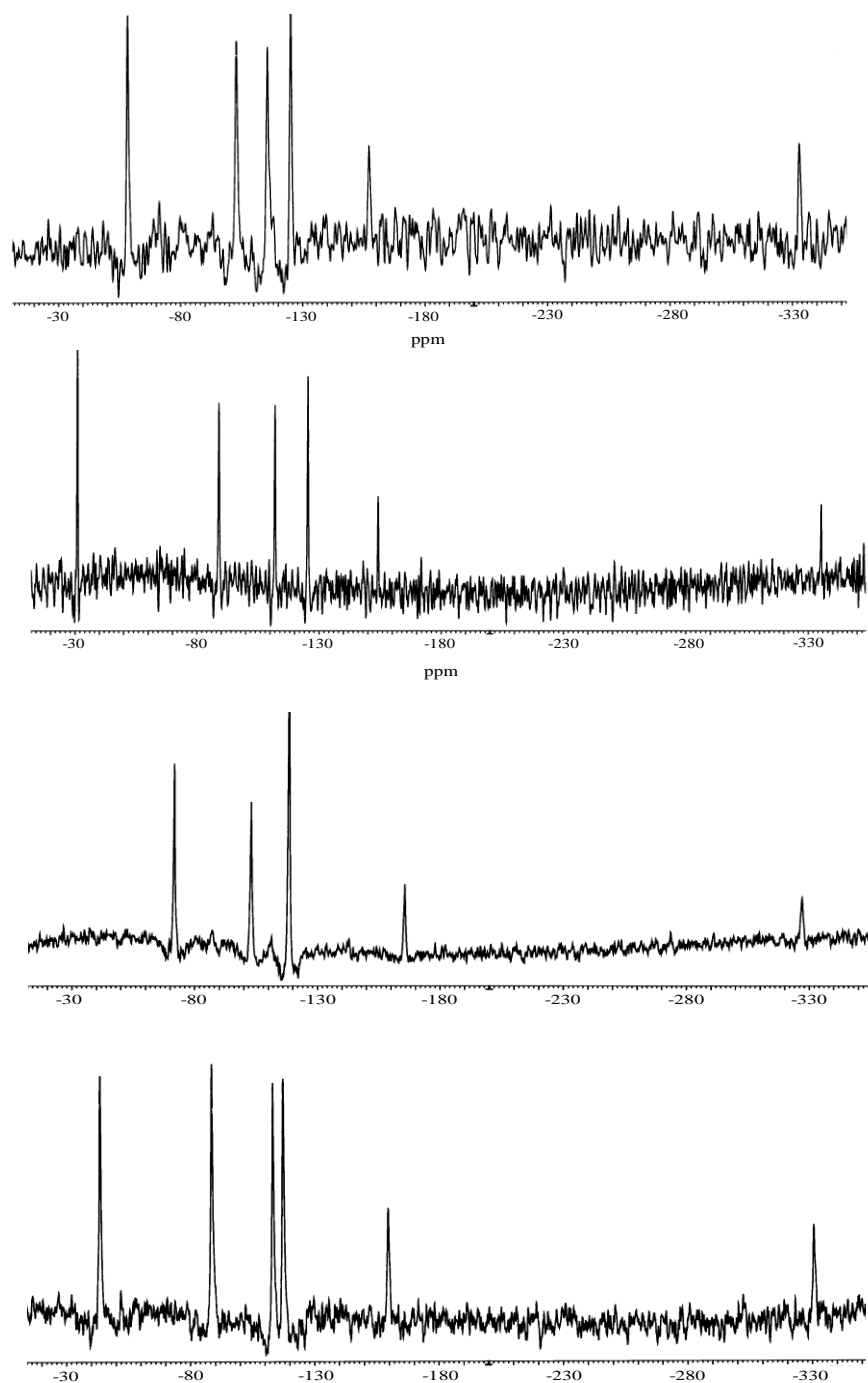
Fig. 4.1 [183]W-NMR spectra of **K,Na-11**, **Cs,Na-12**, **Cs,Na-13** and **Na-14** from top down dissolved in water/D$_2$O
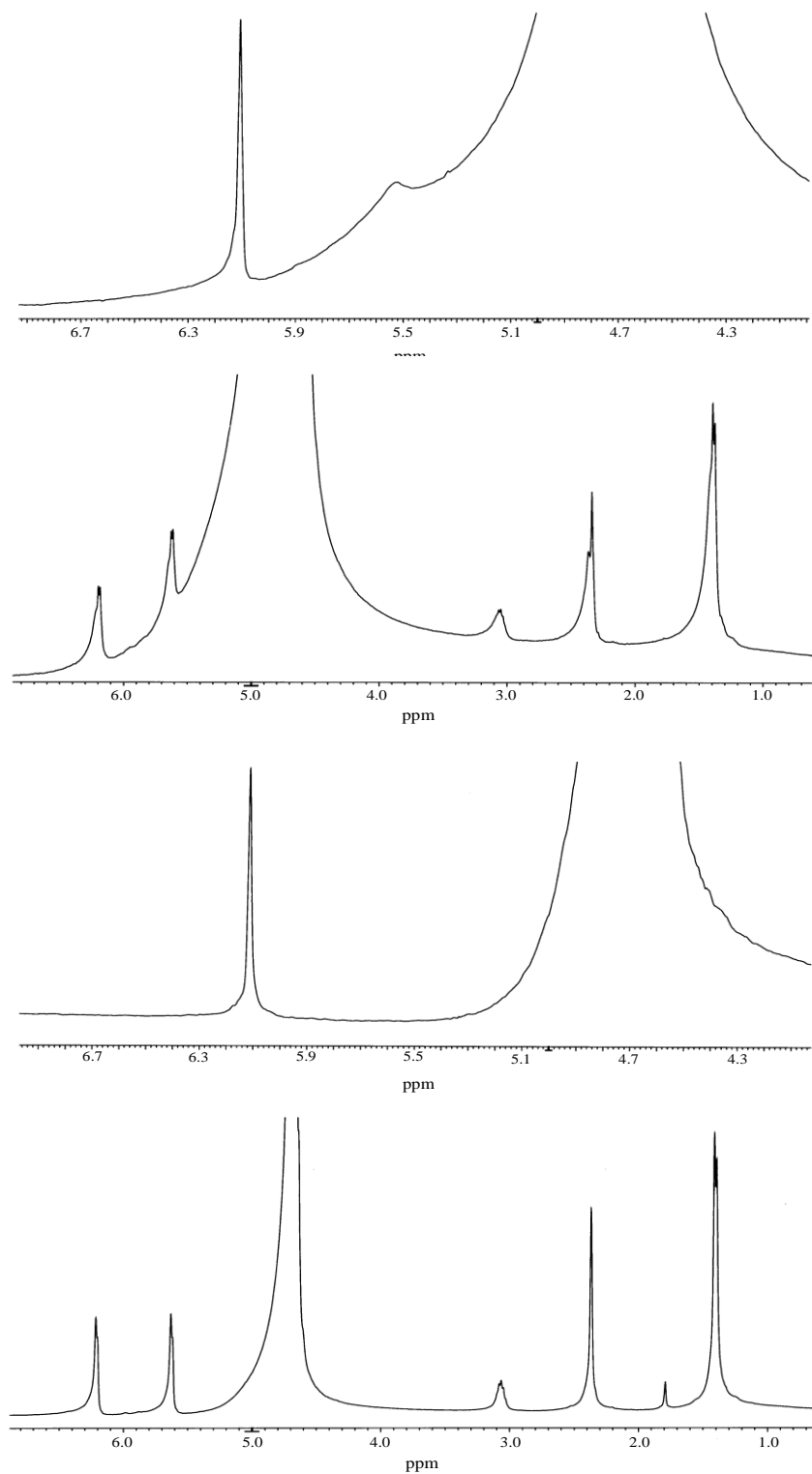
Fig. 4.2 ^{1}H-NMR spectra of **K,Na-11**, **Cs,Na-12**, **Cs,Na-13** and **Na-14** from top down dissolved in water/D_2O
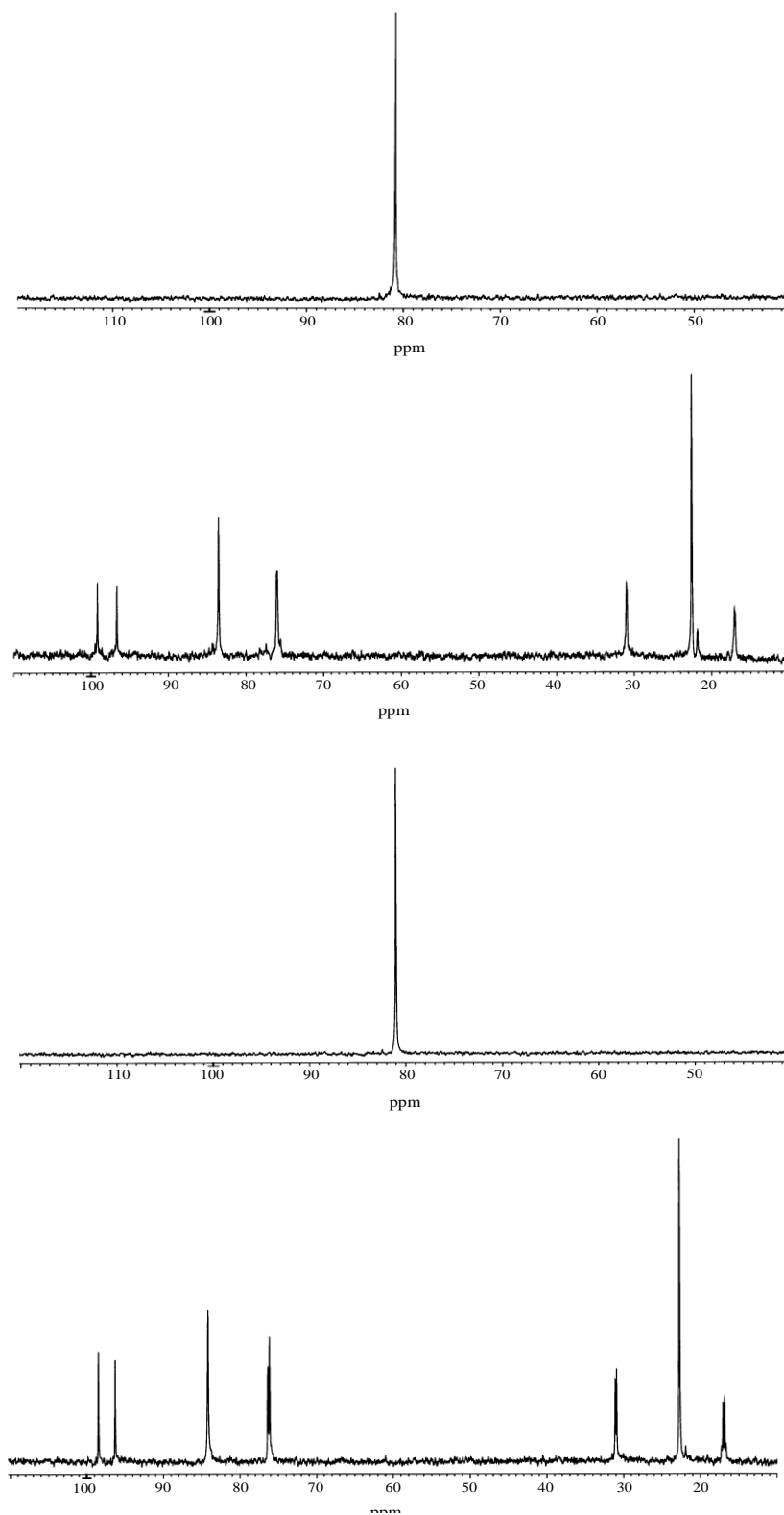
Fig. 4.3 ^{13}C-NMR spectra of **K,Na-11**, **Cs,Na-12**, **Cs,Na-13** and **Na-14** from top down dissolved in water/D_2O

4.1.2 Structure discussion

The synthesis of **11-14** was accomplished by reaction of $[X_2W_{22}O_{74}(OH)_2]^{12-}$ (X = Sb^{III}, Bi^{III}) and $[Ru(arene)Cl_2]_2$ in equimolar ratios in sodium acetate buffer medium (pH 6.0). This indicates that the dimeric Ru-precursor is hydrolyzed at such conditions, providing the reactive mononuclear electrophile in situ. Polyanions **11-14** were also obtained upon reacting $[Ru(arene)Cl_2]_2$ and $[X_2W_{22}O_{74}(OH)_2]^{12-}$ (X = Sb^{III}, Bi^{III}) in higher molar ratios (e.g., 2:1 and 3:1). Polyanion **13** had already been prepared by Proust's group, albeit through a different route by reaction of $[(C_{10}H_{14})\text{-}RuCl_2]_2$ with $Na_2WO_4.2H_2O$ and Sb_2O_3 instead of $Na_{12}[Sb_2W_{22}O_{74}(OH)_2]$ used in this procedure.[12] The benzene derivatives **11** and **12** represent the first examples of lone-pair-containing heteropolytungstates bearing a $Ru(C_6H_6)$ unit. Our group as well as others have already reported some organo-tin derivatives of this class of POMs.[15] Polyanions **11-14** consist of two lacunary B-β-$[XW_9O_{33}]^{9-}$ (X=Sb^{III}, Bi^{III}) Keggin fragments linked via two inner *cis*-WO_2 groups and two outer (arene)Ru^{2+} units leading to a structure with idealized C_{2h} symmetry (Fig 4.4).
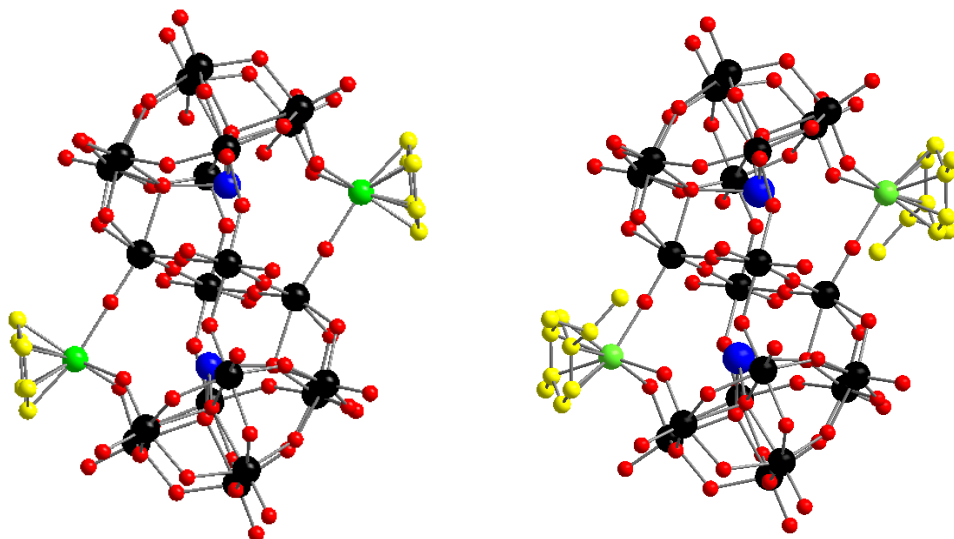
Fig. 4.4 Ball-and-stick representations of polyanions **11** and **12** $[X_2W_{20}O_{70}(RuC_6H_6)_2]^{10-}$ (X = Sb, Bi), left, and polyanions **13** and **14** $[X_2W_{20}O_{70}(RuC_{10}H_{14})_2]^{10-}$ (X = Sb, Bi), right. Color code: black (W), red (O), green (Ru), yellow (C) and blue (Sb or Bi)

Alternatively, these polyanions can be described as a dilacunary $[X_2W_{20}O_{70}]^{14-}$ fragment substituted by two (arene)Ru^{2+} units. The structure of **11-14** is closely related to the parent structure $[X_2W_{22}O_{74}(OH)_2]^{12-}$ and its transition-metal-substituted derivatives $[X_2W_{20}M_2O_{70}(H_2O)_6]^{(14-2n)-}$ (X=Sb^{III}, Bi^{III}; M^{n+} = Fe^{3+}, Co^{2+}, Ni^{2+}, Cu^{2+}, Zn^{2+}).[1a,2a,2c] The only difference is that the two outer WO$_3$ groups in $[X_2W_{22}O_{74}(OH)_2]^{12-}$ and the two transition-metal ions with three aqua ligands each in $[X_2W_{20}M_2O_{70}(H_2O)_6]^{(14-2n)-}$ have been exchanged for (arene)Ru^{2+} in the case of **11-14**. The ruthenium ions in the four polyanions **11-14** are bound via an oxygen atom to one {XW$_9$O$_{33}$} unit, and via two oxygens to the other. Other dimeric organometallic ruthenium containing heteropolytungstates do not exhibit such a binding mode of the Ru center which is most likely dictated by the lone pair repulsion in **11-14**. For example, in $[(PW_9O_{34})_2(cis-WO_2)(cis-RuL^{Me}_2)]^{13-}$ (L^{Me} = 1,3-dimethylimidazolidine-2-ylidene) the ruthenium ion is coordinated to the {P$_2$W$_{19}$O$_{70}$} fragment via four

Ru-O-W bonds, two to each of the {PW$_9$O$_{34}$} units.[10] In the case of [{PW$_{11}$O$_{39}${Ru(arene)}}$_2${WO$_2$}]$^{8-}$ (arene = benzene, toluene), each Ru(arene) group is linked to two oxygen atoms of the lacuna and an oxo ligand of the {WO$_2$} group.[9]

Nevertheless, the Ru-O(W) distances in **11** to **14** fall in a range comparable to what has been reported for the two abovementioned polyanions: 2.08(1)-2.09(1) Å for 1, 2.08(1)-2.10(1) Å for 2, 2.08(2)-2.10(2) Å for 3, and 2.08(2)-2.14(2) Å for 4. The Ru-O-W angles of the four compounds **11-14** are in the range 131.0(7)-177.5(7)° which is larger than 150.3(17)-161.3-(17)°, reported for [{PW$_{11}$O$_{39}${Ru(arene)}}$_2${WO$_2$}]$^{8-}$ (arene = benzene, toluene). Bond-valence sum (BVS) calculations for **11-14** indicate that there are no protonation sites and therefore the charge of the polyanions must be -10. In the solid state these charges are balanced by either one or two types of alkali metal ions (sodium, potassium, cesium). Not all sodium ions could be detected by single-crystal XRD because of disorder. However, the presence of the remaining sodium ions was verified by elemental analysis.

Multinuclear solution NMR studies were performed on the diamagnetic polyanions **11-14** at room temperature, by dissolving the respective salts **K,Na-11**, **Cs,Na-12**, **Cs,Na-13**, and **Na-14** in D$_2$O. The ^{183}W NMR spectra of **11**, **12**, and **14** exhibit the expected six line pattern between -30 and -340 ppm with relative intensities 2:2:2:2:1:1, characteristic of the idealized C$_{2h}$ symmetry of the polyanions. For **13** we only see five instead of the expected six lines, which is almost certainly because of coincidental overlap of two signals within the set of four intense downfield signals. The signal at -118.8 ppm is in fact significantly more intense than the other two corresponding downfield signals (this is fully consistent with the observations of Proust *et al.*).[10] Also for polyanion **14** the two central signals are very close, but can still be distinguished (-113.6 and -117.8 ppm). The ^{1}H- and ^{13}C NMR spectra of **11** and **12** show only one signal, most likely indicating fast rotation of the arene

ligands around the C_6-axis in solution which renders all carbons and protons of the two $Ru(C_6H_6)$ groups magnetically equivalent. This phenomenon was also observed for other organo-Ru supported heteropolytungstates.[7a,b,8d,9,10]

On the other hand, for **13** and **14** we observed five signals in ^1H NMR and seven signals in ^{13}C-NMR, which reflects exactly the number of magnetically inequivalent protons and carbons in p-cymene. This also implies that fast rotation of the sterically more demanding p-cymene (compared to benzene) around the Ru-arene vector is unlikely.

4.1.3 Catalytic experiments

The four polyanions salts were tested for their heterogeneous catalytic efficiency toward the air oxidation of the aromatic hydrocarbon p-xylene. The detailed experimental procedure is as follows:

Five milliliters of p-xylene, 10 mg of the non-dissolved catalyst, and 0.1 g of tert-butylhydroperoxide were stirred in a 25 mL 2-necked-round-bottom flask at 130°C with constant air flow of about 10 mL/min for 12 h. The solution was allowed to cool to ambient temperature, and then the solid product was separated by filtration. The filtrate contained p-tolualdehyde, 4-methylbenzyl alcohol, p-toluic acid, and unreacted p-xylene.

The acids formed were esterified using the following procedure: 300 μL of the sample was taken in a glass vial; 2 mL of 14% borontrifluoride (BF_3) in methanol was added to the vial which was sealed with a Teflon lined stopper and heated for 1 h at 80°C. The sample was cooled to room temperature, and 2 mL of deionized water was added with mild shaking. The esters formed were extracted by the addition of 2 mL of HPLC grade dichloromethane. The lower organic layer containing the product was analyzed by GC.

Hot filtration experiments: reactions were performed with the same conditions as described above for p-xylene or hexadecane oxidation; however,

a 1 mL aliquot was taken from the hot solution after 4 h and transferred to a new vessel containing all starting materials but the catalyst. In this way, any homogeneous contributions to the reaction could be observed by following the progress of the reaction (typically for 3 h) in the second vessel by GC.

4.1.4 Catalytic results

The four Ru-POM salts **K,Na-11**, **Cs,Na-12**, **Cs,Na-13** and **Na-14** were tested as catalysts for the solvent free oxidation of p-xylene. As products we observed mainly p-methyl-benzylalcohol, p-tolualdehyde, and p-toluic acid. No evidence for the formation of the fully oxidized terephthalic acid was found throughout these experiments.

Table 4.1 summarizes the results of the performance of the four Ru-POM catalysts together with the two "all-tungsten" derivatives $Na_{12}[Sb_2W_{22}O_{74}(OH)_2] \cdot 44H_2O$ (Sb_2W_{22}) and $Na_{12}[Bi_2W_{22}O_{74}(OH)_2] \cdot 44H_2O$ (Bi_2W_{22}) and the blank corresponding to the substrate alone. Sb_2W_{22} and Bi_2W_{22} resulted in significantly lower substrate conversions, emphasizing the importance of the ruthenium centers for the catalytic activity. The range of conversions exhibited by the use of the five Ru-POMs is 12 to 16%, with **Cs,Na-12** being the catalyst with the highest-conversion. **K,Na-11**, in contrast, showed the lowest conversion but the best selectivity for p-toluic acid. The main oxidation product of p-xylene was, in general, the alcohol with selectivity of 60 up to 70% in some cases. It is also worth noting that the TOFs for the benzene-containing polyanion salts **K,Na-11** and **Cs,Na-12** were higher than those of the corresponding p-cymene derivatives **Cs,Na-13** and **Na-14**. Hot filtration experiments were performed for all catalysts and no further reaction was observed in the second reaction vessel. The Ru precursor materials $[(C_{10}H_{14})RuCl_2]_2$ and $[(C_6H_6)RuCl_2]_2$ exhibited conversions of 4.6

and 3.6%, respectively. The reactions without catalyst in the presence and absence of TBHP initiator provided only 0.1 and 0% conversions, respectively.

Catalysts	C_8H_{10} Conv. (mol %)[b]	TOF[c] (h^{-1})	Product selectivity (mol %)[d] and distribution		
			A[e]	B[f]	C[g]
Blank	0.1	-	0	100	0
Sb_2W_{22}	0.7	-	59	41	0
Bi_2W_{22}	1.4	-	58	42	0
K,Na-11	12.1	1333	59	17	25
Cs,Na-12	13.5	587	61	26	13
Cs,Na-13	15.9	1431	70	16	13
Na-14	14.0	360	67	20	13

Table 4.1 Catalytic activity of the four Ru-POM catalysts for p-xylene air oxidation.[a]

[a] Reaction conditions: 10 mg catalyst, 5 mL p-xylene, 0.1g TBHP, airflow rate 10 mL/min, temperature 130 °C, reaction time 12 h.

[b] p-xylene conv. (%) = (reacted p-xylene /introduced p-xylene) x 100.

[c] TOF = moles p-xylene converted per mole catalyst per hour.

[d] Product selectivity: nb of mole of product/reacted p-xylene

[e] p-methyl benzyl alcohol

[f] p-tolualdehyde

[g] p-toluic acid

The effect of a radical scavenger (BHT) on the reaction route was assessed and the results are presented in Fig 4.5. We observed the complete suppression of substrate conversion upon addition of BHT. Furthermore, the yields were very low when the reaction was conducted without addition of TBHP, indicating that the reaction most likely proceeds via a free radical mechanism. Under the reaction conditions, the TBHP initiator is expected to

abstract a hydrogen atom from the methyl group of p-xylene which forms a peroxo radical that further reacts to give the final products.
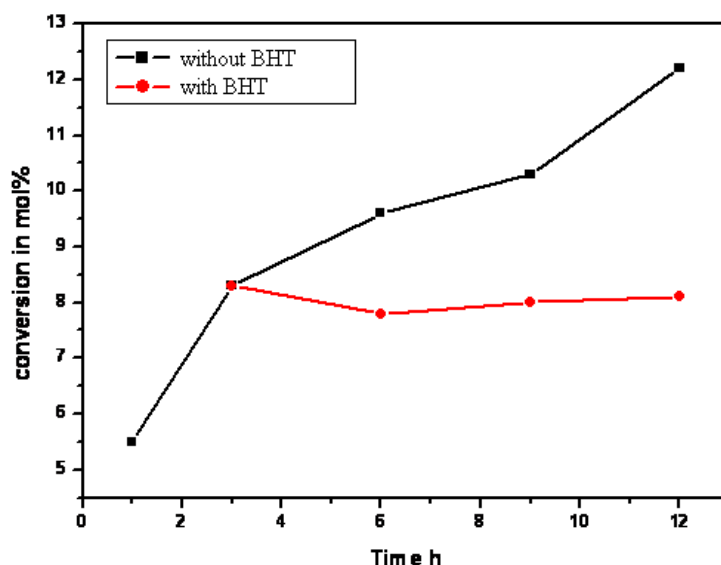
Fig. 4.5 Time profile of air oxidation of p-xylene using **K,Na-11** as a catalyst (black squares) and with the addition of BHT after 3 h of the reaction (red circles)

The time profiles for the reactions using the Ru-POM salts **K,Na-11**, **Cs,Na-12**, **Cs,Na-13**, and **Na-14** are shown in Fig 4.6. For each POM, five reactions were started simultaneously and each was stopped after a different time interval: 1, 3, 6, 9, and 12 h, respectively, followed by subsequent GC-analysis of the products. The graph shows that the conversion increases linearly with time, without induction period because of the presence of the radical initiator. All four POMs maintained their structures after the reactions, as shown by separation of the POM salt and consecutive IR analysis.
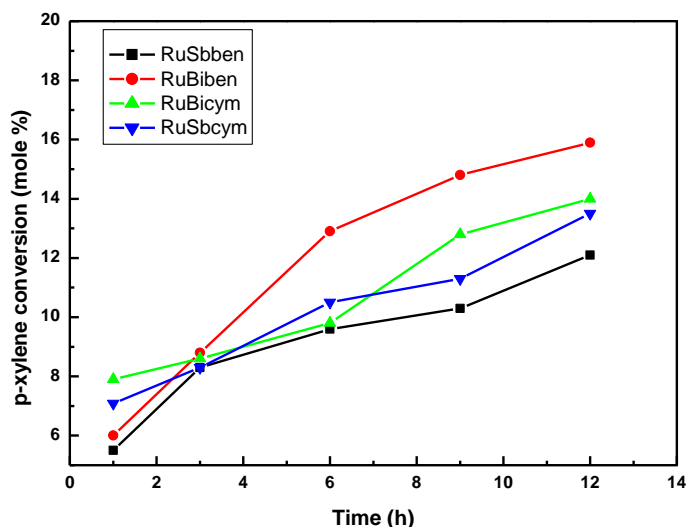
Fig. 4.6 Comparative time profiles for the oxidation of p-xylene using the four different Ru-
POMs as catalysts

4.2 Homogeneous catalysis with Zr/Hf-POMs

The exploration of the interaction between lacunary polyoxometalates POMs
and group 4 (Ti, Zr and Hf) transition metals has been mainly driven by the
fact that potential resulting adducts can serve as catalysts or even as soluble
molecular analogues of the well known Ti and Zr-containing heterogeneous
catalysts.[13] Very few reports are found in literature dealing with the catalytic
performance of Zr/Hf-POMs and these were mainly concerned with the Lewis
acid activity of such species.[14,15]

As opposed to the PW_9O_{34} and SiW_9O_{34} trilacunary Keggin units already
investigated, the lone pair on the As^{III} in AsW_9O_{33} entails different reactivity
and consequently structurally distinctive products.[16] For all the above
mentioned factors and since this kind of interaction has not been so far
reported on, we were motivated for a thorough study on the reaction of

AsW_9O_{33} with zirconium and hafnium. The outcome was two novel structures $Cs_9Na_2[Zr_6(\mu_3\text{-}O)_4(OH)_4(H_2O)_2(CH_3COO)_5(AsW_9O_{33})_2].87H_2O$ (**Cs,Na-15**) and $Cs_{10}Na[Hf_6(\mu_3\text{-}O)_4(OH)_4(H_2O)_2(CH_3COO)_5(AsW_9O_{33})_2].73H_2O$ (**Cs,Na-16**). TBA salts of 1 and 2 were also made to be used as homogeneous catalysts for the oxidation of several organic substrates in acetonitrile solution.

4.2.1 Synthetic procedures, FT-IR and nuclear magnetic resonance spectroscopy data

$Cs_9Na_2[Zr_6(\mu_3\text{-}O)_4(OH)_4(H_2O)_2(CH_3COO)_5(AsW_9O_{33})_2].87H_2O$ **Cs,Na-15**

$Na_9[\alpha\text{-}AsW_9O_{33}]$ (0.246 g, 0.1 mmol) was dissolved in 20 mL of 0.5M lithium acetate buffer solution (pH 4.0) and then of $ZrCl_4$ (0.0466 g, 0.2 mmol) was added. The solution was heated at 80°C for one hour and filtered while hot. Then 1M CsCl (0.05 mL) solution was added after filtration. Slow evaporation at room temperature led to the appearance of white crystalline product after about one week. Evaporation was allowed to continue until the solution level approached the solid product, which was filtered off and air-dried; the yield was 0.112g (50%).

IR of **Cs,Na-15**: 1637(m), 1617(m), 1577(s), 947(s), 870(vs), 783(m), 728(w),691(w), 642(w), 457(m) cm^{-1}.

NMR of **Cs,Na-15** in D_2O at 293 K: [1]H: 1.7 ppm; ^{13}C-NMR: 24.1, 182.0 ppm; [138]W: -98.7, -101.6, -159.5, -186.9, and 227.7 ppm with relative intensities 2:2:2:2:1.

$((n\text{-}C_4H_9)_4N)_7H_4[Zr_6O_4(OH)_4(H_2O)_2(CH_3COO)_5(AsW_9O_{33})_2]$ **TBA$_7$H$_4$-15**
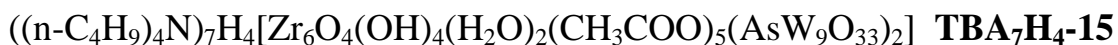
TBA salt of 1 was made by the redissolution of **Cs,Na-15** in H_2O followed by addition of solid TBABr, filtration, washing with plenty of water, and drying in an oven at 50 °C overnight.

$Cs_{10}Na[Hf_6(\mu_3\text{-}O)_4(OH)_4(H_2O)_2(CH_3COO)_5(AsW_9O_{33})_2].73H_2O$ **Cs,Na-16**

$Na_9[\alpha\text{-}AsW_9O_{33}]$ (0.246 g, 0.1 mmol) was dissolved in 20 mL of 0.5M lithium acetate buffer solution (pH 4.0) and then of (0.064 g, 0.2 mmol) of $HfCl_4$ was added. The solution was heated at 80°C for one hour and filtered while hot. Then 1M CsCl (0.05 mL) solution was added after filtration. Slow evaporation at room temperature led to the appearance of white crystalline product after about one week. Evaporation was allowed to continue until the solution level approached the solid product, which was filtered off and air-dried.

IR of **Cs,Na-16**: 1637(m), 1617(m), 1577(m), 948(m), 874(s),784(m), 729(w), 693(w), 649(w), 457(m) cm^{-1}.

NMR of **Cs,Na-16** in D_2O at 293 K: ^{1}H: 2.8 ppm; ^{13}C-NMR: 24.1, 182.2 ppm

$((n-C_4H_9)_4N)_6H_5[Hf_6O_4(OH)_4(H_2O)_2(CH_3COO)_5(AsW_9O_{33})_2]$ **TBA$_6$H$_5$-16**
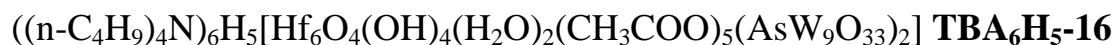
TBA salt of 2 was made by the dissolution of **Cs,Na-16** in H_2O followed by addition of solid TBABr, filtration, washing with plenty of water, and drying in an oven at 50 °C overnight.

NMR of **TBA$_6$H$_5$-16** in CH_3CN at 293 K: [138]W: -73.0, -73.1, -106.9, -162.6, and201.5 ppm with relative intensities 2:2:2:2:1.

[183]W-NMR spectra of the four compounds are shown in Fig. 4.7
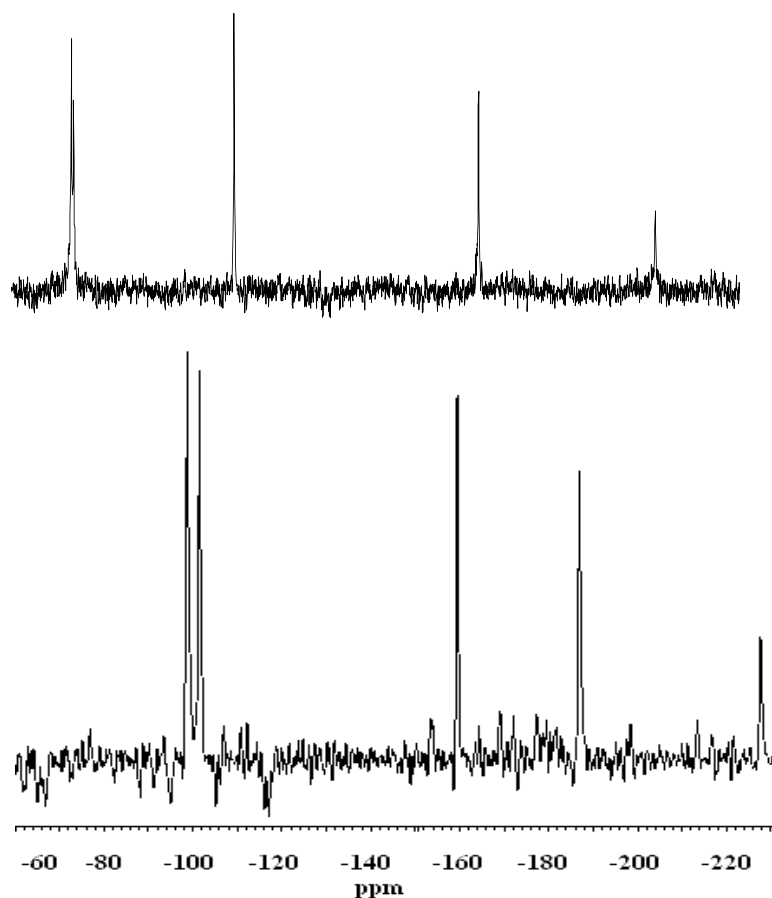
Fig. 4.7 [183]W-NMR spectra of **Cs,Na-15** (bottom) and **TBA$_6$H$_5$-16** (top) dissolved in water/D_2O and acetonitrile respectively

4.2.2 Structure discussion

Polyanions **15** and **16** consist of an unprecedented hexa-zirconium/hafnium core with the metal ions occupying the vertices of an octahedron which is accommodated by two (B-α-AsW$_9$O$_{33}$) fragments. The Zr/Hf ions are octa-coordinated resulting in a square anti-prismatic geometry. The eight faces of the Zr$_6$/Hf$_6$ octahedron are capped by four µ$_3$-O and four µ$_3$-OH bridges, each linking three zirconium/hafnium atoms (Fig. 4.8).
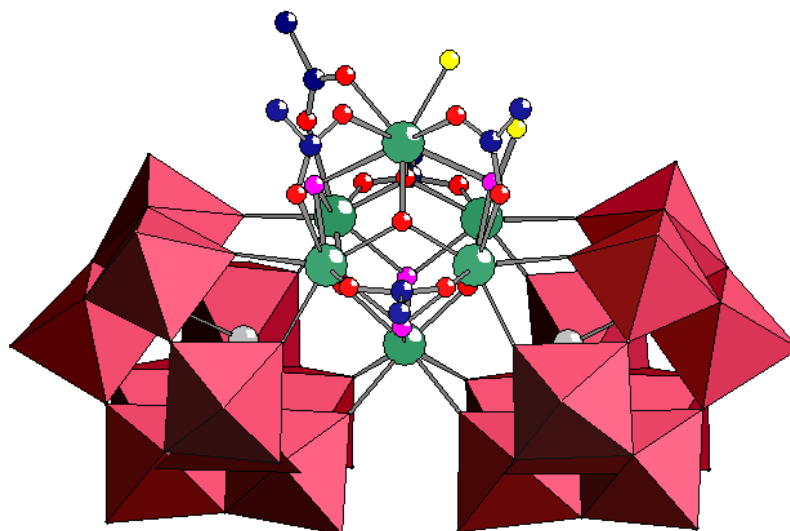
Fig. 4.8 Combined polyhedral/ball-and-stick representation of [M$_6$O$_4$(OH)$_4$(H$_2$O)$_2$(CH$_3$COO)$_5$(AsW$_9$O$_{33}$)$_2$]$^{11-}$ (M = Zr, **15**; Hf, **16**). Color code: WO$_6$ octahedra (dark red), Hf/Zr (green), As (grey), O (red), monoprotonated O (pink), diprotonated O (yellow), C (dark blue), H not shown.

The two (AsW$_9$O$_{33}$) units in **15** and **16** are not eclipsed, but rather lie at an angle of ~74° leaving a cavity perfectly suitable to host the M$_6$ unit. One of the vertices of the M$_6$ octahedron is pointing exactly inside this cavity, while the opposite one is pointing away from the polyanion. The 'equatorial plane' formed by the remaining four vertices serves as a kind of 'ceiling' for the cavity. The five 'inner' Zr/Hf atoms are directly bound to the lacunary site of

the (AsW_9O_{33}) fragments in the expected fashion via two Zr/Hf-O-W bonds involving corner-shared WO_6 octahedra. The outer, unique Zr/Hf atom is bridged by three acetate groups to three of the four Zr/Hf atoms in the equatorial plane of the M_6 octahedron. The unexpected absence of the fourth, symmetry related acetate is due to a slight distortion in the M_6 assembly introduced by bonding to the first three acetates. The outer, unique Zr/Hf has a distance of 3.56/3.54 A to its non-acetate-bridged Zr/Hf neighbour, vs 3.48/3.46 A for the distance to the four equatorial, acetate-bridged Zr/Hf neighbours. This feature is perfectly reproducible for both polyanions **15** and **16**, as seen by single-crystal XRD. The absence of this fourth acetate lowers the point group symmetry of the title polyanions from C_{2v} to C_1. The four equatorial Zr/Hf atoms are linked on the two external sides via two additional acetate groups.

4.2.3 Catalytic experiments

The two polyanions TBA-salts were tested for their homogeneous catalytic efficiency toward the oxidation of the organic substrates, cyclohexene (CyH), methyl phenyl sulfide (MPS) and cyclohexanol (CyHol).

The catalytic oxidations were carried out in temperature-controlled glass vessels at 20-70°C in MeCN solution (total reaction volume 1 mL). Samples were taken during the reaction course by a syringe, and the reaction products were identified by GC-MS and GC using reference compounds. Substrate conversions and product yields were quantified by GC using biphenyl or dodecane as internal standards.

Reaction conditions for CyH oxidation: [CyH]0.2 M, [H_2O_2]0.2 M, [POM] $2 \cdot 10^{-3}$ M, temperature 50°C, reaction time 5 h.

Reaction conditions for MPS oxidation: [MPS] 0.1 M, [H_2O_2] 0.1 M, [POM] $1 \cdot 10^{-3}$ M, temperature 20°C, reaction time 0.5 h

Reaction conditions for CyHol oxidation: [CyHol] 0.1 M, [H_2O_2] 0.4 M, [POM] $4 \cdot 10^{-3}$ M, temperature 70°C, reaction time 1 h.

4.2.4 Catalytic results

Studies were performed with **TBA$_6$H$_5$-15** and **TBA$_7$H$_4$-16** on H_2O_2 dismutation and the oxidation of representative organic substrates with H_2O_2 in MeCN medium, where the POMs are completely soluble. In the absence of an organic substrate, both polyanions caused intensive H_2O_2 decomposition (Fig. 4.9), which is quite typical for Zr-POMs.[17]
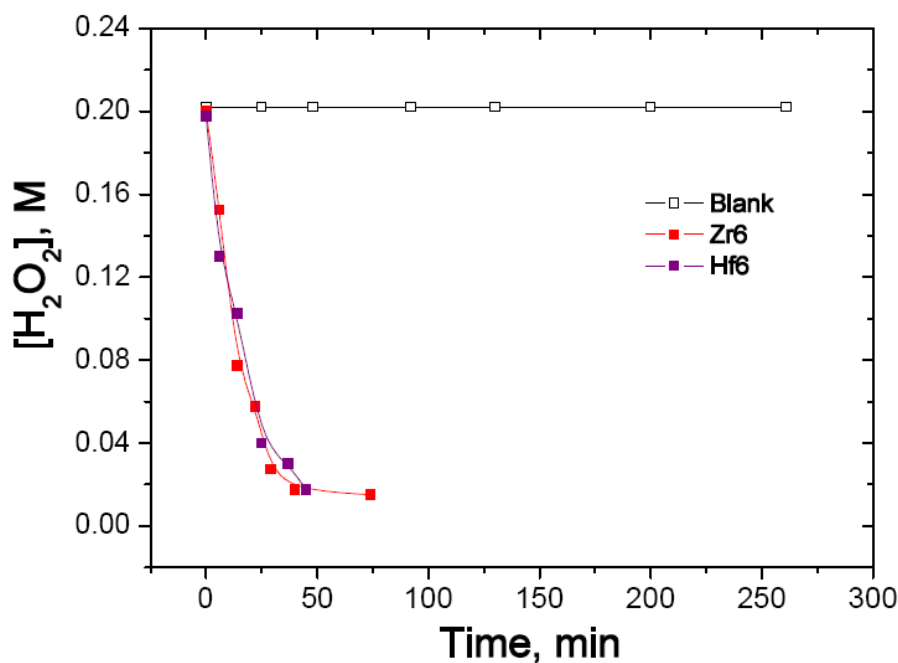
Fig. 4.9 Decomposition of H_2O_2 with time in presence and absence of TBA$_9$H$_2$-**15** and TBA$_8$H$_3$-**16**

The results of the catalytic oxidations are presented in Table 4.2. With one equivalent of H_2O_2 methyl phenyl sulfide (MPS) produced methyl phenyl sulfoxide (MPSO) with 79-82% selectivity at 69-74% substrate conversion using 1 mol % of TBA_6H_5-15 and TBA_7H_4-16, sulfone $(MPSO_2)$ was the only by-product. Interestingly, polyanion 16 was more active than 15 (TOF 876 and 286 h^{-1}, respectively). Cyclohexanol (CyHol) gave mainly cyclohexanone (86-89% selectivity at 59% conversion), while cyclohexene (CyH) produced predominantly epoxide, *trans*-1,2-cyclohexanediol and 2-hydroxycyclohexanone (totally 80-84%) along with further oxidation products, including adipaldehyde and adipic acid. The epoxide to diol ratios were 1.4 and 0.8 for 15 and 16, respectively; the yield of diol and its overoxidation products was also higher for 16, most likely, due to the higher proton content in this salt. Importantly, for both catalysts the amount of the allylic oxidation products, 2-cyclohexene-1-ol and 2-cyclohexene-1-one, did not exceed 5%. This is quite unusual for cyclohexene oxidation over Zr-catalysts, including Zr-POMs,[13b,17]and indicates a dominating heterolytic oxidation mechanism.

Table 4.2 Catalytic activity of the TBA salts of polyanions 15 and 16 in the oxidation of cyclohexene, methylphenyl sulfide and cyclohexanol

Substrate	Catalyst	Conv. %	Selectivity [a] %			TOF [b] h^{-1}
CyH [c]			epox	diol	ketol	
	TBA$_6$H$_5$-15	60	43	30	11	33
	TBA$_7$H$_4$-16	51	27	35	18	36
MPS [d]			MPSO		MPSO$_2$	
	TBA$_6$H$_5$-15	74	82		17	286
	TBA$_7$H$_4$-16	69	79		20	876
CyHol [e]			Cyclohexanone			
	TBA$_6$H$_5$-15	59	89			n.d.
	TBA$_7$H$_4$-16	59	86			52

[a] GC yield based on substrate consumed.

[b] TOF = (moles of substrate consumed)/[(moles of POM) × time];
    determined from the initial rates

[c] Reaction conditions: CyH 0.2 M, H$_2$O$_2$ 0.2 M, POM 2·10^{-3} M, 50°C, 5 h

[d] Reactio conditions: MPS 0.1 M, H$_2$O$_2$ 0.1 M, POM 1·10^{-3} M, 20°C, 0.5 h

[e] Reaction conditions: CyHol 0.1 M, H$_2$O$_2$ 0.4 M, POM 4·10^{-3} M, 70°C, 1 h

4.2.5 Conclusions

In the first part of this chapter, synthesis and structure of four organo-Ru supported lone pair containing heteropolytungstates were described.

The polyanions $[X_2W_{20}O_{70}(RuL)_2]^{10-}$ (X = Sb^{III}, L = benzene, **11**; X = Bi^{III}, L=benzene, **12**; X = Sb^{III}, L = p-cymene, **13**; X = Bi^{III}, L = p-cymene, **14**) consist of two (L)Ru^{2+} units linked to a Krebs-type polyanion $[X_2W_{20}O_{70}]^{14-}$ fragment resulting in an assembly with idealized C$_{2h}$ symmetry.

Oxidation reaction studies using the four organo-ruthenium polyanions as heterogeneous catalysts were conducted for p-xylene oxidation. For all four ruthenium-containing polyanions the yields were comparable and significantly higher than those for the blank and the corresponding "all-

tungsten" derivatives Sb_2W_{22} and Bi_2W_{22}. This is evidence suggesting the importance of the ruthenium centers on the overall catalytic efficiency of the POMs for this type of reactions.

The second part of the chapter dealt with the two novel polyanions $[M_6O_4(OH)_4(H_2O)_2(CH_3COO)_5(AsW_9O_{33})_2]^{11-}$ (M = Zr, **15**; Hf, **16**). They contain an unprecedented octahedral Zr_6/Hf_6 assembly which is stabilized by two (B-α-AsW$_9$O$_{33}$) groups and five terminal acetate ligands. The TBA-salts of both **15** and **16** revealed high catalytic activity and selectivity in the liquid-phase oxidation of organic compounds with aqueous H_2O_2. A heterolytic oxidation mechanism is manifested by the high yields of epoxide and diol in the oxidation of cyclohexene.

4.3 References

[1] Naota, T.; Takaya, H.; Murahashi, S. I. *Chem. Rev.* **1998**, *98*, 2599.

[2] (a) Neumann, R.; Khenkin, A. M.; Dahan, M. *Angew. Chem., Int. Ed.* **1995**, *34*, 1587. (b) Neumann, R.; Dahan, M. *Nature* **1997**, *388*, 353. (c) Neumann, R.; Dahan, M. *J. Am. Chem. Soc.* **1998**, *120*, 11969. (d) Bonchio, M.; Scorrano, G.; Toniolo, P.; Proust, A.; Artero, V.; Conte, V. *Adv. Synth. Catal.* **2002**, *344*, 841. (e) Yamaguchi, K.; Mizuno, N. *New J. Chem.* **2002**, *26*, 972. (f) Adam, W.; Alsters, P. L.; Neumann, R.; Saha-Möller, C. R.; Seebach, D.; Beck, A. K.; Zhang, R. *J. Org. Chem.* **2003**, *68*, 8222. (g) Yin, C. X.; Finke, R. G. *Inorg. Chem.* **2005**, *44*, 4175.

[3] Bösing, M.; Loose, I.; Pohlmann, H.; Krebs, B. *Chem. Eur. J.* **1997**, *3*, 1232.

[4] (a) Loose, I.; Droste, E.; Bösing, M.; Pohlmann, H.; Dickman, M. H.; Roşu, C.; Pope, M. T.; Krebs, B. *Inorg. Chem.* **1999**, *38*, 2688. (b) Krebs, B.; Droste, E.; Piepenbrink, M.; Vollmer, G. *C. R. Acad. Sci. Paris, Ser. IIc* **2000**, *3*, 205. (c) Rusu, D.; Roşu, C.; Crãciun, C.; David, L.; rusu, M.; Marcu, Gh. *J. Mol. Struct.* **2001**, *563-564,* 427. (d) Kortz, U.; Savelieff, M. G.; Bassil, B. S.; Keita, B.; Nadjo, L. *Inorg. Chem.* **2002**, *41*, 783. (e) Limanski, E. M.; Drewes, D.; Droste, E.; Bohner, R.; Krebs, B. *J. Mol. Struct.* **2003**, *656*, 17.

[5] (a) Randall, W. J.; Weakley, T. J. R.; Finke, R. G. *Inorg. Chem.* **1993**, *32*, 1068. (b) Neumann, R.; Khenkin, A. M. *Inorg. Chem.* **1995**, *34*, 5753. (c) Sadakane, M.; Tsukuma, D.; Dickman, M. H.; Bassil, B. S.; Kortz, U.; Capron, M.; Ueda, W. *Dalton Trans.*, **2007**, 2833. (d) Geletii, Y.; Botar B.; Kögerler P.; Hillesheim D.; Musaev D.; Hill C. *Angew. Chem. Int. Ed.* **2008**, 47, 3896. (e) Sartorel A.; Carraro M.; Scorrano G.; De Zorzi R.; Geremia S.; McDaniel N.D.; Bernhard S.; Bonchio M. *J. Am. Chem. Soc*. **2008**, *130*, 5006. (f) Yamaguchi S.; Uehara K.; Kamata K.; Yamaguchi K.; Mizuno N. *Chem. Lett.* **2008**, 37, 328.

[6] (a) Bi, L.-H.; Kortz, U.; Keita, B.; Nadjo, L. *Dalton Trans.* **2004**, 3184. (b) Bi, L. –H.; Dickman, M. H.; Kortz, U.; Dix, I. *Chem. Commun.* **2005**, 3962. (c) Sadakane, M.; Tsukuma, D.; Dickman, M. H.; Bassil, B.S.; Kortz, U.; Higashijima M.; Ueda W. *Dalton Trans.* **2006**, 4271.

[7] (a) Bi, L.-H.; Kortz, U.; Dickman, M. H.; Keita, B.; Nadjo, L. *Inorg. Chem.* **2005,** *44,* 7485. (b) Bi, L.-H.; Chubarova, E. V.; Nsouli, N.H.; Dickman, M.H.; Kortz, U.; Keita,

B.; Nadjo, L. *Inorg. Chem.,* **2006**, *45*, 8575. (c) Mal S.; Nsouli N.; Dickman M.H.; Kortz U. *Dalton Trans.*, **2007**, 2627–2630.

[8] (a) Attanasio, D.; Bachechi, F.; Suber, L. *Dalton Trans.* **1993**, 2373. (b) Day, V. W.; Eberspacher, T. A.; Klemperer, W. G.; Planalp, R. P.; Schiller, P. W.; Yagasaki, A.; Zhong, B. *Inorg. Chem.* **1993**, *32*, 1629. (c) Klemperer, W. G.; Zhong, B.-X. *Inorg. Chem.* **1993**, *32*, 5821. (d) Pohl, M.; Lin, Y.; Weakley, T. J. R.; Nomiya, K.; Kaneko, M.; Weiner, H.; Finke R. G. *Inorg. Chem.* **1995**, *34*, 767.

[9] Artero, V.; Laurencin, D.; Villanneau, R.; Thouvenot, R.; Herson, P.; Gouzerh, P.; Proust, A. *Inorg. Chem.* **2005**, *44*, 2826.

[10] Laurencin, D.; Villanneau, R.; Herson, P.; Thouvenot, R.; Jeannin, Y.; Proust, A. *Chem. Commun.* **2005**, 5524.

[11] Sakai, Y.; Shinohara, A.; Hayashi, K.; Nomiya, K. *Eur. J. Inorg. Chem.* **2006**, 163.

[12] Kato, C. N.; Shinohara, A.; Moriya, N.; Nomiya, K. *Catal. Commun.* **2006**, 7, 413.

[13] (a) Villanneau R.; Carabineiro H.; Carrier X.; Thouvenot R.; Herson P.; Lemos F.; Ribeiro F. R.; Che M. *J. Phys. Chem. B* **2004**, *108*, 12465. (b) Kholdeeva O. A.; Maksimovskaya R. I.; *J. Mol. Catal. A – Chemical* **2007**, *262*, 7. (c) Kikukawa Y.; Yamaguchi S.; Tsuchida K.; Nakagawa Y.; Uehara K.; Yamaguchi K.; Mizuno N. *J. Am. Chem. Soc.* **2008**, *130*, 5472.

[14] Boglio, C.; Micoine, K.; Remy, P.; Hasenknopf, B.; Thorimbert, S.; Lacote, E.; Malacria, M.; Afonso, C.; Tabet, J. C. *Chem. Eur. J.* **2007**, *13,* 5426.

[15] Kikukawa, Y.; Yamaguchi, S.; Tsuchida, K.; Nakagawa, Y.; Uehara, K.; Yamaguchi, K., Mizuno, N. *J. Am. Chem. Soc.* **2008**, *130,* 5472.

[16] (a) Fukaya K.; Yamase T. *Angew. Chem. Int. Edit.* **2003**, *42*, 654. (b) Hussain F.; Reicke M.; Kortz U. *Eur. J. Inorg. Chem.* **2004**, 2733. (c) Hussain F.; Kortz U. *Chem. Comm.* **2005**, 1191. (d) Drewes D.; Piepenbrink M.; Krebs B. *Z. Anorg. Allg. Chem.* **2006**, *632*, 534. (e) Fukaya K.; Yamase T. *J. Alloys Compounds* **2006**, *408*, 915. (f) Hussain F.; Bassil B. S.; Kortz U.; Kholdeeva O. A.; Timofeeva M. N.; de Oliveira P.; Keita B.; Nadjo L. *Chem. Eur. J.* **2007**, *13*, 4733. (g) Hou Y.; Fang X.; Hill C. L. *Chem.-Eur. J.* **2007**, *13*, 9442.

[17] Kholdeeva O. A.; Maksimov G. M.; Maksimovskaya R. I.; Vanina M. P.; Trubitsina T. A.; Naumov D. Y.; Kolesov B. A.; Antonova N. S.; Carbo J. J.; Poblet J. M. *Inorg. Chem.* **2006**, *45*, 7224.

Curriculum Vitae

GHADA AL-KADAMANY

Gender: Female
Date of Birth: Feb 1st, 1981
e-mail: g.alkadamany@jacobs-university.de
gadkad@gmail.com
Tel: +49-152-07521503

EDUCATION

PhD in Inorganic Chemistry (with distinction)   Jun 2010
Jacobs University, Bremen, Germany

MS in Analytical Chemistry (96% grade)   Jul 2006
American University of Beirut, Beirut, Lebanon

BS in Chemistry (94% grade)   Jun 2003
Lebanese University, Beirut, Lebanon

RELEVANT EXPERIENCE

RESEARCH

Jacobs University Bremen, JUB
- Synthesis of titanium-containing polyoxotungstates followed by solid state and solution characterization
- Heterogeneous catalytic studies on Ru-containing polyoxotungstates towards the oxidation of P-xylene using air as an oxidant

Boreskov Institute of Catalysis (one month)
- Homogeneous catalytic studies on Zr and Hf- containing polyoxotungstates towards the oxidation of different organic substrates using H_2O_2 as an oxidant

American University of Beirut, AUB
- Assessment of particulate matter PM_{10} levels in several residential sites in Beirut via active sampling followed by gravimetric analysis and speciation of the PM_{10} ionic content
- Sampling of NO_2 and SO_2 using passive samplers in order to study the contribution of these gases to the variation of inorganic constituents of PM_{10} like NO_3^- and SO_4^{2-}

TEACHING

- Teaching assistantships in AUB and JUB which involve preparing for lab experiments, lab lectures and monitoring students during experiments, for five different lab courses (General, Analytical, Inorganic and Advanced Inorganic Chemistry) throughout MS and PhD
- Supervision of the research work of two undergraduates and one masters student during my PhD work

ANALYTICAL SKILLS

- Good theoretical and practical knowledge of the chromatographic and spectroscopic techniques, IC, GC, FT-IR, NMR and single-crystal XRD

CONFERENCES and MEETINGS

- Oral presentation, Norddeutsches Doktoranden-kolloquium NDDK XI, Braunschweig, Germany   Sep 2008
- Poster presentation, International Symposium on Homogeneous Catalysis, ISHC-XVI, Florence, Italy   Jul 2008
- 59th Lindau Nobel Laureate Meeting   Jul 2009

PUBLICATIONS

- Hexa-Zirconium/Hafnium Containing Tungstoarsenates(III) and their oxidation catalysis properties. (*Manuscript accepted in Chem. Eur. J.*)
- Unique Catalytic Performance of the Polyoxometalate $[Ti_2(OH)_2As_2W_{19}O_{67}(H_2O)]^{8-}$: The Role of 5-Coordinated Titanium in H_2O_2 Activation. *Eur. J. Inorg. Chem.* **2009**; 34; 5134-5141.
- Organo-Ruthenium Supported Heteropolytungstates: Synthesis, Structure, Electrochemistry, and Oxidation Catalysis. *Inorg. Chem.*; **2009**; 48; 10068-10077.
- Cyclic Ti_9 Keggin Trimers with Tetrahedral (PO_4) or Octahedral (TiO_6) Capping Groups. *Inorg. Chem.*; (Communication); **2008**; 47(19); 8574-8576.
- Chapter in the book "*Regional Climate variability and its impacts in the Mediterranean area*". Saliba N.; Kouyoumdjian H.; Al Kadamany G. Springer Netherlands, **2007**, p129-142.
- MS thesis: Characterization of PM_{10} and Selected Gas-phase Compounds in Multiple Indoor Sites in Beirut

LANGUAGES

- Arabic (mother tongue)
- Written and oral fluency in English
- Basic knowledge of German

REFERENCES

- Professor Ulrich Kortz
  Professor of Chemistry, School of Engineering and Science,
  Jacobs University, 28759, Bremen, Germany
  Tel: +49-421-200-3235, Fax: +49-421-200-3229
  E-mail: u.kortz@jacobs-university.de

- Professor Gerd-Volker Röschenthaler
  Professor of Chemistry, School of Engineering and Science,
  Jacobs University, 28759, Bremen, Germany
  Tel: +49-421-200-3138, Fax: +49-421-200-3229
   E-mail: g.roeschenthaler@jacobs-university.de

- Professor Oxana Kholdeeva
  Professor of Chemistry, Boreskov Institute of Catalysis,
  Lavrentina 5, Novosibirsk 630090, Russia
  Tel: +7-3833-269433, Fax: +7-3833-309573
  E-mail: khold@catalysis.ru

Appendix

1. Cyclic Ti9 Keggin Trimers with Tetrahedral (PO4) or octahedral (TiO6) Capping Groups.
   Al-Kadamany, G.; Hussain, F.; Mal, S. S.; Dickman, M. H.; Leclerc-Laronze, N.; Marrot, J.; Cadot, E.; Kortz, U. *Inorg. Chem.*, **2008**, 47, 8574-8576.

2. Organo-Ruthenium Supported Heteropolytungstates: Synthesis, Structure, Electrochemistry, and Oxidation Catalysis.
   Bi, L.-H.; Al-Kadamany, G.; Chubarova, E. V.; Dickman, M. H.; Chen, L.; Gopala, D. S.; Richards, R. M.; Keita, B.; Nadjo, L.; Jaensch, H.; Mathys, G.; Kortz, U. *Inorg. Chem.* **2009**, 48, 10068-10077.

3. Unique Catalytic Performance of the Polyoxometalate $[Ti_2(OH)_2As_2W_{19}O_{67}(H_2O)]^{8-}$: The Role of 5-Coordinated Titanium in H_2O_2 Activation.
   Kholdeeva, O. A.; Donoeva, B. G.; Trubitsina, T. A.; Al-Kadamany, G.; Kortz, U. *Eur. J. Inorg. Chem.* **2009**; 34; 5134-5141.

4. Hexa-Zirconium/Hafnium Containing Tungstoarsenates(III) and Their Oxidation Catalysis Properties.
   Al-Kadamany, G.; Mal, S. S.; Milev, B.; Donoeva, B.; Maksimovskaya, R.; Kholdeeva, O. A.; Kortz, U. *Chem. Eur. J.* (Manuscript in press, **2010**)